



DIPARTIMENTO SCIENZE DELLA VITA

DOTTORATO DI RICERCA IN SCIENZE DELLA VITA

CICLO XXXIV

COORDINATORE Prof. Massimo Valoti

CYP450 expression and regulation in SH-SY5Y cells. Possible role in
neurotoxin-mediated injury

SETTORE SCIENTIFICO-DISCIPLINARE: BIO/14

TUTOR: Prof. Valoti Massimo

DOTTORANDA: Dr.ssa Chiaino Elda

Co-TUTOR: Prof.ssa Maria Frosini

A.A. 2021-2022*

Table of contents

Summary.....	5
Abbreviations	7
1. Background.....	8
1.1. Neurodegeneration	9
1.1.2. Parkinson’s disease.....	11
1.1.3. Mitochondrial dysfunction and PD	13
1.2. Cytochrome P450	15
1.2.1. The CYP450 in the brain	17
1.2.2. CYP1A1	19
1.2.3. CYP2D6	20
1.2.4. CYP2E1.....	21
1.2.5. CYP2B6	23
1.2.6. CYP3A4	24
1.3. CYP450 induction.....	26
1.3.1. β -naphthoflavone	27
1.3.2. Ethanol	29
1.3. Neurotoxins	29
1.3.1. MPP ⁺	31
1.3.2. Rotenone	34
1.4. <i>In vitro</i> model for PD research	36
1.4.1. Human neuroblastoma SH-SY5Y cell line.....	39
1.4.3. SH-SY5Y Cell differentiation.....	40
1.5. Aim of the study.....	44
2. Common Materials and Methods.....	47
2.1. Materials.....	48
2.1.1. Substances purchased by Sigma Merck (Darmstadt, Germany):.....	48
2.1.2. Substances purchased by Euroclone (Pero, Italy):.....	49
2.1.3. Substances purchased by BioRad (Hercules, California, USA):	49
2.1.4 Substances purchased by others:	49
2.2. Solutions	50
2.3. Instruments.....	54
2.4. Cell culture.....	57
2.4.2. Sub-culturing	57

2.4.3. Cell counting.....	57
2.4.4. Cell freezing.....	58
2.4.5. Cell seeding.....	58
3. Task 1. SH-SY5Y cell differentiation	60
3.1. Introduction.....	61
3.2. Methods.....	64
3.2.1. Cell Differentiation	64
3.2.2. Morphological analysis	65
3.2.3. Western blot analysis	65
3.2.4. Quantitative real-time PCR.....	68
3.3. Results.....	72
3.3.1. Effect of differentiation with RA-TPA and RA-BDNF on SH-SY5Y: morphological analysis	72
3.3.2. Expression of specific neuronal markers	74
3.3.3. Effect of RA-BDNF and RA-TPA differentiation on basal CYP450 expression.....	77
3.4. Discussion	78
4. Task 2. Induction of Cytochrome P450 isoforms in SH-SY5Y cells	85
4.1. Introduction.....	86
4.2. Methods.....	87
4.2.1. Cell culture and cell differentiation	87
4.2.2. CYP-induction	88
4.2.3. Quantitative real-time PCR.....	88
4.3. Results.....	88
4.4. Discussion	92
5. Task 3.....	96
Role of CYP450 against dopaminergic neurotoxins-promoted damage.....	96
5.1. Introduction.....	97
5.2. Methods.....	98
5.2.1. Cell treatments	98
5.2.2. MTT viability assay.....	99
5.2.3. Propidium Iodide viability assay	100
5.2.4. Annexin V/PI assay.....	100
5.2.5. Analysis of Cell cycle	101
5.2.6. Intracellular ROS.....	102
5.2.7. Mitochondrial Membrane Potential measure	102

5.2.8. Mitochondrial complex I activity	103
5.3. Statistical analysis	104
5.4. Results.....	104
5.4.1. Effects of β NF and EtOH on MPP ⁺ - and Rotenone-mediated injury in UD and differentiated SH-SY5Y.....	104
5.4.2. Effects of β NF and EtOH on cell cycle changes promoted by MPP ⁺ and Rotenone in UD SH-SY5Y	116
5.4.3. Effects of β NF and EtOH on intracellular ROS formation promoted by MPP ⁺ and Rotenone in UD and differentiated SH-SY5Y.....	118
5.4.4. Effects of β NF and EtOH on $\Delta\psi$ m loss promoted by MPP ⁺ in UD SH-SY5Y cells.....	121
5.4.5. Effects of β NF and EtOH Complex I disruption promoted by MPP ⁺ in UD SH-SY5Y cells	122
5.5. Discussion	123
6. Conclusions.....	129
6.1 Conclusions	130

Summary

The Cytochrome P450 isozymes involved in xenobiotic metabolism are ubiquitous enzymes, predominantly expressed in the liver in comparison to the extrahepatic tissues. In the brain, CYP expression is approximately 0.5-2% of that in liver microsomes, and most of the isoforms appears to be very low for playing a role in overall total body clearance. Brain basal expression and up-regulation can however significantly affect local disposition of xenobiotic or endogenous compounds. Several reports, in fact, indicate that environmental toxins may play a role in the pathogenesis of neurodegenerative disorders by directly damaging neurons or by CYPs-mediated their bioactivation into toxic compounds. Among the different isoforms, CYP2D6 is particularly involved in the metabolism of exogenous drugs, neurotoxins such as 1-methyl-4-phenyl-1,2,3,6-tetrahydropyridine (MPTP, which selectively target nigrostriatal dopaminergic pathways), as well as endogenous compounds, including dopamine. Moreover, CYP2D6 extended polymorphism is significantly associated with an increased PD risk, owing to a lower capability in the metabolism of neurotoxic compounds such as pesticides. On the contrary, other studies did not support the association between PD and the poor CYP2D6-dependent metabolism, thus suggesting that PD is most likely the result of interactions between multiple genetic and environmental factors.

The aim of the present study was to increase the knowledge on the role of neuronal CYP-dependent oxidative metabolism and to clarify whether it might affect xenobiotic-promoted neurodegeneration by using an in vitro model based on human neuroblastoma-derived SH-SY5Y cells.

The first step was to promote the differentiation of neuroblastoma cells into mature human dopaminergic neurons phenotype. Two different protocols based on retinoic acid and phorbol ester or retinoic acid and brain derived neurotrophic factor were set up. The switch into dopaminergic phenotype was assessed by studying the cell morphology and the expression of the most important proteins recognized as neuronal biomarkers. Results showed that after differentiation, SH-SY5Y cells demonstrated extensive and elongated neuritic projections, a significant increased content of NeurineN, Synaptophysin, and β -tubulin III, as well as dopamine transporter.

Two well know inducers such as β -naphthoflavone (β NF) and ethanol (EtOH) were then used for promoting CYPs induction in both undifferentiated (UD) and differentiated SH-SY5Y cells. qRT-PCR analysis showed that both compounds significantly increased the mRNA expression of CYP2E1 and CYP2D6 isoforms in all SH-SY5Y cells population, while 1A1 and 3A4 were substantially unaffected.

To explore the role of CYP in the protection toward neurotoxicity, SH-SY5Y cells possessing increased CYPs content were treated with 1-methyl-4-phenylpyridinium (MPP⁺), the MAO-B-dependent toxic metabolite of MPTP, or rotenone, two neurotoxins widely used to reproduce PD models *in vivo* and *in vitro*.

The treatment with EtOH and β NF protected UD cells against MPP⁺ toxicity, whereas only β NF partially reverted the cytotoxic insult promoted by Rotenone. Moreover, the differentiated SH-SY5Y cells resulted to be less sensitive to the cytotoxic effects caused by the neurotoxins and consequently less responsive to the protection promoted by the CYPs induction. Furthermore, both β NF and EtOH treatments partially reverted the loss in mitochondria membrane potential, complex I impairment, as well as the increased ROS formation when UD were exposed to MPP⁺ or rotenone.

Taken together, these results support the possible role of CYP isoforms in the neuroprotection against xenobiotic insult, especially as far as concerned the metabolic activity of CYP2D6 and CYP2E1. However, it would be interesting to investigate the induction dynamics of the CYPs here analysed and to understand the pathways triggered by β NF and EtOH leading to CYP induction. In conclusion, the impact that these isoforms have in the metabolism of other drugs, together with the present results, bring new insights on the role of brain CYPs in the effects of drugs and can drive future therapeutic approaches for ameliorating the therapy of neurological diseases.

Abbreviations

AHR	Aryl hydrocarbon receptors
ATP	Adenosine triphosphate
BDNF	Brain-Derived Neurotrophic Factor
BNF	β -naphthoflavone
BSA	Bovine serum albumin
CAR	Constitutive androstane receptor
cDNA	Complementary DNA
CNS	Central nervous system
C _T	Average threshold cycle
DA	Dopamine
DAERGIC	Dopaminergic
DAT	Dopamine transporter
DMSO	Dimethylsulfoxide
DPBS	Dulbecco's phosphate buffered saline
DTT	Dithiothreitol
ETC	Electron transport chain
FACS	Fluorescent-activated cell sorting
FBS	Fetal bovine serum
MAO	Monoamine oxidase
MPP ⁺	1-methyl-4phenylpyridinium iodide
MPTP	1-methyl-4-phenyl-1,2,3,6-tetrahydropyridine
mRNA	Messenger RNA
MTT	Thiazolyl Blue Tetrazolium Bromide
NADH	Nicotinamide adenine dinucleotide (reduced form)
NeuN	Neuronal nuclei protein
PD	Parkinson's disease
PI	Propidium Iodide
PVDF	Polyvinylidene fluoride
PXR	Pregnane X Receptor
qRT-PCR	Quantitative Real Time-polymerase chain reaction
RA	Retinoic acid
ROS	Reactive oxygen species
SDS	Sodium dodecyl sulfate
SEM	Standard error of the mean
TH	Tyrosine hydroxylase
TPA	12-O-tetradecanoyl-phorbol-13 acetate
TRIS	Tris(hydroxymethyl)aminomethane
TRITON-X	Iso-octylphenoxy polyethoxyethanol
WB	Western blot
$\Delta\Psi_M$	Mitochondrial membrane potential

1. Background

1.1. Neurodegeneration

Neurodegenerative diseases are characterized by progressive and selective loss of specific neuronal populations. Depending on the affected area and the type of damaged cells, the symptoms of these diseases may vary but the outcome is always severely disabling. These pathologies are generally late-onset disorders and show sporadic epidemiology, like Alzheimer's disease (AD), Parkinson's disease (PD), Huntington's disease (HD) and Amyotrophic lateral sclerosis (ALS). As life expectancy continues to advance in developed countries, the incidence of these disorders increases and will continue for the foreseeable future. Although neurodegenerative diseases are rather heterogeneous from an etiological, clinical, and epidemiological point of view, many prominent studies suggest that they share common pathogenetic mechanisms. These pathologies are generally late-onset disorders and show sporadic epidemiology, like Alzheimer's disease (AD), Parkinson's disease (PD), Huntington's disease (HD) and Amyotrophic lateral sclerosis (ALS). As life expectancy continues to advance in developed countries, the incidence of these disorders increases and will continue to do so. In recent decades, major efforts have been made to understand the mechanisms of the neurodegeneration process that underlies these disorders. From these intense investigations, it is increasingly evident that in the complex set of events leading to cell death, mitochondrial dysfunction occupies a prominent role (Figure 1).

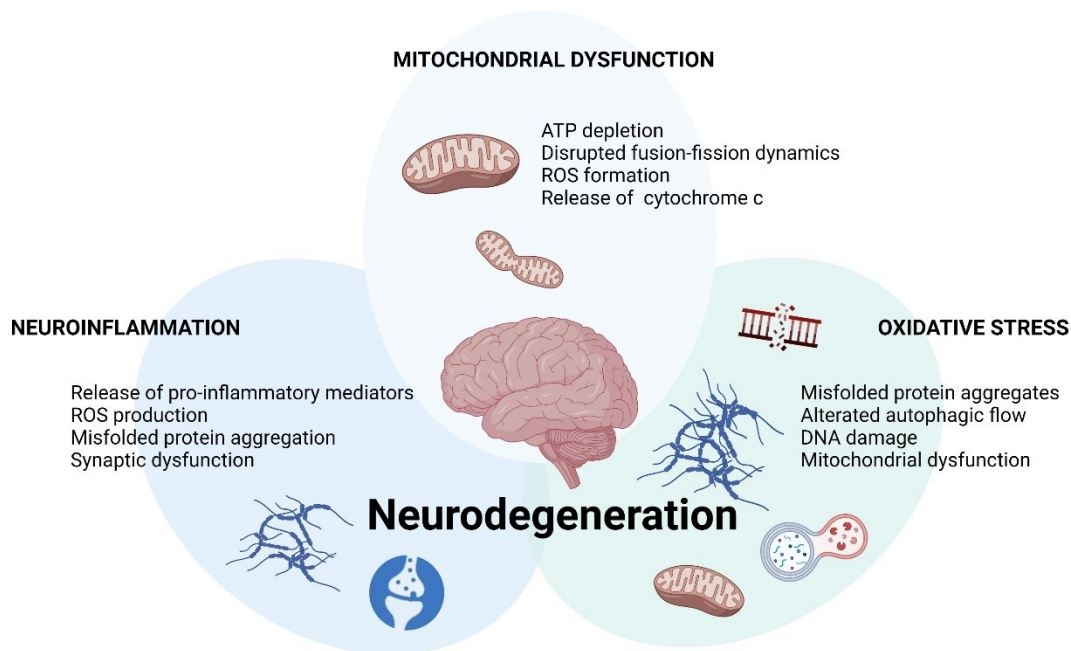


Figure 1. Causes contributing to the onset and development of the neurodegenerative process.

The selective vulnerability of neurons in certain regions of the brain appears to be an intrinsic feature, indicating a particular sensitivity to injury under adverse conditions, while other neurons are relatively resistant. The selective vulnerability of some neurons often consists in structural and functional changes that may lead to cell death.¹

A primary aspect to consider is the energy requirement. The metabolic activity of the brain has high energy requirements, accounting for about 20-25% of the whole glucose and oxygen use. Therefore, a reduced metabolism and energy production can be significantly correlated to neuronal dysfunction. Given the role of mitochondria as the primary energy source of the cell, their impairment would lead to a consistent metabolic imbalance and a resulting consequent cascade dysfunctions in other cellular districts.

Neuroinflammation seems to be another pivotal part of the pathophysiological cascade that leads to neurodegenerative disorders, but it is not yet clear whether it plays a crucial role in the onset of diseases or if it is a consequence that contribute to accelerate its progress.

The pro/anti-inflammatory balance in the brain is finely regulated by microglia, a type of cells involved in inducing and modulating a broad spectrum of cellular responses to regulate brain development, maintenance of neuronal networks, and injury response. Some of the findings in animal model studies confirmed microglia activation, observed in post mortem PD brains, and upregulation of pro-inflammatory mediators such as cytokines following noxious stimulus.² The increase in the level of peripheral cytokines act on the endothelial cells of the blood brain barrier (BBB) and causes an altered vascular permeability.³ A wide range of antigens can activate microglia, such as infectious agents, foreign pathogens, prions, or other pathologically-modified CNS proteins, aggregates of β -amyloid and α -synuclein.⁴ In the context of neurodegenerative diseases, neuroinflammation tends to be a chronic process that fails to resolve by itself and is considered a crucial factor of the disorder.

¹ Wang, X., Michaelis, M. L., & Michaelis, E. K. (2010). Functional genomics of brain aging and Alzheimer's disease: focus on selective neuronal vulnerability. *Current genomics*, *11*(8), 618–633

² Marogianni, C., Sokratous, M., Dardiotis, E., Hadjigeorgiou, G. M., Bogdanos, D., & Xiromerisiou, G. (2020). Neurodegeneration and Inflammation-An Interesting Interplay in Parkinson's Disease. *International journal of molecular sciences*, *21*(22), 8421

³ Varatharaj, A., & Galea, I. (2017). The blood-brain barrier in systemic inflammation. *Brain, behavior, and immunity*, *60*, 1–12

⁴ Colonna, M., & Butovsky, O. (2017). Microglia Function in the Central Nervous System During Health and Neurodegeneration. *Annual review of immunology*, *35*, 441–468

Interconnected with the inflammatory process and mitochondrial dysfunction, oxidative stress represents another critical regulatory element in the onset of neurodegenerative process. As also occurs in neuroinflammation, oxidative stress represents a consequence of an imbalance between the production of reactive oxygen species (ROS) and their elimination through the body's antioxidants defense systems. The formation of ROS is a physiologically phenomenon, as oxygen is involved in various cellular activities such as signal transduction, gene transcription and oxidative phosphorylation in mitochondria. A significant increase in ROS formation can lead to major damage in different cellular districts: oxidative stress can lead to an alteration of mitochondrial function, with depletion of ATP and release of cytochrome *c*. ROS are also involved in DNA damage⁵, alteration of autophagic flow and aberrant aggregation of proteins, such as α -synuclein and amyloid- β ⁶.

Multiple lines of evidence provide strong support for the involvement of these mechanisms in the onset and development of the neurodegenerative process. It is therefore natural to focus on the mechanisms involved in the development of ground-breaking therapeutic strategies.

1.1.2. Parkinson's disease

PD is the second most common neurodegenerative disorder after AD, strongly correlated to age, that affect millions of the older population with an incidence rate of 13.43/100,000 in 2019⁷. The major pathological hallmark of PD is the formation of intracellular aggregates of α -synuclein that elicit the selective loss of DAergic neurons within the substantia nigra, which can lose up to 50-70% of its neurons compared to the same region in unaffected individuals. This disorder is clinically characterized by motor symptoms like rigidity, resting tremor, bradykinesia, and postural instability, while in the advanced stages of the disease dementia and depression may arise (Figure 2).⁸

⁵ Mariani, E., Polidori, M. C., Cherubini, A., & Mecocci, P. (2005). Oxidative stress in brain aging, neurodegenerative and vascular diseases: an overview. *Journal of chromatography. B, Analytical technologies in the biomedical and life sciences*, 827(1), 65–75.

⁶ Tönnies, E., & Trushina, E. (2017). Oxidative Stress, Synaptic Dysfunction, and Alzheimer's Disease. *Journal of Alzheimer's disease : JAD*, 57(4), 1105–1121.

⁷ Zejin O., Jing P., Shihao T., Danping D., Danfeng Y., Huiqi N., Zhi W. (2021). Global Trends in the Incidence, Prevalence, and Years Lived With Disability of Parkinson's Disease in 204 Countries/Territories From 1990 to 2019 *Frontiers in Public Health* (9)

⁸ Spillantini, M. G., Schmidt, M. L., Lee, V. M., Trojanowski, J. Q., Jakes, R., & Goedert, M. (1997). Alpha-synuclein in Lewy bodies. *Nature*, 388(6645), 839–840.

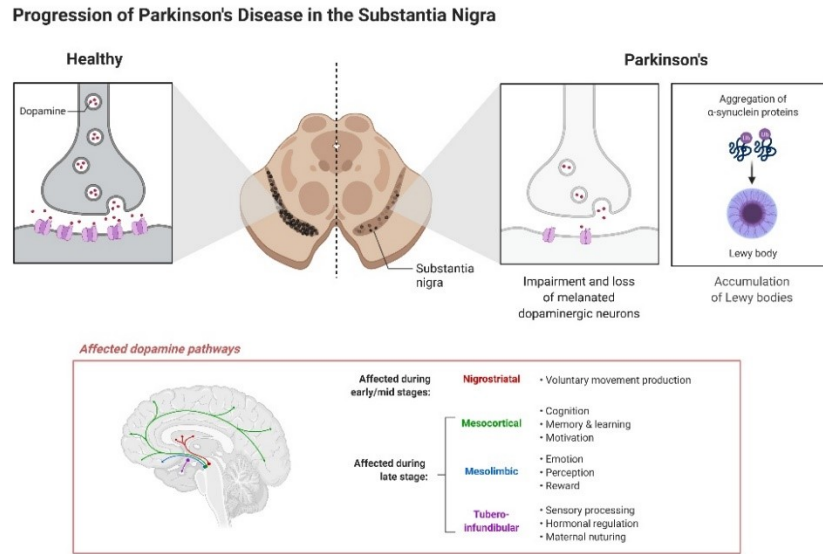


Figure 2. Pathogenesis and affected area of PD.⁹

PD is a multifactorial disorder with complex etiology. Apart from the purely hereditary "genetic" forms of PD (about 10% of total cases), in the idiopathic form the most important risk factor is aging, followed by environmental exposures and genetic susceptibility. Many reports have shown that exposure to environmental toxins is associated with an increased risk of developing PD. In fact, it has been showed that people living in rural areas are at significantly increased risk of getting PD caused by exposure to potential neurotoxins present in pesticides.¹⁰ One of the first assessments regarding the correlation between the onset of PD and exposure to environmental toxins was the observation that a byproduct of the synthesis of the narcotic meperidine, namely 1-methyl-4-phenyl-1, 2,3,6-tetrahydropyridine (MPTP), caused irreversible parkinsonism. MPTP, in fact, is highly lipophilic and easily crosses the blood brain barrier and is converted to its toxic metabolite the 1- methyl-4-phenylpyridinium (MPP⁺) in astrocytes. MPP⁺ is an excellent substrate for the dopamine transporter (DAT), which explains its selectivity for DAergic neurons., where it inhibits complex I of the mitochondrial electron transport chain. As a result, a rapid and selective loss in dopaminergic neurones occurs in the striatum and substantia nigra pars compacta (SNpc), thus resulting in a PD-

⁹ www.biorender.com, last access April 2022

¹⁰ Kline, E. M., Houser, M. C., Herrick, M. K., Seibler, P., Klein, C., West, A., & Tansey, M. G. (2021). Genetic and Environmental Factors in Parkinson's Disease Converge on Immune Function and Inflammation. *Movement disorders: official journal of the Movement Disorder Society*, 36(1), 25–36.

like disease.¹¹ Pesticide exposures have gained special focus ever since the neurotoxic MPP⁺ was first described as causing Parkinsonism in humans in the eighties. Moreover, some insecticides and pesticides causing mitochondrial dysfunction, such as Paraquat and Rotenone.

1.1.3. Mitochondrial dysfunction and PD

The pivotal role of mitochondrial dysfunction in the onset of PD has been greatly highlighted from research over the last decades. The first evidence of mitochondrial dysfunction involvement in the pathogenesis of PD emerged following the observation of a significant and specific reduction in the mitochondrial complex I activity in substantia nigra samples of PD patients.¹² Furthermore, evidence for dysfunctional mitochondrial metabolism in PD arises from studies on the effects caused by MPP⁺ on electron transport chain (ETC), suggesting that apoptosis resulting from Complex I deficiency may be related to the primary disease process (Figure 3).¹³

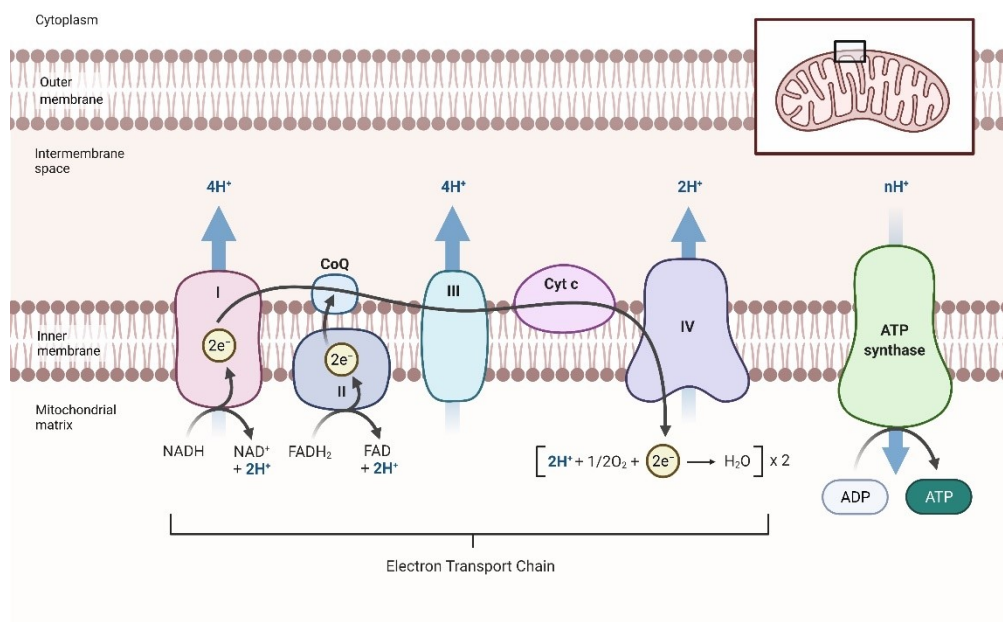


Figure 3. Primary ETC metabolic function inside the inner membrane of the mitochondrion.¹⁴

¹¹ Lickteig, B., Wimalasena, V. K., & Wimalasena, K. (2019). N-Methyl-4-phenylpyridinium Scaffold-Containing Lipophilic Compounds Are Potent Complex I Inhibitors and Selective Dopaminergic Toxins. *ACS chemical neuroscience*, 10(6), 2977–2988.

¹² Schapira AH, Cooper JM, Dexter D, Jenner P, Clark JB, Marsden CD. Mitochondrial complex I deficiency in Parkinson's disease. *Lancet*. 1989 Jun 3;1(8649):1269.

¹³ Javitch JA, D'Amato RJ, Strittmatter SM, Snyder SH. Parkinsonism-inducing neurotoxin, N-methyl-4-phenyl-1,2,3,6-tetrahydropyridine: uptake of the metabolite N-methyl-4-phenylpyridine by dopamine neurons explains selective toxicity. *Proc Natl Acad Sci U S A*. 1985 Apr;82(7):2173-7. doi: 10.1073/pnas.82.7.2173. PMID: 3872460; PMCID: PMC397515.

¹⁴ www.biorender.com, last access April 2022

In addition to the impairment of ETC, other mitochondrial alterations might be responsible for processes triggering dopaminergic neurons death. For example, the mitochondrial fission/fusion machinery contributes for the full-mitochondrial lifecycle and any pathological changes in these dynamics lead to mitochondrial fragmentation and thus neuronal death.¹⁵¹⁶ Disruption of mitochondria physiological functions can increase the generation of ROS, which promote the formation of protein aggregates¹⁷, induce DNA damage, alter autophagic flux¹⁸, and the ubiquitin proteasomal system (UPS)¹⁹. In a study conducted on post-mortem substantia nigra samples from brains with PD, several markers of oxidative stress were found to be present to a greater extent than control samples.²⁰ Furthermore, when dysfunctional, mitochondria may release more calcium into the cytosol, thereby increasing cellular excitotoxicity (Figure 4).²¹

The relevance of the altered mitochondrial function in the complex and varied phenomenon of neurodegeneration prompted us to focus on every element that can influence its functionality. Therefore, in this context it is necessary to consider the role of Cytochrome P450 and the effects of CYP-mediated oxidative metabolism on the maintenance of cellular homeostasis.

¹⁵ Chen, H., Chomyn, A., & Chan, D. C. (2005). Disruption of fusion results in mitochondrial heterogeneity and dysfunction. *The Journal of biological chemistry*, 280(28), 26185–26192.

¹⁶ Parone, P. A., Da Cruz, S., Tondera, D., Mattenberger, Y., James, D. I., Maechler, P., Barja, F., & Martinou, J. C. (2008). Preventing mitochondrial fission impairs mitochondrial function and leads to loss of mitochondrial DNA. *PLoS one*, 3(9), e3257.

¹⁷ Rocha, E. M., De Miranda, B., & Sanders, L. H. (2018). Alpha-synuclein: Pathology, mitochondrial dysfunction and neuroinflammation in Parkinson's disease. *Neurobiology of disease*, 109(Pt B), 249–257.

¹⁸ Arduíno, D. M., Esteves, A. R., & Cardoso, S. M. (2013). Mitochondria drive autophagy pathology via microtubule disassembly: a new hypothesis for Parkinson disease. *Autophagy*, 9(1), 112–114.

¹⁹ Bragoszewski, P., Turek, M., & Chacinska, A. (2017). Control of mitochondrial biogenesis and function by the ubiquitin-proteasome system. *Open biology*, 7(4), 170007.

²⁰ Yoritaka, A., Hattori, N., Uchida, K., Tanaka, M., Stadtman, E. R., & Mizuno, Y. (1996). Immunohistochemical detection of 4-hydroxynonenal protein adducts in Parkinson disease. *Proceedings of the National Academy of Sciences of the United States of America*, 93(7), 2696–2701.

²¹ Sheehan, J. P., Swerdlow, R. H., Parker, W. D., Miller, S. W., Davis, R. E., & Tuttle, J. B. (1997). Altered calcium homeostasis in cells transformed by mitochondria from individuals with Parkinson's disease. *Journal of neurochemistry*, 68(3), 1221–1233.

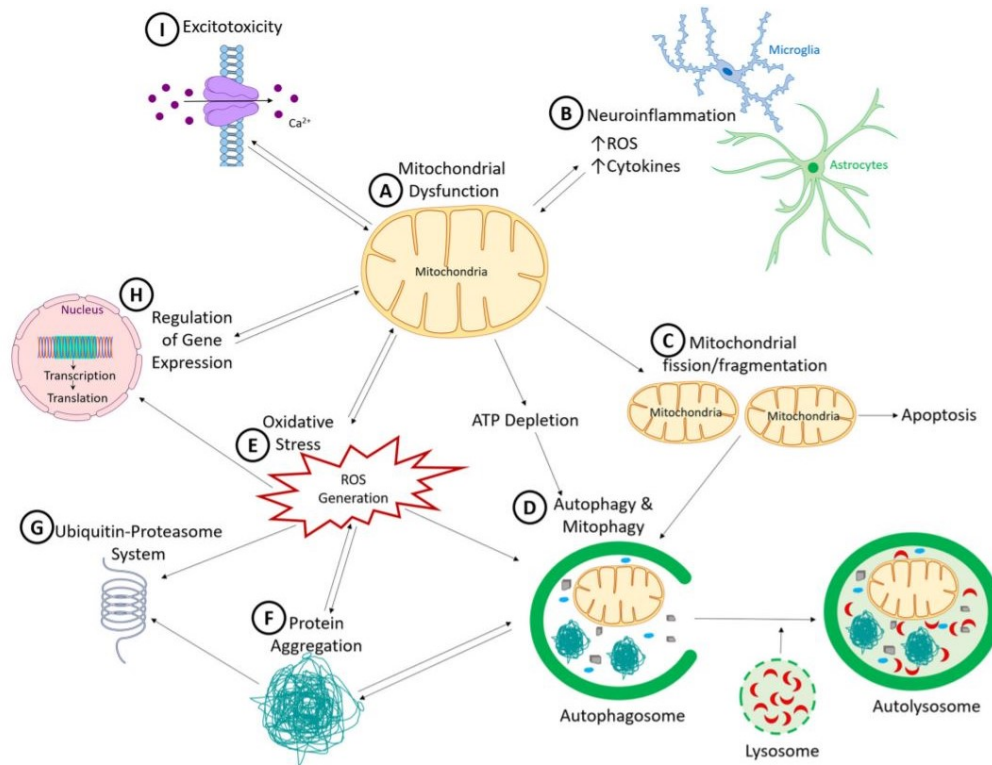


Figure 4. Crosstalk between pathogenic mechanisms in neurodegenerative diseases: (A) mitochondrial dysfunction, (B) neuroinflammation, (C) disruption of mitochondrial dynamics, (D) altered autophagy, (E) oxidative stress, (F) abnormal protein aggregation, (G) impairment of UPS, (H) altered regulation of gene expression, (I) excitotoxicity.²²

1.2. Cytochrome P450

The cytochrome P450 (CYP) family is a heterogeneous superfamily of hemoproteins, present in all living organisms, belonging to a known class of enzymes called mixed-function oxidase or monooxygenase. These hemoproteins contain a prosthetic group, a heme group, an iron-protoporphyrin IX. Iron can form six coordination bonds, two with axial ligands and four with the nitrogen atoms of the porphyrin ring. The two axial bonds are named proximal and distal, respectively. The first is established with the sulfhydryl group of a cysteine residue of the carboxy-terminal end of the cytochrome P450 itself, while the other is a variable bond that can be occupied by various ligands during the catalytic cycle of CYP (Figure 5). CYP450 represent the main group of enzymes of phase I metabolism. They are in fact involved in the oxidative biotransformation of both

²² Helley, M. P., Pinnell, J., Sportelli, C., & Tieu, K. (2017). Mitochondria: A Common Target for Genetic Mutations and Environmental Toxicants in Parkinson's Disease. *Frontiers in genetics*, 8, 177. 7

endogenous (hormones, fatty acids, neurotransmitters) and exogenous (drugs, environmental chemicals) compounds.

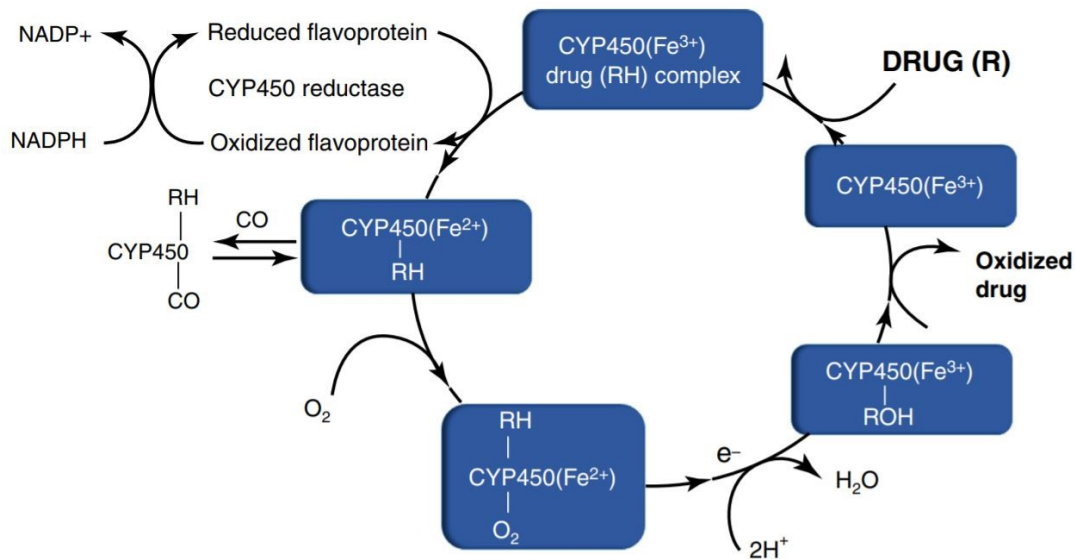


Figure 5. CYP450 catalytic cycle. Cytochrome P450 enzymes chemically oxidize or reduce drugs using a reactive heme ring, with an iron atom as the ultimate electron acceptor or donor, and NADPH as a necessary co-factor²³

The main types of reactions catalysed by CYP are C-Oxidation (hydroxylation, epoxydation, peroxydation), N-oxidation and S-oxidation as well as oxidative O-, S-, and N-dealkylation. The nomenclature used to classify the CYP isoforms is based on a common identifier "CYP", then each CYP family member is designated by a number, each subfamily by a letter and each member of the subfamily by a second number (Figure 6). Each isoform acts on a specific substrate pool.

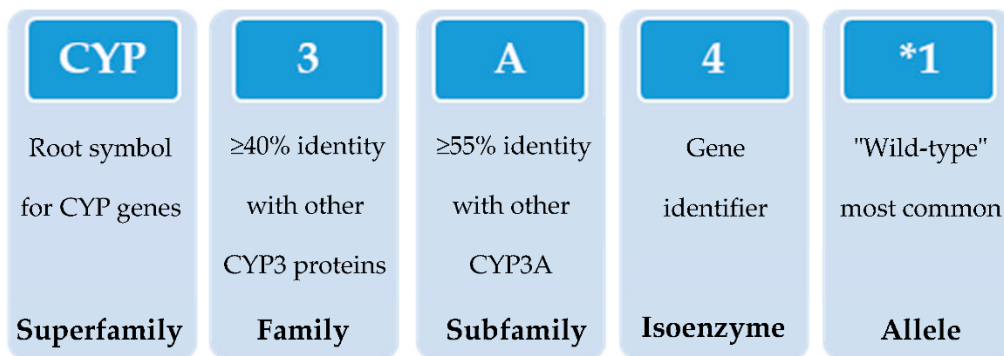


Figure 6. Schematic representation of the nomenclature system of CYP genes.

²³ Ghosh, C., Hossain, M., Solanki, J., Dadas, A., Marchi, N., & Janigro, D. (2016). Pathophysiological implications of neurovascular P450 in brain disorders. *Drug discovery today*, 21(10), 1609–1619.

Cytochromes P450 are expressed in almost all tissues, with particularly high levels in barrier organs such as lungs, gastrointestinal tract, kidneys, central nervous system, and especially in the liver. At the cellular level, CYP enzymes are mainly part of the microsomal system, that is, the set of vesicles linked to the smooth endoplasmic reticulum; they are then found in the mitochondrial membrane, in lysosomes and in the nucleus.

1.2.1. The CYP in the brain

The regulatory function performed by CYP in the brain is increasing the subject of neuroscientific research. Brain CYP isoforms are generated through alternative splicing²⁴ and distributed with a diverse pattern compared to the liver, resulting in different biotransformation of drugs in the CNS. The main subfamilies identified are CYP1A, CYP1B, CYP2B, CYP2C, CYP2D, CYP2E and CYP2J (Figure 7).

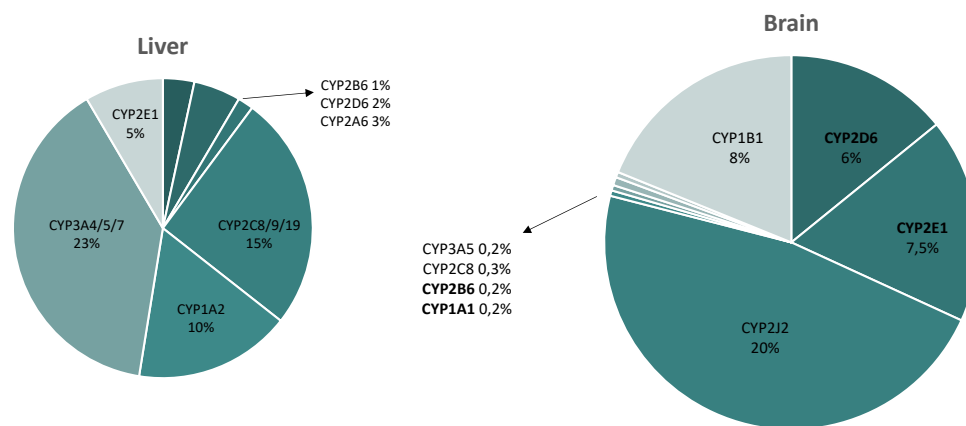


Figure 7. CYPs expression in liver and brain.²⁵

In recent years, new studies have been conducted on their activity, which show how local brain CYP-mediated metabolism can significantly influence the central effects of a substance or the onset of

²⁴ Turman, C. M., Hatley, J. M., Ryder, D. J., Ravindranath, V., & Strobel, H. W. (2006). Alternative splicing within the human cytochrome P450 superfamily with an emphasis on the brain: The convolution continues. *Expert opinion on drug metabolism & toxicology*, 2(3), 399–418.

²⁵ Stingl, J. C., Brockmüller, J., & Viviani, R. (2013). Genetic variability of drug-metabolizing enzymes: the dual impact on psychiatric therapy and regulation of brain function. *Molecular psychiatry*, 18(3), 273–287.

diseases²⁶. Although the expression is relatively low compared to the liver²⁷ and the CYP-dependent metabolism is unlikely to contribute to the overall clearance of xenobiotics, their function can be of relevance on a local level. Brain CYPs may play a role in modulating brain activity, behaviour, susceptibility to CNS diseases and treatment outcomes. Moreover, individual differences in brain CYP metabolism, due to inducers, inhibitors, or genetic variation, can influence sensitivity and response to centrally acting drugs.²⁸ This is due to several factors: the localization of brain CYPs to specific regions and cell types allows for a potentially considerable impact on metabolism in certain brain microenvironments and the brain as a whole. The levels of CYPs in specific neurons may be comparable to, or even higher than levels in hepatocytes.²⁹

The tissue-specific expression of CYP also occurs at the subcellular level. Several studies have shown that, in the CNS, the drug-metabolizing enzymes (DME) CYP isoforms activity has been found primarily in the mitochondrial subcellular fraction, while the liver CYP are active mainly in the endoplasmic reticulum or microsomal fraction (human³⁰, monkey³¹ and rat).

Similarly to the liver, human brain CYP are responsive to foreign chemicals and can be induced. The induction of many CYP occurs by the ligand activation of key receptor transcription factors including pregnane X receptor (PXR), constitutive androstane receptor (CAR) and aryl hydrocarbon receptor (AhR) that leads to increased transcription. An alternative mechanism of CYP induction involves compounds that stabilize translation or inhibit the protein degradation pathway, as in the case of ethanol which can induce the CYP2E1 isoform³².

²⁶ Miksys, S., & Tyndale, R. F. (2013). Cytochrome P450-mediated drug metabolism in the brain. *Journal of psychiatry & neuroscience: JPN*, 38(3), 152–163.

²⁷ Stamou, M., Wu, X., Kania-Korwel, I., Lehmler, H. J., & Lein, P. J. (2014). Cytochrome p450 mRNA expression in the rodent brain: species-, sex-, and region-dependent differences. *Drug metabolism and disposition: the biological fate of chemicals*, 42(2), 239–244.

²⁸ McMillan, D. M., & Tyndale, R. F. (2018). CYP-mediated drug metabolism in the brain impacts drug response. *Pharmacology & therapeutics*, 184, 189–200.

²⁹ Ferguson, C. S., & Tyndale, R. F. (2011). Cytochrome P450 enzymes in the brain: emerging evidence of biological significance. *Trends in pharmacological sciences*, 32(12), 708–714.

³⁰ Gherzi-Egea, J. F., Perrin, R., Leininger-Muller, B., Grassiot, M. C., Jeandel, C., Floquet, J., Cuny, G., Siest, G., & Minn, A. (1993). Subcellular localization of cytochrome P450, and activities of several enzymes responsible for drug metabolism in the human brain. *Biochemical pharmacology*, 45(3), 647–658.

³¹ Iscan, M., Reuhl, K., Weiss, B., & Maines, M. D. (1990). Regional and subcellular distribution of cytochrome P-450-dependent drug metabolism in monkey brain: the olfactory bulb and the mitochondrial fraction have high levels of activity. *Biochemical and biophysical research communications*, 169(3), 858–863.

³² Woodcroft, K. J., & Novak, R. F. (1998). Xenobiotic-enhanced expression of cytochromes P450 2E1 and 2B in primary cultured rat hepatocytes. *Drug metabolism and disposition: the biological fate of chemicals*, 26(4), 372–378.

1.2.2. CYP1A1

The Cytochrome P4501A (CYP1A) subfamily has been the object of attention in toxicological research for its metabolic function towards exogenous and endogenous compounds. CYP1A2 is predominantly a form expressed in the liver, while CYP1A1 exhibits more marked expression in extrahepatic tissues³³ such as the respiratory system (trachea and lungs), and to lesser extent in the liver, adrenal gland, bladder, heart, kidney, ovary, placenta, prostate, testicle, thyroid, salivary gland, spleen, and brain³⁴.

As mentioned above, the hepatic and extrahepatic expression of CYP1A subfamily can be induced by many substrates by multiple pathways, the most important known to occur at the transcription level mediated by the cytosolic aryl hydrocarbon receptor (AhR)³⁵. Moreover, CYP1A isoforms can be induced by the CAR³⁶ and peroxisome proliferator-activated receptor α (PPAR α) (Figure 8)³⁷.

³³ Guengerich F. P. (1992). Characterization of human cytochrome P450 enzymes. *FASEB journal: official publication of the Federation of American Societies for Experimental Biology*, 6(2), 745–748.

³⁴ Choudhary, D., Jansson, I., Stoilov, I., Sarfarazi, M., & Schenkman, J. B. (2005). Expression patterns of mouse and human CYP orthologs (families 1-4) during development and in different adult tissues. *Archives of biochemistry and biophysics*, 436(1), 50–61.

³⁵ Ye, W., Chen, R., Chen, X., Huang, B., Lin, R., Xie, X., Chen, J., Jiang, J., Deng, Y., & Wen, J. (2019). AhR regulates the expression of human cytochrome P450 1A1 (CYP1A1) by recruiting Sp1. *The FEBS journal*, 286(21), 4215–4231.

³⁶ Yoshinari, K., Yoda, N., Toriyabe, T., & Yamazoe, Y. (2010). Constitutive androstane receptor transcriptionally activates human CYP1A1 and CYP1A2 genes through a common regulatory element in the 5'-flanking region. *Biochemical pharmacology*, 79(2), 261–269.

³⁷ Séréé, E., Villard, P. H., Pascussi, J. M., Pineau, T., Maurel, P., Nguyen, Q. B., Fallone, F., Martin, P. M., Champion, S., Lacarelle, B., Savouret, J. F., & Barra, Y. (2004). Evidence for a new human CYP1A1 regulation pathway involving PPAR- α and 2 PPRE sites. *Gastroenterology*, 127(5), 1436–1445.

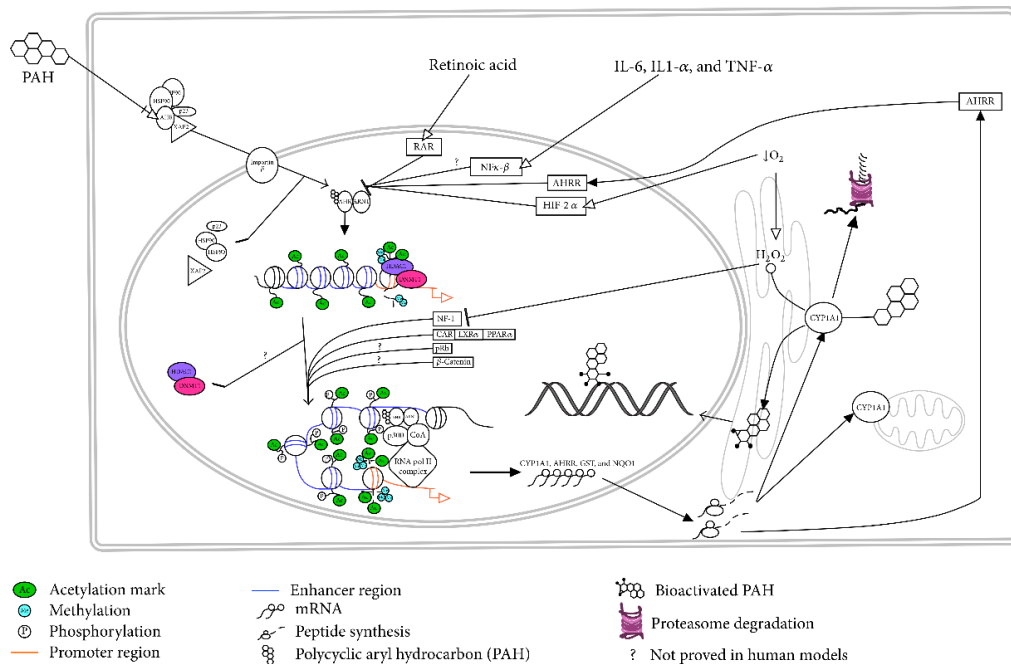


Figure 8. Mechanisms involved in the CYP1A1 regulation.³⁸

The presence of this isoform in several areas of human brain (detected in cerebellum; midbrain; basal ganglia; frontal cortex; and temporal cortex³⁹) suggest an important CYP1A1 local metabolic involvement of CYP1A1. In fact, this enzyme appears to be involved in the local CNS metabolism of fatty acids⁴⁰, necessary for neuronal outgrowth and maintenance, activation of procarcinogenic xenobiotics such as polycyclic aromatic hydrocarbons and other environmental compounds.

1.2.3. CYP2D6

Among all known isoforms of the human CYP2C subfamily, CYP2D6 stands out as the most relevant element for neuroscientific research. CYP2D6 is involved in the biotransformation of many substrates endogenous (dopamine and tyramine⁴¹) several drugs and various neurotoxic compounds. Furthermore, the CYP2D6 locus exhibits a high degree of genetic polymorphism that clearly has been

³⁸ Santes-Palacios, R., Ornelas-Ayala, D., Cabañas, N., Marroquín-Pérez, A., Hernández-Magaña, A., Del Rosario Olguín-Reyes, S., Camacho-Carranza, R., & Espinosa-Aguirre, J. J. (2016). Regulation of Human Cytochrome P4501A1 (hCYP1A1): A Plausible Target for Chemoprevention? *BioMed research international*, 2016, 5341081

³⁹ McFadyen, M., Melvin, W. T., & Murray, G. I. (1998). Regional distribution of individual forms of cytochrome P450 mRNA in normal adult human brain. *Biochemical pharmacology*, 55(6), 825–830.

⁴⁰ Schwarz, D., Kisselev, P., Ericksen, S. S., Szklarz, G. D., Chernogolov, A., Honeck, H., Schunck, W. H., & Roots, I. (2004). Arachidonic and eicosapentaenoic acid metabolism by human CYP1A1: highly stereoselective formation of 17(R),18(S)-epoxyeicosatetraenoic acid. *Biochemical pharmacology*, 67(8), 1445–1457.

⁴¹ Hiroi, T., Imaoka, S., & Funae, Y. (1998). Dopamine formation from tyramine by CYP2D6. *Biochemical and biophysical research communications*, 249(3), 838–843.

linked to the variable pharmacological response to a variety of analgesic⁴², cardiovascular, and antidepressant drugs⁴³.

It is expressed in the liver, intestinal tissue, lymphoid cells, lungs⁴⁴ and markedly in the brain⁴⁵. CYP2D6 in fact has been identified by *in situ* hybridization in neurons located within the substantia nigra, the area of midbrain as well as in pyramidal cells in neocortex and hippocampus.⁴⁶

Its importance in the CNS, and for PD, consists in being among the main DME isoforms expressed and in its recognized role as the enzyme responsible for the metabolic inactivation of neurotoxins. Results from several studies suggested that brain CYP2D6 may play an important role in neuroprotection and that interindividual variation in the expression of this enzyme can alter the risk of developing idiopathic form of PD. Indeed, people who have genetically lower CYP2D6 activity may have a reduced ability to inactivate the PD-causing neurotoxins.^{47,48}

1.2.4. CYP2E1

CYP2E1 is a member of the cytochrome P450-dependent monooxygenase superfamily, which has been extensively studied for its relevance in the related oxidative metabolism of chemical compounds. At the CNS level, this isoform is largely distributed in brain regions; CYP2E1 mRNA was detected in cortex, cerebellum, basal ganglia, hippocampus, substantia nigra and medulla oblongata with an extremely variable expression pattern.

Similar to CYP2D6, CYP2E1 has also been related to polymorphisms, which appears to have important role in cancer and drug metabolism. In the CNS this isoform is involved in the metabolism of several

⁴² Flores, C. M., & Mogil, J. S. (2001). The pharmacogenetics of analgesia: toward a genetically based approach to pain management. *Pharmacogenomics*, 2(3), 177–194.

⁴³ Eichelbaum, M., Kroemer, H. K., & Fromm, M. F. (1997). Impact of P450 genetic polymorphism on the first-pass extraction of cardiovascular and neuroactive drugs. *Advanced drug delivery reviews*, 27(2-3), 171–199.

⁴⁴ Guidice, J. M., Marez, D., Sabbagh, N., Legrand-Andreolletti, M., Spire, C., Alcaïde, E., Lafitte, J. J., & Broly, F. (1997). Evidence for CYP2D6 expression in human lung. *Biochemical and biophysical research communications*, 241(1), 79–85.

⁴⁵ McFadyen, M., Melvin, W. T., & Murray, G. I. (1998). Regional distribution of individual forms of cytochrome P450 mRNA in normal adult human brain. *Biochemical pharmacology*, 55(6), 825–830.

⁴⁶ Siegle, I., Fritz, P., Eckhardt, K., Zanger, U. M., & Eichelbaum, M. (2001). Cellular localization and regional distribution of CYP2D6 mRNA and protein expression in human brain. *Pharmacogenetics*, 11(3), 237–245.

⁴⁷ Mann, A., Miksys, S. L., Gaedigk, A., Kish, S. J., Mash, D. C., & Tyndale, R. F. (2012). The neuroprotective enzyme CYP2D6 increases in the brain with age and is lower in Parkinson's disease patients. *Neurobiology of aging*, 33(9), 2160–2171. 4

⁴⁸ Lu, Y., Peng, Q., Zeng, Z., Wang, J., Deng, Y., Xie, L., Mo, C., Zeng, J., Qin, X., & Li, S. (2014). CYP2D6 phenotypes and Parkinson's disease risk: a meta-analysis. *Journal of the neurological sciences*, 336(1-2), 161–168.

endogenous substrates, such as fatty acids, in the regulation of dopamine levels in the substantia nigra, and in exogenous substances, such as alcohol⁴⁹, acetaminophen and procarcinogens found in tobacco smoke (nitrosamine compounds)⁵⁰. In the brain, CYP2E1 has been found in different cell compartments, including plasma membrane, the Golgi apparatus, and the endoplasmic reticulum. However, recent studies indicate that it is also present in the mitochondrial fraction, where it promotes oxidative stress during the production of acetaldehyde.

The peculiarity of being induced in the liver by various compounds, such as alcohol and nicotine⁵¹, has led to hypothesize a similar possibility within the brain as well. In fact, CYP2E1 appears to be inducible in CNS tissue by many of its substrates by complex mechanisms involving transcriptional, translational, and posttranslational effects.⁵²

In the CNS, a distinctive feature of this isoform is the ability to metabolize and be induced by ethanol. After chronic ethanol consumption, CYP2E1 activity and expression increases, associated with proliferation of the smooth endoplasmic reticulum (SER).⁵³ Alcohol-mediated induction of CYP2E1 is not accompanied by de novo RNA and protein synthesis, suggesting that a post-transcriptional stabilization mechanism of CYP2E1 mRNA is involved.⁵⁴

⁴⁹ Howard, L. A., Miksys, S., Hoffmann, E., Mash, D., & Tyndale, R. F. (2003). Brain CYP2E1 is induced by nicotine and ethanol in rat and is higher in smokers and alcoholics. *British journal of pharmacology*, 138(7), 1376–1386.

⁵⁰ García-Suástegui, W. A., Ramos-Chávez, L. A., Rubio-Osornio, M., Calvillo-Velasco, M., Atzin-Méndez, J. A., Guevara, J., & Silva-Adaya, D. (2017). The Role of CYP2E1 in the Drug Metabolism or Bioactivation in the Brain. *Oxidative medicine and cellular longevity*, 2017, 4680732.

⁵¹ Lieber C. S. (1999). Microsomal ethanol-oxidizing system (MEOS): the first 30 years (1968-1998), a review. *Alcoholism, clinical and experimental research*, 23(6), 991–1007.

⁵² Howard, L. A., Miksys, S., Hoffmann, E., Mash, D., & Tyndale, R. F. (2003). Brain CYP2E1 is induced by nicotine and ethanol in rat and is higher in smokers and alcoholics. *British journal of pharmacology*, 138(7), 1376–1386.

⁵³ Lieber C. S. (2004). The discovery of the microsomal ethanol oxidizing system and its physiologic and pathologic role. *Drug metabolism reviews*, 36(3-4), 511–529.

⁵⁴ Novak, R. F., & Woodcroft, K. J. (2000). The alcohol-inducible form of cytochrome P450 (CYP 2E1): role in toxicology and regulation of expression. *Archives of pharmacal research*, 23(4), 267–282.

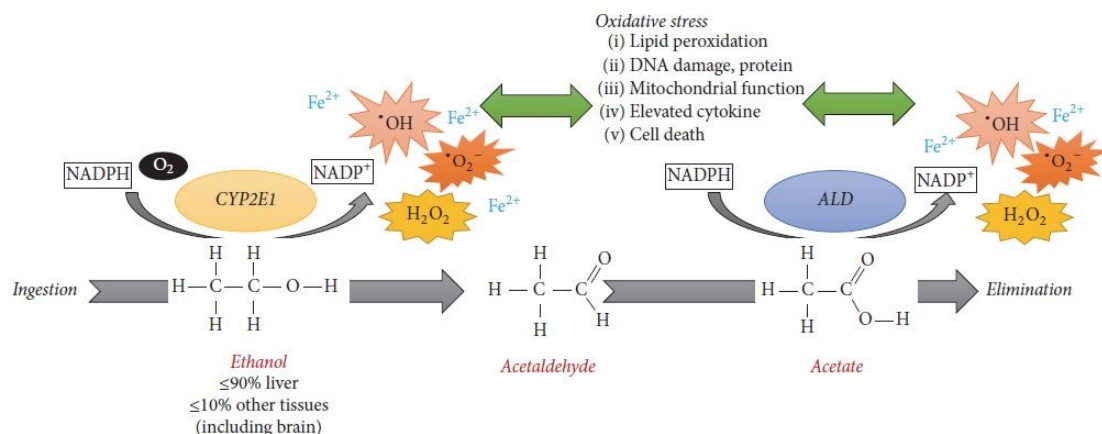


Figure 9. Oxidation process of ethanol by CYP2E1. This event causes an increase in ROS production, with consequent oxidative stress damaging the biomolecules⁵⁵

Consequent to its metabolic activity, studies in CYP2E1-null mice has demonstrated the possible role of CYP2E1 in ROS production (Figure 9). In fact, depending on the metabolized substrates, CYP2E1 can produce electrophilic compounds capable of causing cellular toxicity by reacting with cellular macromolecules of the brain tissue.

Furthermore, recent findings have reported that the brains of PD patients exhibit reduced CYP2E1 methylation resulting in increased CYP2E1 mRNA levels, suggesting that its epigenetic variability may play a role in the susceptibility to PD development.⁵⁶

1.2.5. CYP2B6

CYP2B6 is one of the less well-characterized human CYP isoforms. It was initially thought to constitute only a small percentage of the total hepatic CYP450 pool and that it plays a negligible role in drug metabolism in humans.⁵⁷ It was then proved instead that CYP2B6 is highly expressed in the liver, and

⁵⁵ García-Suástegui, W. A., Ramos-Chávez, L. A., Rubio-Osornio, M., Calvillo-Velasco, M., Atzin-Méndez, J. A., Guevara, J., & Silva-Adaya, D. (2017). The Role of CYP2E1 in the Drug Metabolism or Bioactivation in the Brain. *Oxidative medicine and cellular longevity*, 2017, 4680732.

⁵⁶ Kaut, O., Schmitt, I., & Wüllner, U. (2012). Genome-scale methylation analysis of Parkinson's disease patients' brains reveals DNA hypomethylation and increased mRNA expression of cytochrome P450 2E1. *Neurogenetics*, 13(1), 87–91.

⁵⁷ Desta, Z., El-Boraie, A., Gong, L., Somogyi, A. A., Lauschke, V. M., Dandara, C., Klein, K., Miller, N. A., Klein, T. E., Tyndale, R. F., Whirl-Carrillo, M., & Gaedigk, A. (2021). PharmVar GeneFocus: CYP2B6. *Clinical pharmacology and therapeutics*, 110(1), 82–97.

to a certain extent in the extrahepatic tissues such as brain, kidney, digestive tract and the lungs.⁵⁸ Moreover, it is fully or partially involved in the catalytic biotransformation of numerous substrates of clinical interest, such as anticancers⁵⁹, antidepressants⁶⁰, and anxiolytics⁶¹. CYP2B6 expression in the human brain has mainly been identified in the neuron and astrocytes in a regional and cell-specific manner and significantly higher levels of CYP2B6 have been observed in the brains of smokers and alcoholics⁶².

As already reported for the well-known CYP2D6 isoform, CYP2B6 expression possess interindividual variability in a range of 20- to 250-fold possibly owing to polymorphism⁶³ and transcriptional activation by inducers.

In response to xenobiotic exposure, changes in CYP2B6 protein expression and catalytic function occurs through transcriptional activation of the corresponding gene, a process mediated by a series of nuclear receptors, such as CAR (Constitutive Androstane Receptor) and the Pregnane X receptor (PXR).⁶⁴

1.2.6. CYP3A4

One of the best-known subfamilies of enzymes is CYP3A4, the predominant isoform constitutively expressed in the adult human liver. This isoform is also expressed in many extrahepatic tissues

⁵⁸ GTEx Consortium (2013). The Genotype-Tissue Expression (GTEx) project. *Nature genetics*, 45(6), 580–585.

⁵⁹ Evans, W. E., & Relling, M. V. (2004). Moving towards individualized medicine with pharmacogenomics. *Nature*, 429(6990), 464–468.

⁶⁰ Sarfo, F. S., Zhang, Y., Egan, D., Tetteh, L. A., Phillips, R., Bedu-Addo, G., Sarfo, M. A., Khoo, S., Owen, A., & Chadwick, D. R. (2014). Pharmacogenetic associations with plasma efavirenz concentrations and clinical correlates in a retrospective cohort of Ghanaian HIV-infected patients. *The Journal of antimicrobial chemotherapy*, 69(2), 491–499.

⁶¹ Bielinski, S. J., Olson, J. E., Pathak, J., Weinshilboum, R. M., Wang, L., Lyke, K. J., Ryu, E., Targonski, P. V., Van Norstrand, M. D., Hathcock, M. A., Takahashi, P. Y., McCormick, J. B., Johnson, K. J., Maschke, K. J., Rohrer Vitek, C. R., Ellingson, M. S., Wieben, E. D., Farrugia, G., Morrisette, J. A., Kruckeberg, K. J., ... Kullo, I. J. (2014). Preemptive genotyping for personalized medicine: design of the right drug, right dose, right time-using genomic data to individualize treatment protocol. *Mayo Clinic proceedings*, 89(1), 25–33.

⁶² Miksys, S., Lerman, C., Shields, P. G., Mash, D. C., & Tyndale, R. F. (2003). Smoking, alcoholism, and genetic polymorphisms alter CYP2B6 levels in human brain. *Neuropharmacology*, 45(1), 122–132.

⁶³ Zanger, U. M., Klein, K., Saussele, T., Bliedernicht, J., Hofmann, M. H., & Schwab, M. (2007). Polymorphic CYP2B6: molecular mechanisms and emerging clinical significance. *Pharmacogenomics*, 8(7), 743–759.

⁶⁴ Langmia, I. M., Just, K. S., Yamoune, S., Brockmüller, J., Masimirembwa, C., & Stingl, J. C. (2021). CYP2B6 Functional Variability in Drug Metabolism and Exposure Across Populations-Implication for Drug Safety, Dosing, and Individualized Therapy. *Frontiers in genetics*, 12, 692234.

including the intestine, kidney, lung, adrenal gland, prostate, and brain.⁶⁵ CYP3A4 activity contributes to steroid metabolism and is responsible for the majority of P450-related metabolism of all therapeutic drugs in use. The activity and behavior of this enzyme are fairly well characterized in liver and gut, but its involvement in the homeostasis of other tissues is still poorly defined.

In the CNS, CYP3A4 has been localized in mitochondrial and/or microsomal fractions in cortical neurons, pyramidal neurons of the hippocampus and reticular neurons of the midbrain⁶⁶. In different compartments of the brain, the variety of the cell type- and regio-specific expression pattern allows CYP3A4 to reach levels comparable to that found in hepatocytes. Furthermore, CYP3A4 activity is influenced by a combination of mechanisms and factors including genetic polymorphisms, induction by exogenous compounds, regulation by cytokines, hormones, and disease states in different ways respect to the liver isoforms.⁶⁷

It is well-known that nuclear hormone receptors PXR and CAR modulate both constitutive expression and induction of CYP3A in the liver.⁶⁸ The regulation of CYP in the brain is complex, with brain region- and cell-specificity for a particular inducer, and occurs by transcriptional, post-transcriptional and post-translational mechanisms.

The active site of CYP3A4 is large and flexible and can accommodate large substrates such as immunosuppressants, macrolide antibiotics, and anticancer drugs, but smaller molecules are also accepted including ifosfamide, tamoxifen, benzodiazepines, and others.⁶⁹

Although CYP3A4 does not directly promote PD, it participates in the metabolism of some therapeutic drugs used for its treatment and is involved in other CNS diseases⁷⁰

⁶⁵ Woodland, C., Huang, T. T., Gryz, E., Bendayan, R., & Fawcett, J. P. (2008). Expression, activity and regulation of CYP3A in human and rodent brain. *Drug metabolism reviews*, 40(1), 149–168.

⁶⁶ Agarwal, V., Kommaddi, R. P., Valli, K., Ryder, D., Hyde, T. M., Kleinman, J. E., Strobel, H. W., & Ravindranath, V. (2008). Drug metabolism in human brain: high levels of cytochrome P4503A43 in brain and metabolism of anti-anxiety drug alprazolam to its active metabolite. *PloS one*, 3(6), e2337.

⁶⁷ Zanger, U. M., & Schwab, M. (2013). Cytochrome P450 enzymes in drug metabolism: regulation of gene expression, enzyme activities, and impact of genetic variation. *Pharmacology & therapeutics*, 138(1), 103–141.

⁶⁸ Stanley, L. A., Horsburgh, B. C., Ross, J., Scheer, N., & Wolf, C. R. (2006). PXR and CAR: nuclear receptors which play a pivotal role in drug disposition and chemical toxicity. *Drug metabolism reviews*, 38(3), 515–597.

⁶⁹ Zanger, U. M., & Schwab, M. (2013). Cytochrome P450 enzymes in drug metabolism: regulation of gene expression, enzyme activities, and impact of genetic variation. *Pharmacology & therapeutics*, 138(1), 103–141.

⁷⁰ Agúndez, J. A., García-Martín, E., Alonso-Navarro, H., & Jiménez-Jiménez, F. J. (2013). Anti-Parkinson's disease drugs and pharmacogenetic considerations. *Expert opinion on drug metabolism & toxicology*, 9(7), 859–874.

1.3. CYP450 induction

As mentioned above, CYP450 isoforms are a major source of variability in drug pharmacokinetics and response. Expression of each CYP is multifactorially regulated in a variety of ways including genetic variation, and xenobiotic (Table 1) and endogenous (cytokines and hormones) induction and repression.⁷¹

CYP isoform	Induction	
	Liver	Brain
CYP1A1-2	Via AhR receptor activation: polycyclic aromatic hydrocarbons, β -naphthoflavone, Omeprazole, Primaquine, natural combustion products, dietary constituents, chemical manufacturing by-products Via CAR receptor activation: phenobarbital Nicotine	β -naphthoflavone, TCDD (2,3,7,8-tetrachlorodibenzo- <i>p</i> -dioxin), 3-methylcholanthrene,
CYP2B6	Via nuclear receptor CAR: phenobarbital, rifampicin, barbiturates Via PXR receptor activation: rifampicin, and barbiturates And Cyclophosphamide, Artemisinin, Carbamazepine, Efavirenz and several statins, Nicotine	phenobarbital
CYP2D6	smoking, ethanol	Testosterone/ ethanol nicotine
CYP2E1	Ethanol, acetone, Isoniazid, pyrazole	Nicotine, ethanol, acetone
CYP3A4	Via PXR and CAR receptors: g barbiturates, Rifampicin, statins, Amprenavir, Carbamazepine, Dexamethasone, Efavirenz, Ginkgo biloba	Anti-epileptic drugs, Cyclophosphamide

Table 1. CYPs modulation by natural/synthetic agents in the liver and the brain.⁷²⁷³⁷⁴⁷⁵⁷⁶⁷⁷⁷⁸⁷⁹

⁷¹ Zanger, U. M., & Schwab, M. (2013). Cytochrome P450 enzymes in drug metabolism: regulation of gene expression, enzyme activities, and impact of genetic variation. *Pharmacology & therapeutics*, 138(1), 103–141.

⁷² Tukey, R. H., Hannah, R. R., Negishi, M., Nebert, D. W., & Eisen, H. J. (1982). The Ah locus: correlation of intranuclear appearance of inducer-receptor complex with induction of cytochrome P1-450 mRNA. *Cell*, 31(1), 275–284.

⁷³ Chen, Y. Y., & Chan, K. M. (2018). Modulations of TCDD-mediated induction of zebrafish cyp1a1 and the AHR pathway by administering Cd²⁺ in vivo. *Chemosphere*, 210, 577–587

⁷⁴ Zanger, U. M., & Schwab, M. (2013). Cytochrome P450 enzymes in drug metabolism: regulation of gene expression, enzyme activities, and impact of genetic variation. *Pharmacology & therapeutics*, 138(1), 103–141.

⁷⁵ Navarro-Mabarak, C., Camacho-Carranza, R., & Espinosa-Aguirre, J. J. (2018). Cytochrome P450 in the central nervous system as a therapeutic target in neurodegenerative diseases. *Drug metabolism reviews*, 50(2), 95–108.

⁷⁶ Howard, L. A., Miksys, S., Hoffmann, E., Mash, D., & Tyndale, R. F. (2003). Brain CYP2E1 is induced by nicotine and ethanol in rat and is higher in smokers and alcoholics. *British journal of pharmacology*, 138(7), 1376–1386.

⁷⁷ Schilter, B., Andersen, M. R., Acharya, C., & Omiecinski, C. J. (2000). Activation of cytochrome P450 gene expression in the rat brain by phenobarbital-like inducers. *The Journal of pharmacology and experimental therapeutics*, 294(3), 916–922.

⁷⁸ Sánchez-Catalán, M. J., Hipólito, L., Guerri, C., Granero, L., & Polache, A. (2008). Distribution and differential induction of CYP2E1 by ethanol and acetone in the mesocorticolimbic system of rat. *Alcohol and alcoholism (Oxford, Oxfordshire)*, 43(4), 401–407.

⁷⁹ Tripathi, V. K., Kumar, V., Pandey, A., Vatsa, P., Dhasmana, A., Singh, R. P., Appikonda, S., Hwang, I., & Lohani, M. (2017). Monocrotophos Induces the Expression of Xenobiotic Metabolizing Cytochrome P450s (CYP2C8 and CYP3A4) and Neurotoxicity in Human Brain Cells. *Molecular neurobiology*, 54(5), 3633–3651.

CYP-mediated drug metabolism occurs predominantly in the liver, but the role of CYP oxidative metabolism within the brain has emerged as another source responsible of drug response.

CYPs in the brain appear to be especially sensitive to induction following xenobiotic exposure. Furthermore, cerebral CYP activity appears to be differently regulated in comparison to the corresponding hepatic isoforms (e.g. in monkeys, phenobarbital is able to increase CYP2B expression in both the liver and brain, but increases CYP2E expression only in the brain⁸⁰⁸¹). Numerous exogenous compounds are responsible for the induction of brain CYP isoforms expression (table x), so a further understanding of their functional significance may be valuable in developing more effective approaches to treat and prevent CNS diseases and to improve drug development.

1.3.1. β -naphthoflavone

β -naphthoflavone is a polyaromatic hydrocarbon known to be a CYP450 inducer, acting as an agonist on the AhR⁸²(Figure 10). The AhR is a transcription factor that resides in its inactivated state in the cytoplasm, where it forms a complex with different chaperone proteins HSP90, XAP2 and p23. After a ligand is bound, the complex translocates into the nucleus, leading to AHR/ARNT (AhR Receptor Nuclear Translocation) heterodimer formation. This heterodimer modulates the expression of targets by binding to xenobiotic responsive elements (XRE). Activated AhR induces the cytochromes of the 1-P450 family (1A1, 1A2, 1B1).⁸³

The effect of β NF through the AhR receptor activation is well documented in the liver, as the β NF intraperitoneal injection caused a strong induction response of monooxygenase activities associated with CYP1A, and increased expression of the CYP1A-like protein and mRNA in microsomes of the heart and kidneys.⁸⁴

⁸⁰ Lee, A. M., Joshi, M., Yue, J., & Tyndale, R. F. (2006). Phenobarbital induces monkey brain CYP2E1 protein but not hepatic CYP2E1, in vitro or in vivo chlorzoxazone metabolism. *European journal of pharmacology*, 552(1-3), 151–158.

⁸¹ Lee, A. M., Miksys, S., Palmour, R., & Tyndale, R. F. (2006). CYP2B6 is expressed in African Green monkey brain and is induced by chronic nicotine treatment. *Neuropharmacology*, 50(4), 441–450.

⁸² Chirulli, V., Marvasi, L., Zaghini, A., Fiorio, R., Longo, V., & Gervasi, P. G. (2007). Inducibility of AhR-regulated CYP genes by beta-naphthoflavone in the liver, lung, kidney and heart of the pig. *Toxicology*, 240(1-2), 25–37.

⁸³ Brauze, D., Fijalkiewicz, K., Szaumkessel, M., Kiwerska, K., Bednarek, K., Rydzanicz, M., Richter, J., Grenman, R., & Jarmuz-Szymczak, M. (2014). Diversified expression of aryl hydrocarbon receptor dependent genes in human laryngeal squamous cell carcinoma cell lines treated with β -naphthoflavone. *Toxicology letters*, 231(1), 99–107.

⁸⁴ Pretti, C., Salvetti, A., Longo, V., Giorgi, M., & Gervasi, P. G. (2001). Effects of beta-naphthoflavone on the cytochrome P450 system, and phase II enzymes in gilthead seabream (*Sparus aurata*). *Comparative biochemistry and physiology. Toxicology & pharmacology: CBP*, 130(1), 133–144.

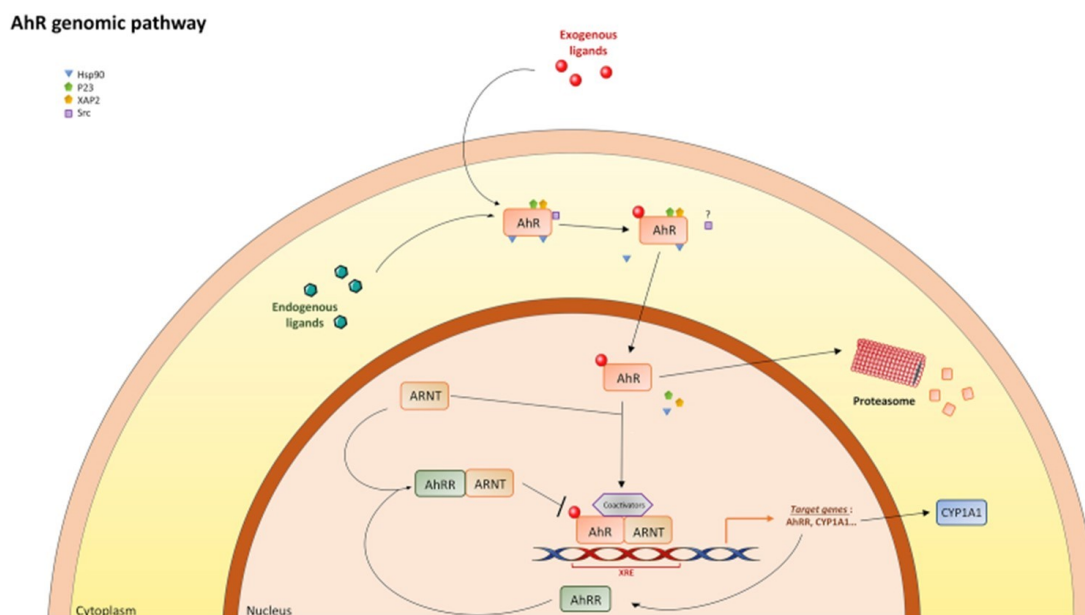


Figure 10. Agonist-mediated activation of the AHR.⁸⁵

Furthermore, many studies on animal models (pig⁸⁶, juvenile lake trout⁸⁷ and primary culture of rat hepatocytes⁸⁸) have demonstrated the induction of CYP1A1 and CYP1A2 in the CNS after treatment with β NF. Given these premises, it is therefore necessary to analyze the direct consequences of this increased activity of cytochromial enzymes on the homeostasis of the tissues involved. Studies on mouse have shown that β NF can protect against hyperoxic lung damage, highlighting an inverse correlation between lung and hepatic CYP1A expression and the extent of the damage, thus supporting the hypothesis that the CYP1A enzyme plays a protective role.⁸⁹

Moreover, the pretreatment with β NF and cigarette smoke exert neuroprotective effects in response to toxicity promoted by MPTP in mice owing to the CYP induction elicited by β NF⁹⁰.

⁸⁵Larigot, L., Juricek, L., Dairou, J., & Coumoul, X. (2018). AhR signaling pathways and regulatory functions. *Biochimie open*, 7, 1–9.

⁸⁶Nannelli, A., Rossignolo, F., Tolando, R., Rossato, P., Longo, V., & Gervasi, P. G. (2009). Effect of beta-naphthoflavone on AhR-regulated genes (CYP1A1, 1A2, 1B1, 2S1, Nrf2, and GST) and antioxidant enzymes in various brain regions of pig. *Toxicology*, 265(3), 69–79.

⁸⁷Chung-Davidson, Y. W., Rees, C. B., Wu, H., Yun, S. S., & Li, W. (2004). beta-naphthoflavone induction of CYP1A in brain of juvenile lake trout (*Salvelinus namaycush* Walbaum). *The Journal of experimental biology*, 207(Pt 9), 1533–1542. 9

⁸⁸Lněničková, K., Skálová, L., Stuchlíková, L., Szoťáková, B., & Matoušková, P. (2018). Induction of xenobiotic-metabolizing enzymes in hepatocytes by beta-naphthoflavone: Time-dependent changes in activities, protein and mRNA levels. *Acta pharmaceutica (Zagreb, Croatia)*, 68(1), 75–85.

⁸⁹Sinha, A., Muthiah, K., Jiang, W., Couroucli, X., Barrios, R., & Moorthy, B. (2005). Attenuation of hyperoxic lung injury by the CYP1A inducer beta-naphthoflavone. *Toxicological sciences: an official journal of the Society of Toxicology*, 87(1), 204–212.

⁹⁰Shahi, G. S., Das, N. P., & Mochhala, S. M. (1991). 1-Methyl-4-phenyl-1,2,3,6-tetrahydropyridine-induced neurotoxicity: partial protection against striato-nigral dopamine depletion in C57BL/6J mice by cigarette smoke exposure and by beta-naphthoflavone-pretreatment. *Neuroscience letters*, 127(2), 247–250.

1.3.2. Ethanol

Ethanol (EtOH) is a linear alkyl chain alcohol with known CNS effects. It was found to be a substrate and a potent inducer of the CYP2E1 isoform in rat brains, being specific by region and cell type (frontal cortex, olfactory bulb, hippocampus, and cerebellum)⁹¹. Specifically, the ethanol-mediated induction of CYP2E1 can be initiated through signaling pathways p38 and ERK1 / 2 and through the PKC / JNK / SP1 signaling pathway.⁹² In brains of African green monkeys EtOH produced a dose-dependent increase in CYP2D levels without modifying hepatic levels of the same isoform, suggesting organ, regio and cell-specific activity (in the absence of transcriptional mechanisms).⁹³

Furthermore, a correlation between the levels of mRNA and CYP2D6 was demonstrated in alcoholics patients brain regions susceptible to alcoholic damage (e.g., Purkinje cells, cerebellum, and pyramidal cells of the hippocampus).⁹⁴

1.3. Neurotoxins

The triggers for dysfunctional mechanisms in sporadic PD are only just beginning to be elucidated. As discussed above, several epidemiologic studies underlined the possible role of chronic exposure to environmental dopaminergic toxins in the loss of SNpc dopaminergic neurons and the risk of developing PD^{95,96} and highlighted their potential involvement in modulating neuronal toxicity and the onset of neurodegenerative disease.⁹⁷ Despite the complexities due to the multifactorial neurodegenerative mechanism in PD and the extent of gene-environment interactions, the results of

⁹¹ Howard, L. A., Miksys, S., Hoffmann, E., Mash, D., & Tyndale, R. F. (2003). Brain CYP2E1 is induced by nicotine and ethanol in rat and is higher in smokers and alcoholics. *British journal of pharmacology*, 138(7), 1376–1386.

⁹² Na, S., Li, J., Zhang, H., Li, Y., Yang, Z., Zhong, Y., Dong, G., Yang, J., & Yue, J. (2017). The induction of cytochrome P450 2E1 by ethanol leads to the loss of synaptic proteins via PPAR α down-regulation. *Toxicology*, 385, 18–27.

⁹³ Miller, R. T., Miksys, S., Hoffmann, E., & Tyndale, R. F. (2014). Ethanol self-administration and nicotine treatment increase brain levels of CYP2D in African green monkeys. *British journal of pharmacology*, 171(12), 3077–3088.

⁹⁴ Miksys, S., Rao, Y., Hoffmann, E., Mash, D. C., & Tyndale, R. F. (2002). Regional and cellular expression of CYP2D6 in human brain: higher levels in alcoholics. *Journal of neurochemistry*, 82(6), 1376–1387. x

⁹⁵ McCormack, A. L., Thiruchelvam, M., Manning-Bog, A. B., Thiffault, C., Langston, J. W., Cory-Slechta, D. A., & Di Monte, D. A. (2002). Environmental risk factors and Parkinson's disease: selective degeneration of nigral dopaminergic neurons caused by the herbicide paraquat. *Neurobiology of disease*, 10(2), 119–127.

⁹⁶ Sherer, T. B., Kim, J. H., Betarbet, R., & Greenamyre, J. T. (2003). Subcutaneous rotenone exposure causes highly selective dopaminergic degeneration and alpha-synuclein aggregation. *Experimental neurology*, 179(1), 9–16.

⁹⁷ Ferguson, C. S., & Tyndale, R. F. (2011). Cytochrome P450 enzymes in the brain: emerging evidence of biological significance. *Trends in pharmacological sciences*, 32(12), 708–714.

studies on environmental factors can have far-reaching implications, including the development of preventive strategies that could identify people at risk and limit the exposure to harmful agents.

The most compelling evidence of environmental neurotoxic compounds as a causal source of PD was obtained in the 1980s following accidental exposure to a drug contaminated with 1-methyl-4-phenyl-1,2,3,6-tetrahydropyridine (MPTP), an inhibitor of mitochondrial complex I, that resulted in irreversible parkinsonian syndromes and has drawn attention to the pivotal role of mitochondrial impairment in the onset of PD.⁹⁸ Further characterisation of MPTP-induced parkinsonism confirmed its similarity to PD, but also pointed to important differences, such as the lack of Lewy-body pathology.⁹⁹ These differences suggest that the pathological features of PD are unlikely to be caused by a single toxic insult, but rather involve multifactorial events, such as exposure to multiple toxins, gene-toxin interactions, and age-related effects.

Metals (transition metals [eg, iron and copper] in particular), have been investigated as potential risk factors on the basis of their accumulation in the substantia nigra and their participation in harmful oxidative reactions.¹⁰⁰ Epidemiological evidence supporting a relationship between metal exposure and PD still remains inconclusive, but some of their peculiarities such as the interaction with α -synuclein that promotes fibrillation *in vitro*,¹⁰¹ and pieces of evidence on long-term exposure (e.g., lead with iron and iron with copper)¹⁰² suggest their possible involvement with the increased risk of the onset of PD pathology and related pathological mechanisms.

A considerable body of evidence epidemiologically links exposure to environmental pesticides and herbicides like rotenone and paraquat (also known to inhibit mitochondrial respiration)¹⁰³ with

⁹⁸ Langston, J. W., Ballard, P., Tetrud, J. W., & Irwin, I. (1983). Chronic Parkinsonism in humans due to a product of meperidine-analog synthesis. *Science (New York, N.Y.)*, 219(4587), 979–980. 1

⁹⁹ Langston, J. W., Forno, L. S., Tetrud, J., Reeves, A. G., Kaplan, J. A., & Karluk, D. (1999). Evidence of active nerve cell degeneration in the substantia nigra of human's years after 1-methyl-4-phenyl-1,2,3,6-tetrahydropyridine exposure. *Annals of neurology*, 46(4), 598–605.

¹⁰⁰ Dexter, D. T., Wells, F. R., Lees, A. J., Agid, F., Agid, Y., Jenner, P., & Marsden, C. D. (1989). Increased nigral iron content and alterations in other metal ions occurring in brain in Parkinson's disease. *Journal of neurochemistry*, 52(6), 1830–1836.

¹⁰¹ Uversky, V. N., Li, J., & Fink, A. L. (2001). Metal-triggered structural transformations, aggregation, and fibrillation of human alpha-synuclein. A possible molecular NK between Parkinson's disease and heavy metal exposure. *The Journal of biological chemistry*, 276(47), 44284–44296.

¹⁰² Gorell, J. M., Johnson, C. C., Rybicki, B. A., Peterson, E. L., Kortsha, G. X., Brown, G. G., & Richardson, R. J. (1997). Occupational exposures to metals as risk factors for Parkinson's disease. *Neurology*, 48(3), 650–658.

¹⁰³ Tanner, C. M., Kamel, F., Ross, G. W., Hoppin, J. A., Goldman, S. M., Korell, M., Marras, C., Bhudhikanok, G. S., Kasten, M., Chade, A. R., Comyns, K., Richards, M. B., Meng, C., Priestley, B., Fernandez, H. H., Cambi, F., Umbach, D. M., Blair, A.,

harmful effects on the nigrostriatal pathway and a high risk of PD. The results were consistent with a dose-dependent effect; in agricultural workers, risk was increased with duration of pesticide use.¹⁰⁴ New findings in studies with rotenone and paraquat emphasize that dopaminergic selective neurodegeneration may be caused by the intrinsically greater susceptibility of dopaminergic neurons to toxin-induced damage and not only from specific chemicals properties of certain xenobiotics. In particular, models based on rotenone-mediated insult suggest that dopaminergic neurons may be more vulnerable than other cell populations to the effects of complex I inhibition and oxidative stress.¹⁰⁵ The epidemiological data regarding the effect of exposure to these substances on neurodegeneration are not unequivocal, but they support the hypothesis of an intricate mechanism between the neurotoxin-mediated injury and the inter-individual genetic differences.

Based on the evidence in the literature regarding the validity of the models¹⁰⁶¹⁰⁷¹⁰⁸¹⁰⁹ and on previous projects carried out in our laboratory,¹¹⁰ the following xenobiotics were selected for this project: 1-Methyl-4-phenylpyridinium (MPP⁺) and Rotenone (Rt).

1.3.1. MPP⁺

MPP⁺ (1-methyl-4-phenylpyridinium) is the toxic metabolite resulting from the bioconversion of MPTP (1-methyl-4-phenyl-1, 2, 3, 6-tetrahydropyridine), a by-product of the chemical synthesis of a Meperidine analogue. Its use as a research tool became important in the early 1980s following the

Sandler, D. P., & Langston, J. W. (2011). Rotenone, paraquat, and Parkinson's disease. *Environmental health perspectives*, 119(6), 866–872.

¹⁰⁴ Petrovitch, H., Ross, G. W., Abbott, R. D., Sanderson, W. T., Sharp, D. S., Tanner, C. M., Masaki, K. H., Blanchette, P. L., Popper, J. S., Foley, D., Launer, L., & White, L. R. (2002). Plantation work and risk of Parkinson disease in a population-based longitudinal study. *Archives of neurology*, 59(11), 1787–1792.

¹⁰⁵ Di Monte, D. A., Lavasani, M., & Manning-Bog, A. B. (2002). Environmental factors in Parkinson's disease. *Neurotoxicology*, 23(4-5), 487–502.

¹⁰⁶ Ramalingam, M., Huh, Y. J., & Lee, Y. I. (2019). The Impairments of α -Synuclein and Mechanistic Target of Rapamycin in Rotenone-Induced SH-SY5Y Cells and Mice Model of Parkinson's Disease. *Frontiers in neuroscience*, 13, 1028.

¹⁰⁷ Park, H. J., & Kim, H. J. (2013). Inhibitory effect of nicardipine on rotenone-induced apoptosis in SH-SY5Y human neuroblastoma cells. *Molecular medicine reports*, 7(3), 941–946.

¹⁰⁸ Liu, H., Wang, J., Zhang, Q., Geng, L., Yang, Y., & Wu, N. (2020). Protective Effect of Fucoidan against MPP⁺-Induced SH-SY5Y Cells Apoptosis by Affecting the PI3K/Akt Pathway. *Marine drugs*, 18(6), 333.

¹⁰⁹ Chen, J., Sun, J., Jiang, J., & Zhou, J. (2018). Cyanidin Protects SH-SY5Y Human Neuroblastoma Cells from 1-Methyl-4-Phenylpyridinium-Induced Neurotoxicity. *Pharmacology*, 102(3-4), 126–132.

¹¹⁰ Fernandez-Abascal, J., Ripullone, M., Valeri, A., Leone, C., & Valoti, M. (2018). β -Naphthoflavone and Ethanol Induce Cytochrome P450 and Protect towards MPP⁺ Toxicity in Human Neuroblastoma SH-SY5Y Cells. *International journal of molecular sciences*, 19(11), 3369.

identification of its specific neurotoxic activity targeting dopaminergic neurons, which causes a Parkinsonian-like syndrome in humans.¹¹¹

MPTP is a very lipophilic compound, therefore it rapidly crosses the blood-brain barrier and is metabolized with two successive oxidations by MAO-B in glial cells into MPDP, which is further oxidized into the toxic metabolite MPP⁺ (Figure 11).

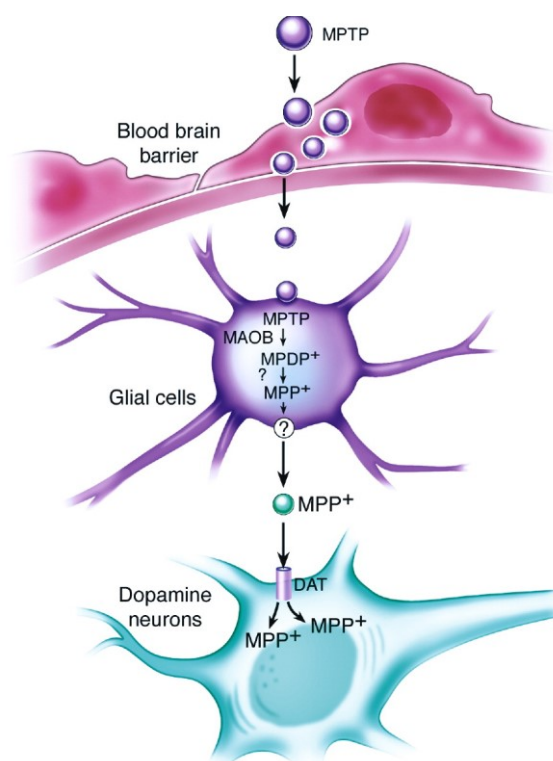


Figure 11. Metabolism of MPTP to MPP⁺ in glial cells.¹¹²

After the release in the synaptic cleft, MPP⁺ is taken up in dopaminergic neurons by the dopamine transporter (DAT). Once inside the cell, MPP⁺ is partly stored in the synaptic vesicles via the vesicular monoamine transporter VMAT2 and is accumulated in the mitochondria. At this level, the compound carries out its primary neurotoxic activity via the impairment of mitochondrial Complex I and causing accordingly a reduction in cellular adenosine triphosphate (ATP) (Figure 12).¹¹³ Moreover, MPP⁺

¹¹¹ Langston, J. W., Ballard, P., Tetrud, J. W., & Irwin, I. (1983). Chronic Parkinsonism in humans due to a product of meperidine-analog synthesis. *Science (New York, N.Y.)*, 219(4587), 979–980.

¹¹² Dauer, W., & Przedborski, S. (2003). Parkinson's disease: mechanisms and models. *Neuron*, 39(6), 889–909.

¹¹³ Nicklas, W. J., Vyas, I., & Heikkila, R. E. (1985). Inhibition of NADH-linked oxidation in brain mitochondria by 1-methyl-4-phenyl-pyridine, a metabolite of the neurotoxin, 1-methyl-4-phenyl-1,2,5,6-tetrahydropyridine. *Life sciences*, 36(26), 2503–2508.

promotes neuroinflammation through microglial activation¹¹⁴ and cause oxidative stress by producing ROS¹¹⁵.

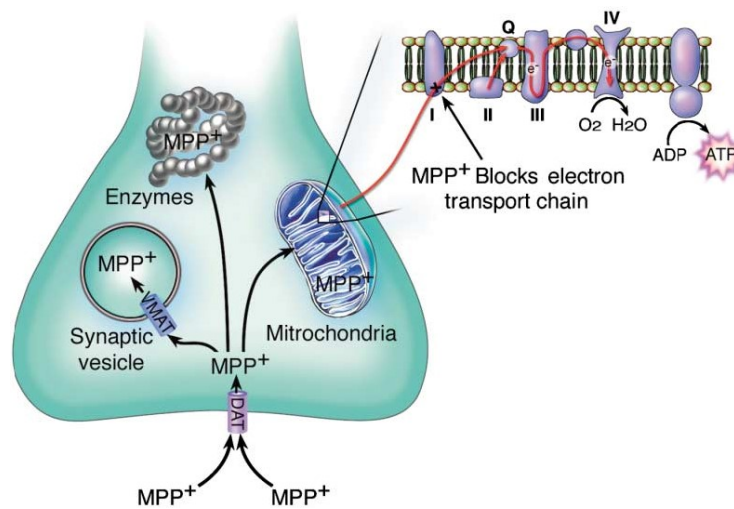


Figure 12. MPP intracellular toxicity.¹¹⁶

MPP⁺ selectively damages the brain dopaminergic pathways in a pattern like that occurring in PD, including neurodegeneration of the substantia nigra pars compacta (SNpc) and a preferential loss of neurons in the ventral and lateral segments of the SNpc^{117,118}, besides dopaminergic neurons that contain neuromelanin are more susceptible to MPTP-induced degeneration¹¹⁹.

The selective dopaminergic toxicity appears not necessarily to occur through specific uptake by DAT of MPP⁺ and related toxins. Instead, the high vulnerability of dopaminergic cells to these toxins seems to be due to their intrinsic high propensity to produce excessive ROS in response to effective

¹¹⁴ Lee, E., Hwang, I., Park, S., Hong, S., Hwang, B., Cho, Y., Son, J., & Yu, J. W. (2019). MPTP-driven NLRP3 inflammasome activation in microglia plays a central role in dopaminergic neurodegeneration. *Cell death and differentiation*, 26(2), 213–228.

¹¹⁵ Lee, H. S., Park, C. W., & Kim, Y. S. (2000). MPP(+) increases the vulnerability to oxidative stress rather than directly mediating oxidative damage in human neuroblastoma cells. *Experimental neurology*, 165(1), 164–171.

¹¹⁶ Dauer, W.T., & Przedborski, S. (2003). Parkinson's Disease Mechanisms and Models. *Neuron*, 39, 889-909.

¹¹⁷ Varastet M, Riche D, Maziere M, Hantraye P. Chronic MPTP treatment reproduces in baboons the differential vulnerability of mesencephalic dopaminergic neurons observed in Parkinson's disease. *Neuroscience*. 1994 Nov;63(1):47-56.

¹¹⁸ Sirinathsinghji DJ, Kupsch A, Mayer E, Zivin M, Pufal D, Oertel WH. Cellular localization of tyrosine hydroxylase mRNA and cholecystokinin mRNA-containing cells in the ventral mesencephalon of the common marmoset: effects of 1-methyl-4-phenyl-1,2,3,6-tetrahydropyridine. *Brain Res Mol Brain Res*. 1992 Jan;12(1-3):267-74.

¹¹⁹ Herrero MT, Hirsch EC, Kastner A, Ruberg M, Luquin MR, Laguna J, Javoy-Agud F, Obeso JA, Agud Y. Does neuromelanin contribute to the vulnerability of catecholaminergic neurons in monkeys intoxicated with MPTP? *Neuroscience*. 1993 Sep;56(2):499-511.

inhibition of complex I and associated downstream effects, compared to non-dopaminergic neurons.¹²⁰¹²¹

Therefore, the use of MPP⁺ allows researchers to investigate the molecular events that occur during the neurodegeneration of dopaminergic neurons to shed light on the pathophysiology of PD.

1.3.2. Rotenone

Rotenone is a compound with an isoflavone structure, used as a broad-spectrum insecticide and pesticide. Like MPTP, rotenone has been reported to promote highly selective toxicity on DA neurons *in vitro*. It is a lipophilic compound that easily crosses the blood-brain barrier and the phospholipid bilayer of cell membranes, accumulating inside the cell organelles. The half-life of rotenone is relatively short (>3 days) so contamination of food is an unlikely exposure route; however, epidemiological studies have demonstrated an increased risk of 1.5–3-fold of PD development in individuals who utilized rotenone in agriculture or lived in close proximity to its use.¹²² Nevertheless, the role of rotenone in the induction of PD risk is most likely through low chronic exposure rather than acute toxicity.

Rotenone is a potent selective mitochondrial complex I inhibitor, which can cause oxidative stress and lead to selective degeneration of striatal–nigral DA neurons. Once in the mitochondria, it binds with high affinity to Complex I of ETC, and thus it induces apoptosis due to disrupting membrane potential and depleting ATP¹²³ (Figure 13).

¹²⁰ Wimalasena K. (2016). The inherent high vulnerability of dopaminergic neurons toward mitochondrial toxins may contribute to the etiology of Parkinson's disease. *Neural regeneration research*, 11(2), 246–247. 0

¹²¹ Lickteig, B., Wimalasena, V. K., & Wimalasena, K. (2019). N-Methyl-4-phenylpyridinium Scaffold-Containing Lipophilic Compounds Are Potent Complex I Inhibitors and Selective Dopaminergic Toxins. *ACS chemical neuroscience*, 10(6), 2977–2988. 4

¹²² Tanner, C. M., Kamel, F., Ross, G. W., Hoppin, J. A., Goldman, S. M., Korell, M., Marras, C., Bhudhikanok, G. S., Kasten, M., Chade, A. R., Comyns, K., Richards, M. B., Meng, C., Priestley, B., Fernandez, H. H., Cambi, F., Umbach, D. M., Blair, A., Sandler, D. P., & Langston, J. W. (2011). Rotenone, paraquat, and Parkinson's disease. *Environmental health perspectives*, 119(6), 866–872.

¹²³ Sherer, T. B., Betarbet, R., Stout, A. K., Lund, S., Baptista, M., Panov, A. V., Cookson, M. R., & Greenamyre, J. T. (2002). An in vitro model of Parkinson's disease: linking mitochondrial impairment to altered alpha-synuclein metabolism and oxidative damage. *The Journal of neuroscience: the official journal of the Society for Neuroscience*, 22(16), 7006–7015.

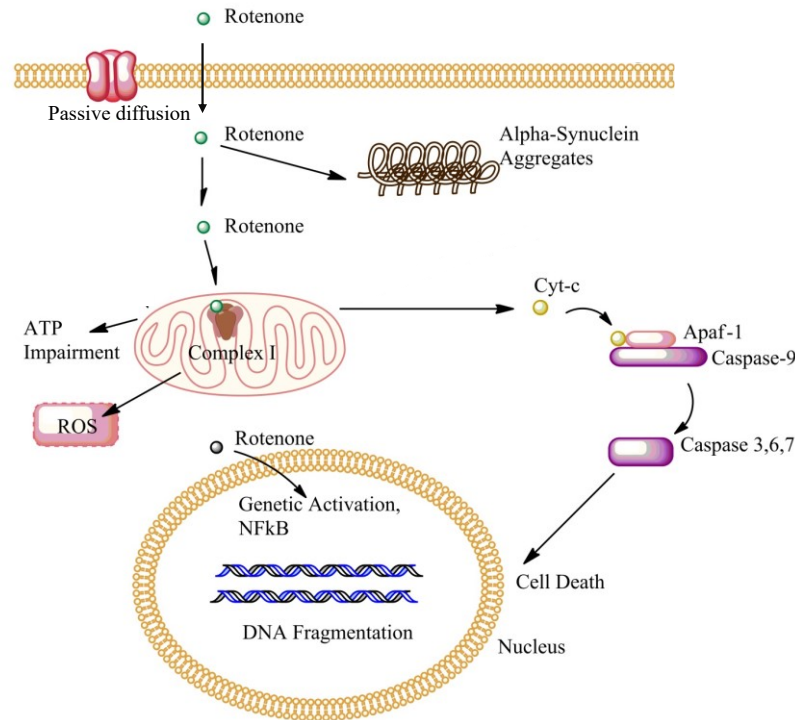


Figure 13. Rotenone-induced mechanism of neuronal cell death.¹²⁴

Other effective contributor to Rotenone-mediated neurotoxicity is the oxidative stress by increasing reactive oxygen species (ROS) production. Excess ROS is involved in DNA damage¹²⁵, lipid peroxidation, mitochondrial dysfunction and α -synuclein alteration¹²⁶. Moreover, in a study conducted on a rodent model, Rotenone caused the selective and progressive death of dopaminergic neurons by promoting neuroinflammation through the activation of microglia and astrocytes, while the surviving neurons show histopathology similar to the substantia nigra of postmortem human Parkinson's.¹²⁷ Based on its capability of reproducing most of the features that occurring in PD, Rotenone has been used extensively for *in vivo* and *in vitro* models.¹²⁸

¹²⁴ Ricardo Cabezas, Marco Fidel Avila, Daniel Torrente, Ramon Santos, El-Bachá, Ludis Morales, Janneth Gonzalez and George E. Barreto (May 15th, 2013). Astrocytes Role in Parkinson: A Double-Edged Sword, Neurodegenerative Diseases, Uday Kishore, IntechOpen, DOI: 10.5772/54305. Available from: <https://www.intechopen.com/chapters/44546>

¹²⁵ Wang, X., Qin, Z. H., Leng, Y., Wang, Y., Jin, X., Chase, T. N., & Bennett, M. C. (2002). Prostaglandin A1 inhibits rotenone-induced apoptosis in SH-SY5Y cells. *Journal of neurochemistry*, 83(5), 1094–1102.

¹²⁶ Giasson, B. I., Duda, J. E., Murray, I. V., Chen, Q., Souza, J. M., Hurtig, H. I., Ischiropoulos, H., Trojanowski, J. Q., & Lee, V. M. (2000). Oxidative damage linked to neurodegeneration by selective alpha-synuclein nitration in synucleinopathy lesions. *Science (New York, N.Y.)*, 290(5493), 985–989.

¹²⁷ Norazit, A., Meedeniya, A. C., Nguyen, M. N., & Mackay-Sim, A. (2010). Progressive loss of dopaminergic neurons induced by unilateral rotenone infusion into the medial forebrain bundle. *Brain research*, 1360, 119–129.

¹²⁸ Xiong, N., Long, X., Xiong, J., Jia, M., Chen, C., Huang, J., Ghoorah, D., Kong, X., Lin, Z., & Wang, T. (2012). Mitochondrial complex I inhibitor rotenone-induced toxicity and its potential mechanisms in Parkinson's disease models. *Critical reviews in toxicology*, 42(7), 613–632. 1

1.4. *In vitro* model for PD research

Despite the intense effort to find better treatments, the pathogenesis of PD remains unknown. One of the major difficulties in identifying new disease-modifying therapies for PD is the lack of a truly representative mammalian model that accurately summarizes the progressive loss of dopaminergic neurons in the CNS as well as the distribution of human disease (i.e. Lewy bodies or aggregates of α -synuclein)¹²⁹, mainly because some specific neuropathological and/or behavioral characteristics of PD are missing. Each currently available models have their advantages and limitations: while some are more suitable for studying the pathogenesis of PD, others are more appropriate for testing therapeutic treatments, thus highlighting the need of developing new models of PD capable of reproducing the human condition as much as possible (Figure 14).

Presently, animal models of PD provide valuable insight into potential new targets for disease intervention. Their use has contributed to the discovery of new therapeutic targets but none of them cover all the aspects of the disease. The classical models based on neurotoxins (such as 6-hydroxydopamine (6-OHDA) or MPTP that selectively target dopaminergic neurons and those using pesticides or herbicides like rotenone or paraquat have been traditionally the most used.¹³⁰ The major advantages are their reproducibility and simplicity, which have allowed for efficient screening of antiparkinsonian compounds to date. Although these models do not mimic entirely the pathology of human PD, they have proven extremely useful in furthering our understanding of the disease. Indeed, the MPTP-treated animals model served to identify the neuronal circuits responsible for the cardinal motor features of PD leading to the development of subthalamic surgical ablation and later deep brain stimulation (the current therapeutic gold standard treatment for PD), for testing potential therapies in modifying dyskinesias, for the development of cell-based therapies, and for the advancement of novel biotechnological approaches such as gene therapy.¹³¹¹³² However, neurotoxin-

¹²⁹ Blesa, J., & Przedborski, S. (2014). Parkinson's disease: animal models and dopaminergic cell vulnerability. *Frontiers in neuroanatomy*, 8, 155.

¹³⁰ Blesa, J., & Przedborski, S. (2014). Parkinson's disease: animal models and dopaminergic cell vulnerability. *Frontiers in neuroanatomy*, 8, 155.

¹³¹ Wichmann, T., Bergman, H., & DeLong, M. R. (2018). Basal ganglia, movement disorders and deep brain stimulation: advances made through non-human primate research. *Journal of neural transmission (Vienna, Austria: 1996)*, 125(3), 419–430.

¹³² Vermilyea, S. C., & Emborg, M. E. (2018). The role of nonhuman primate models in the development of cell-based therapies for Parkinson's disease. *Journal of neural transmission (Vienna, Austria: 1996)*, 125(3), 365–384.

based models remain limited for studying disease-modifying therapies due to their inability to replicate the progressive loss of dopaminergic neurons and the absence of LB pathology.

Non-mammalian models do not exhibit human anatomical connections such as primates or rodents, but still offer numerous advantages: they are able to reproduce some pivotal hallmarks of PD such as LB-like inclusions and DA neurodegeneration. They also have other maintenance conveniences such as low cost, small size and short lifespan, worms (*Caenorhabditis elegans*) and flies (*Drosophila melanogaster*) in fact are ideal candidates for drug screening and quick identification of modifiers. Furthermore, these models are easy to manipulate, as for example *Caenorhabditis elegans* lacks a functional blood brain barrier (BBB) and its body is permeable to dissolved molecules, while a toxin-induced fly model of PD can easily be created by simply exposing them to parkinsonian neurotoxins. As an example of their current usefulness, these types of models allowed to unravel the genetic and functional interactions between several PD-related genes that were subsequently confirmed in neurons and in transgenic mice¹³³, and to identify different age-related genes (*sir-2.1* / SIRT1 and *lagr-1* / LASS2).¹³⁴

Small fish including zebrafish and medaka fish have also been used recently as new PD models. Indeed, their use is growing and is one of the most used in recent times. Certainly, most of the benefits of fish, including transparency, genetics, and the viability of drug screening, are still in development.¹³⁵

In vitro experimental models are used extensively in PD research because they present a controlled environment that enables the direct investigation of the early molecular mechanisms that are potentially involved with dopaminergic degeneration, as well as for the screening of potential therapeutic drugs. However, also these models have limitations, such as the difficulty in mimicking the central nervous system complexity *in vitro*.¹³⁶

¹³³ Dhungel, N., Eleuteri, S., Li, L. B., Kramer, N. J., Chartron, J. W., Spencer, B., Kosberg, K., Fields, J. A., Stafa, K., Adame, A., Lashuel, H., Frydman, J., Shen, K., Masliah, E., & Gitler, A. D. (2015). Parkinson's disease genes VPS35 and EIF4G1 interact genetically and converge on α -synuclein. *Neuron*, 85(1), 76–87. 7

¹³⁴ van Ham, T. J., Thijssen, K. L., Breitling, R., Hofstra, R. M., Plasterk, R. H., & Nollen, E. A. (2008). *C. elegans* model identifies genetic modifiers of alpha-synuclein inclusion formation during aging. *PLoS genetics*, 4(3), e1000027.

¹³⁵ Trigo-Damas, I., Del Rey, N. L., & Blesa, J. (2018). Novel models for Parkinson's disease and their impact on future drug discovery. *Expert opinion on drug discovery*, 13(3), 229–239.

¹³⁶ Freshney I. (2001). Application of cell cultures to toxicology. *Cell biology and toxicology*, 17(4-5), 213–230.

The development of new dopaminergic cell-based models and a better understanding of those already existing is important for the advancement of PD research. Using cell lines, large panels of drugs can be quickly selected through high-throughput screening approaches and with gene overexpression and knockout it is possible to produce genetically engineered cell lines to evaluate the role of a specific gene of interest. This approach has led to the identification of most neuroprotective compounds that have progressed in preclinical studies.¹³⁷¹³⁸

To mimic PD pathology in cell lines, genetics or toxin-based models can be generated. The major advantages of these models are as follows: (1) their indefinite proliferation allows high-throughput experimentation using a wide variety of experimental techniques and endpoints; (2) it has high reproducibility when compared to primary and organotypic cultures because these cells represent homogenous populations; (3) some cell lines express important enzymes for DA metabolism and synapse formation (e.g., SH-SY5Y, LUHMES, PC12, MN9D, N27).¹³⁹ On the other hand, cell lines have many disadvantages.

They present a high proliferative rate which is in sharp contrast to neurons behavior¹⁴⁰, immortalized cells are unable to express significant levels of synaptic proteins compared to primary neurons and organotypic cultures. Furthermore, constant proliferation produces mutations that promote proliferation and survival, thereby causing successive generations of cell lines to lose dopaminergic phenotype compared to their parental lines.

Over the years, several human and mouse neuronal cell lines such as SH-SY5Y cells, PC12 (clonal cell line derived from a pheochromocytoma of the rat adrenal medulla) cells, and Lund human mesencephalic cells have been extensively used to model PD *in vitro*.

¹³⁷ Radio, N. M., & Mundy, W. R. (2008). Developmental neurotoxicity testing in vitro: models for assessing chemical effects on neurite outgrowth. *Neurotoxicology*, 29(3), 361–376.

¹³⁸ Stuchbury, G., & Münch, G. (2010). Optimizing the generation of stable neuronal cell lines via pre-transfection restriction enzyme digestion of plasmid DNA. *Cytotechnology*, 62(3), 189–194.

¹³⁹ Lopes, F. M., Bristot, I. J., da Motta, L. L., Parsons, R. B., & Klamt, F. (2017). Mimicking Parkinson's Disease in a Dish: Merits and Pitfalls of the Most Commonly used Dopaminergic In Vitro Models. *Neuromolecular medicine*, 19(2-3), 241–255.

¹⁴⁰ Luchtman, D. W., & Song, C. (2010). Why SH-SY5Y cells should be differentiated. *Neurotoxicology*, 31(1), 164–166.

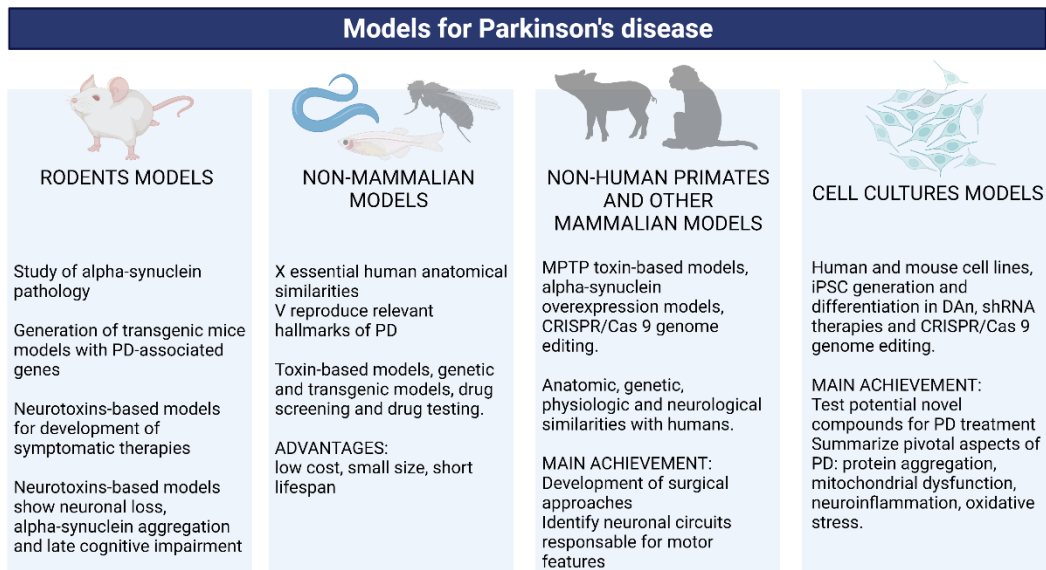


Figure 14. Different types of *in vivo* and *in vitro* models used in research for Parkinson's disease.

1.4.1. Human neuroblastoma SH-SY5Y cell line

The immortalized human neuroblastoma cell line SH-SY5Y is a thrice cloned subline of SK-N-SH cells, which were originally established from a bone marrow biopsy of a neuroblastoma patient in 1970, and since then is one of the widely used cell-based models in neuroscience. Their susceptibility to several dopaminergic xenobiotics such as MPP⁺, 6-hydroxydopamine (6-OHDA), or Rotenone and their ability to mimic many dynamics underlying DAergic neuron death make them one of the most widely used *in vitro* model for PD research. The SH-SY5Y cell line has large-scale expansion capabilities, with a modest cost and relative ease of management compared to primary neuron cultures and as an immortalized cell line, no ethical concerns arise compared to human primary cultures. Moreover, SH-SY5Y cell line exhibits specific proteins, protein isoforms and preserved signaling pathways of interest to neurotoxicological research otherwise absent in animal models.

In the undifferentiated (UD) form, SHSY5Y are morphologically characterized by non-polarized neuroblast-like cell bodies, have few truncated processes, show rapid proliferation, and tend to grow in clusters. The SH-SY5Y cell line has been reported to contain two different cellular phenotypes: neuroblastic-like cells (N-type) and epithelial-like cells (S-type), each with distinct morphologies and

behaviors. S-type cells resemble glial precursor cells and are highly substrate adherent, while N-type cells have a neuronal morphology and are less substrate adherent.

Cells with neuroblast-like morphology are positive for tyrosine hydroxylase (TH) and dopamine- β -hydroxylase characteristic of catecholaminergic neurons, whereas the epithelial-like counterpart cells lacked these enzymatic activities¹⁴¹, therefore an attempt is made to obtain a cell population of SH-SY5Y with N-type majority.

The undifferentiated SH-SY5Y presents a phenotype like immature neurons, with moderate activity of dopamine- β -hydroxylase and negligible levels of choline acetyltransferase, acetylcholinesterase, and butyryl-cholinesterase¹⁴², basal noradrenaline (NA) release and tyrosine hydroxylase activity¹⁴³. The expression of DAT¹⁴⁴ and the ability to synthesize both DA e NA allows defining the phenotype of SH-SY5Y as catecholaminergic. To replicate PD pathology in this cell model, both genetic and toxin-based approaches have been used, for which 6-OHDA and MPTP are the most employed.

1.4.3. SH-SY5Y Cell differentiation

The SH-SY5Y cell line, under specific growth conditions, can be manipulated to obtain a different phenotype based on research needs. After treatment with differentiation-inducing agents, SH-SY5Y cells undergo morphological and biochemical changes that make them more similar to primary neurons with the formation of a greater number of neuritic processes, the cell body becomes distinctly polarized and proliferation rate decreases, as cells are withdrawn from the cell cycle. The most common substances used for the differentiation processes are retinoic acid (RA), phorbol esters such as 12-O-Tetradecanoylphorbol-13-acetate (TPA), brain-derived neurotrophic factor (BDNF) and dibutyryl-cAMP. These characteristics have pointed to this cell line as a useful research tool of research for the study of PD.

¹⁴¹ Kovalevich, J., Santerre, M., & Langford, D. (2021). Considerations for the Use of SH-SY5Y Neuroblastoma Cells in Neurobiology. *Methods in molecular biology (Clifton, N.J.)*, 2311, 9–23.

¹⁴² Biedler, J. L., Roffler-Tarlov, S., Schachner, M., & Freedman, L. S. (1978). Multiple neurotransmitter synthesis by human neuroblastoma cell lines and clones. *Cancer research*, 38(11 Pt 1), 3751–3757.

¹⁴³ Ross, R. A., & Biedler, J. L. (1985). Presence and regulation of tyrosinase activity in human neuroblastoma cell variants in vitro. *Cancer research*, 45(4), 1628–1632.

¹⁴⁴ Takahashi, T., Deng, Y., Maruyama, W., Dostert, P., Kawai, M., & Naoi, M. (1994). Uptake of a neurotoxin-candidate, (R)-1,2-dimethyl-6,7-dihydroxy-1,2,3,4-tetrahydroisoquinoline into human dopaminergic neuroblastoma SH-SY5Y cells by dopamine transport system. *Journal of neural transmission. General section*, 98(2), 107–118. 4

1.4.3.1. Retinoic acid

Retinoic acid (RA) is a Vitamin A-derived compound. RA is an established signaling compound that is involved in neuronal patterning, differentiation, and axon outgrowth.

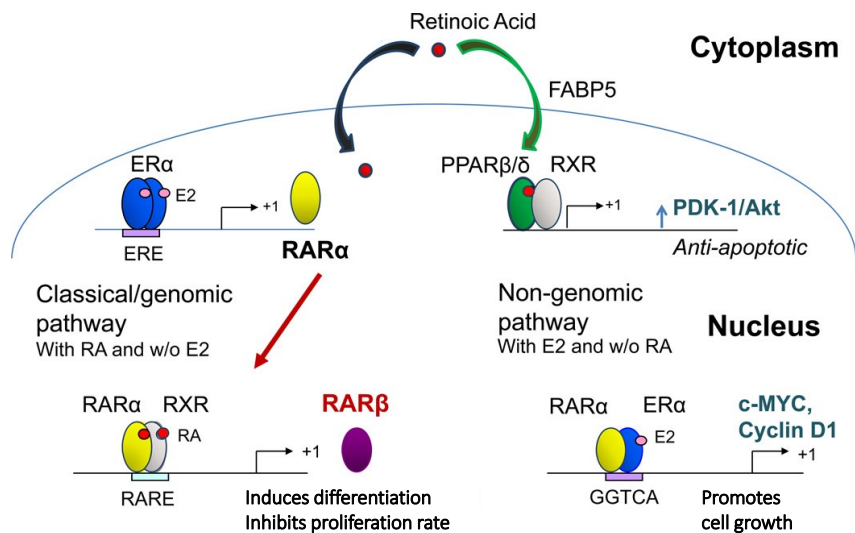


Figure 15. RA-regulated pathways and transcriptional regulators.¹⁴⁵

In cell culture protocols, RA-mediated differentiation occurs through transcriptional and homeostatic regulators, such as nuclear Retinoic Acid Receptors (RARs) α , β and γ , Retinoic X Receptors (RXRs) and PPAR (Figure 15). The binding of ligands with RARs and RXRs promotes the formation of heterodimers and the activation of their downstream effectors¹⁴⁶. This pathway plays a key role in cell differentiation, cell proliferation (with the blockade of cells in G_0 phase of the cell cycle¹⁴⁷), and eventual apoptosis. Instead, RA-mediated activation of the PPAR β/δ results in the upregulation of survival genes through the phosphatidylinositol 3-kinase/Akt signaling pathway¹⁴⁸. RA-mediated differentiation in SH-SY5Y promotes profound changes on morphological and biochemical features,

¹⁴⁵ Connolly, R. M., Nguyen, N. K., & Sukumar, S. (2013). Molecular pathways: current role and future directions of the retinoic acid pathway in cancer prevention and treatment. *Clinical cancer research: an official journal of the American Association for Cancer Research*, 19(7), 1651–1659.

¹⁴⁶ Connolly, R. M., Nguyen, N. K., & Sukumar, S. (2013). Molecular pathways: current role and future directions of the retinoic acid pathway in cancer prevention and treatment. *Clinical cancer research: an official journal of the American Association for Cancer Research*, 19(7), 1651–1659.

¹⁴⁷ Melino, G., Thiele, C. J., Knight, R. A., & Piantini, M. (1997). Retinoids and the control of growth/death decisions in human neuroblastoma cell lines. *Journal of neuro-oncology*, 31(1-2), 65–83.

¹⁴⁸ López-Carballo, G., Moreno, L., Masiá, S., Pérez, P., & Baretino, D. (2002). Activation of the phosphatidylinositol 3-kinase/Akt signaling pathway by retinoic acid is required for neural differentiation of SH-SY5Y human neuroblastoma cells. *The Journal of biological chemistry*, 277(28), 25297–25304.

such as the increase of number and length of neuritic processes, the polarized cell body, the synthesis of neuro-specific enzymes and neurotransmitters and electrophysiologic changes similar to mature neurons.

1.4.3.2. Phorbol ester

SH-SY5Y cells have been shown to further differentiate when treated with phorbol esters, such as 12-O-tetradecanoyl-phorbol-13 acetate (TPA), after treatment with RA. Indeed, the combined treatment with RA and TPA results in cells with longer processes, growth-inhibited, with an increased relative NSE activity compared to undifferentiated cells.¹⁴⁹ Moreover, many lines of evidence showed increased expression of TH, DAT, D2 and D3 receptors has been shown to increase in TPA-differentiated cells. In contrast, TPA-differentiated cell population reduced levels of VMAT compared to the UD neuroblastoma cells.¹⁵⁰

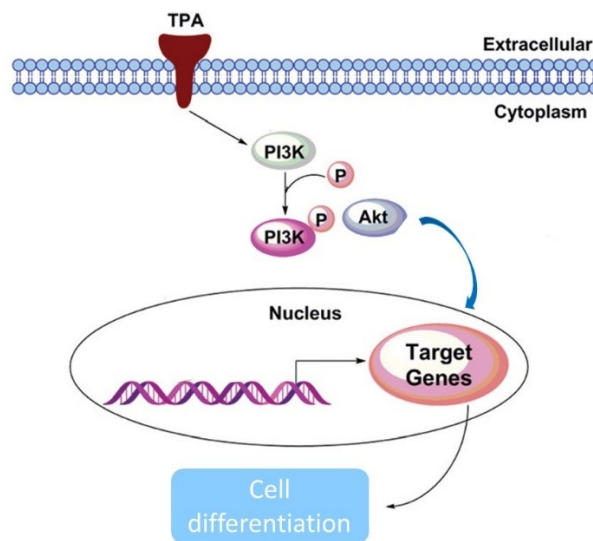


Figure 16. TPA-mediated signaling pathway leading to cell differentiation.¹⁵¹

¹⁴⁹ Kovalevich, J., Santerre, M., & Langford, D. (2021). Considerations for the Use of SH-SY5Y Neuroblastoma Cells in Neurobiology. *Methods in molecular biology (Clifton, N.J.)*, 2311, 9–23. <https://doi.org/10.1007/978-1-0716-1437-2>

¹⁵⁰ Presgraves, S. P., Ahmed, T., Borwege, S., & Joyce, J. N. (2004). Terminally differentiated SH-SY5Y cells provide a model system for studying neuroprotective effects of dopamine agonists. *Neurotoxicity research*, 5(8), 579–598.

¹⁵¹ Liu, W., Li, Y., Zheng, X., Zhang, K., & Du, Z. (2015). Potent inhibitory effect of silibinin from milk thistle on skin inflammation stimuli by 12-O-tetradecanoylphorbol-13-acetate. *Food & function*, 6(12), 3712–3719.

TPA has been shown to be involved in the Akt/PI3K signaling pathway in the same way as RA (Figure 16). According to distinct studies in literature, cells treated with RA and TPA subsequently reflect a final neuronal phenotype similar to mature adrenergic ganglial cells¹⁵² or DAergic neurons.¹⁵³

1.4.3.3. Brain-derived neurotrophic factor (BDNF)

Brain-derived neurotrophic factor (BDNF) is one of the most distributed and well-known neurotrophins in the CNS. It plays a pivotal role in the regulation of CNS functions by binding and activating the TrkB signaling pathway (Figure 17).¹⁵⁴

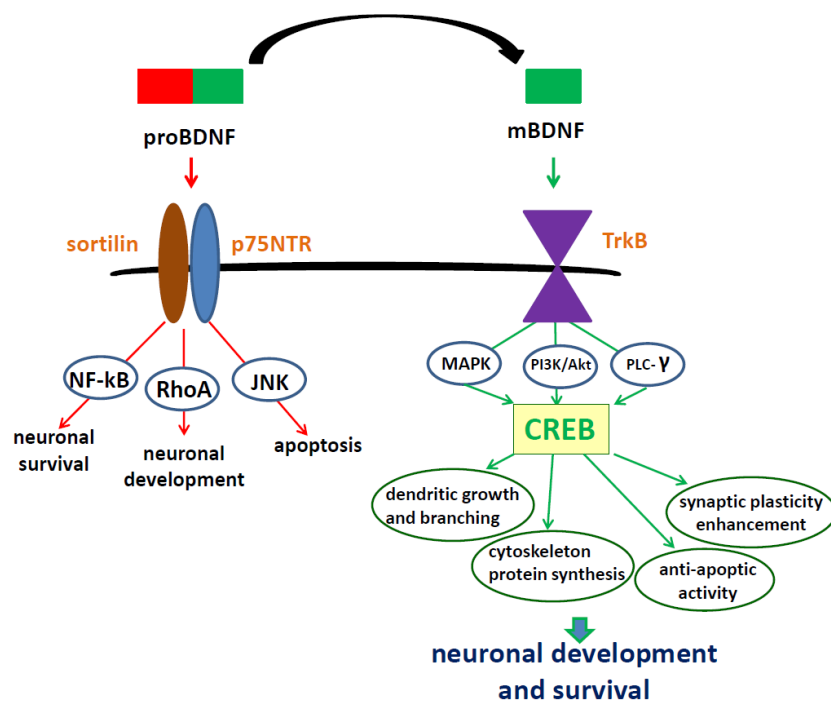


Figure 17. BDNF-activated signaling pathway by interaction with cell surface receptors.

¹⁵²Scott, I. G., Akerman, K. E., Heikkilä, J. E., Kaila, K., & Andersson, L. C. (1986). Development of a neural phenotype in differentiating ganglion cell-derived human neuroblastoma cells. *Journal of cellular physiology*, 128(2), 285–292.

¹⁵³Presgraves, S. P., Ahmed, T., Borwege, S., & Joyce, J. N. (2004). Terminally differentiated SH-SY5Y cells provide a model system for studying neuroprotective effects of dopamine agonists. *Neurotoxicity research*, 5(8), 579–598.

¹⁵⁴ Colucci-D'Amato, L., Speranza, L., & Volpicelli, F. (2020). Neurotrophic Factor BDNF, Physiological Functions and Therapeutic Potential in Depression, Neurodegeneration and Brain Cancer. *International journal of molecular sciences*, 21(20), 7777.

BDNF-TrkB-signaling pathways influence and regulate multiple processes, such as survival of neurons¹⁵⁵, cell differentiation, dendritic growth¹⁵⁶, synaptogenesis, and synaptic plasticity¹⁵⁷.

In neuroscientific research, is commonly used for cell differentiation in a procedure that leads to a homogeneous neuron-like cells population. The RA-treatment induces expression of functional TrkB-receptors making cells responsive to BDNF. BDNF enhances the differentiating effects of RA and activates phosphatidylinositol 3 kinase (PI 3-K) and extracellular regulated kinase (ERK) pathways that mediate survival and neuritogenesis. Another consistent feature of cells generated by sequential exposure to RA and BDNF is its progressive withdrawal from the cell cycle. In previous studies, RA-BDNF-treated cells showed significant norepinephrine release upon carbachol stimulation, increased expression of a neuronal marker (neurofilament NF-H) and maintained NSE levels similar to undifferentiated SH-SY5Y cells.¹⁵⁸ Moreover, differentiation with BDNF did not increase TH-immunoreactive cells.¹⁵⁹ Considering the above evidence, although several neuronal markers have been detected, the phenotype of the BDNF-differentiated cell population is not yet fully defined.

1.5. Aim of the study

In humans, individual differences in CYP-metabolism in the brain, for example due to induction, inhibition, or genetic variation, may contribute to observed differences in the sensitivity to neurotoxins and psychoactive drugs and may also impact endogenous signaling systems. For this reason, the understanding of the functional significance of brain CYPs may be helpful in developing more effective approaches to prevent neurodegenerative diseases.¹⁶⁰ Considering the impact of various brain CYP isoforms on drug/toxin sensitivity and response, the aim of the present study was

¹⁵⁵ Patel, A. V., & Krimm, R. F. (2010). BDNF is required for the survival of differentiated geniculate ganglion neurons. *Developmental biology*, 340(2), 419–429. 4

¹⁵⁶ Gorski, J. A., Zeiler, S. R., Tamowski, S., & Jones, K. R. (2003). Brain-derived neurotrophic factor is required for the maintenance of cortical dendrites. *The Journal of neuroscience: the official journal of the Society for Neuroscience*, 23(17), 6856–6865. 3

¹⁵⁷ Leal, G., Bramham, C. R., & Duarte, C. B. (2017). BDNF and Hippocampal Synaptic Plasticity. *Vitamins and hormones*, 104, 153–195. <https://doi.org/10.1016/bs.vh.2016.10.004> Leal, G., Bramham, C. R., & Duarte, C. B. (2017). BDNF and Hippocampal Synaptic Plasticity. *Vitamins and hormones*, 104, 153–195. 4

¹⁵⁸ Encinas, M., Iglesias, M., Liu, Y., Wang, H., Muhaisen, A., Ceña, V., Gallego, C., & Comella, J. X. (2000). Sequential treatment of SH-SY5Y cells with retinoic acid and brain-derived neurotrophic factor gives rise to fully differentiated, neurotrophic factor-dependent, human neuron-like cells. *Journal of neurochemistry*, 75(3), 991–1003. x

¹⁵⁹ Ducray, A. D., Wiedmer, L., Herren, F., Widmer, H. R., & Mevissen, M. (2020). Quantitative Characterization of Phenotypical Markers After Differentiation of SH-SY5Y Cells. *CNS & neurological disorders drug targets*, 19(8), 618–629.

¹⁶⁰ Ferguson, C. S., & Tyndale, R. F. (2011). Cytochrome P450 enzymes in the brain: emerging evidence of biological significance. *Trends in pharmacological sciences*, 32(12), 708–714.

to elucidate whether well known CYP inducers affect the expression of specific CYP isoforms in the brain and to investigate whether specific CYP induction may protect against neurotoxic damage promoted by xenobiotics.

To verify this hypothesis, the experimental work was organized in three tasks as follows:

Task 1. To set up of a cellular experimental model for studying dopaminergic neurodegeneration and thus the possible neuroprotective role of the CYP(s) induction. The development of a reliable method to generate human neuronal cultures is imperative to allow researchers to perform translational experiments that accurately model the human nervous system. Human SH-SY5Y cells were thus differentiated from a neuroblast-like state into mature human neurons through different approaches including different serum concentrations, the use of RA, phorbol esters, and specific neurotrophins such as brain-derived neurotrophic factor (BDNF), with the final aim to obtain dopaminergic specific neuron subtypes. Different protocols were used and developed in terms of timing and agents employed. At the end SH-SY5Y differentiation was checked for cell morphology, expression of several dopaminergic neuronal markers (NeuN, DAT, Synaptophysin, β tubulin III), some CYP isoforms (CYP1A1, CYP2B6, CYP2D6, CYP2E1, CYP3A4) and MAO A and MAO B. Data were also compared with undifferentiated SH-SY5Y cells.

Task 2. Evaluation of CYP induction performed by EtOH and β NF in human differentiated SH-SY5Y cells. This task was achieved by studying the changes in mRNA levels of the isoforms CYP1A1, CYP2B6, CYP2D6, CYP2E1 and CYP3A4 (i.e. the isoforms most responsible for the xenobiotics oxidative metabolism in the CNS) by qRT-PCR. Data were also compared with undifferentiated SH-SY5Y cells.

Task 3. To assess if the induction of specific CYP isoform protects differentiated human neuroblastoma cells from MPP⁺- and Rotenone-mediated damage. MPP⁺ toxicity appears to be partially linked to the activity of CYPs. In fact, the inhibition of both CYP2D6 and CYP3A caused an

additive effect on MPP⁺ neurotoxicity in neuroblastoma SH-SY5Y cells,¹⁶¹ while CYP2E1 inhibitors partially or almost abolished astrocytes injury induced by the same neurotoxin.¹⁶²

Rotenone is another neurotoxin currently used in PD research for its ability to produce selective and reproducible damage to the nigrostriatal DA system in a very similar way to what occurs in PD owing to mechanisms linked to CYP in a lower extent.

¹⁶¹ Mann, A., & Tyndale, R. F. (2010). Cytochrome P450 2D6 enzyme neuroprotects against 1-methyl-4-phenylpyridinium toxicity in SH-SY5Y neuronal cells. *The European journal of neuroscience*, *31*(7), 1185–1193.

¹⁶² Hao, C., Liu, W., Luan, X., Li, Y., Gui, H., Peng, Y., Shen, J., Hu, G., & Yang, J. (2010). Aquaporin-4 knockout enhances astrocyte toxicity induced by 1-methyl-4-phenylpyridinium ion and lipopolysaccharide via increasing the expression of cytochrome P4502E1. *Toxicology letters*, *198*(2), 225–231.

2. Common Materials and Methods

2.1. Materials

2.1.1. Substances purchased by Sigma Merck (Darmstadt, Germany):

Product	Product Code
1-Methyl-4phenylpyridinium Iodide (MPP ⁺)	D048
2',7'-Dichlorofluorescein Diacetate	D6883
Albumin bovine serum, fatty acid free (BSA)	A8806
All-Trans Retinoic Acid	R2625
Ammonium Persulfate, For Electrophoresis	A3678
Antibody Anti-Dopamine Transporter Rabbit	D6944
Antibody Anti-Synaptophysin Rabbit	SAB4502906
Antibody Anti- β Actin Mouse	A5441
Anti-Rabbit IgG–Peroxidase Antibody Produced in Goat	A0545
Bradford Reagent	B6916
Brain-Derived Neurotrophic Factor (BDNF)	B3795
Dimethylsulfoxide (DMSO)	D4540
Dimethylsulfoxide Sterile-Filtered	D2438
Dulbecco's Phosphate Buffered Saline w/o CaCl ₂ and MgCl ₂	D8537
L-glutamine	59202C
L-Glutamine	59202C
Mitochondrial Membrane Potential Kit	MAK160
Monoclonal Anti-Tub β 3 Antibody, Mouse	SAB700544
Non-Fat Dried Milk Bovine	M7409
Penicillin/Streptomycin Solution	P0781
Phorbol Ester (12-O-Tetradecanoyl-Phorbol-13 Acetate)	P1585
Phosphatase Inhibitor Cocktail	P5726
Ponceau S Solution	P7170
Propidium Iodide (PI)	81845
Protease Inhibitor Cocktail	P8340
Ribonuclease A	R6513
Rotenone	R8875
Thiazolyl Blue Tetrazolium Bromide (MTT)	M2128
Thiazolyl Blue Tetrazolium Bromide (MTT)	M5655
Trypan Blue	T8154
Trypsin-EDTA	T3924
Valinomycin, ready solution	V3639
β NF	N3633

2.1.2. Substances purchased by Euroclone (Pero, Italy):

Product	Product Code
DMEM Low Glucose	ECM0749L
Fetal Bovine Serum (FBS)	ECS5000L

2.1.3. Substances purchased by BioRad (Hercules, California, USA):

Product	Product Code
40% Acrylamide/Bis Solution	1610149
Clarity Western Ecl Substrate	1705061
Goat Anti-Mouse IgG (H + L)-Hrp Conjugate	1706516
Prec Plus Protein Dual Color Stds	1610374
SsoAdvanced™ Universal SYBR® Green Supermix	1725271
TEMED	1610800
XT Sample Buffer 4X	1610791

2.1.4 Substances purchased by others:

Product	Company	Product Code
2-Propanol	PanReac AppliChem (Nova Chimica Srl, Cinisello Balsamo, Italy)	131090.1211
Dead Cell Apoptotic Kit with Annexin Alexa Fluor™ 488 & Propidium Iodide	Thermo Fisher Scientific (Waltham, Massachusetts, USA)	V13245
Ethanol absolute anhydrous	Carlo Erba (Cornaredo, Italy)	4146052
High-Capacity cDNA Reverse Transcription Kit	Thermo Fisher Scientific (Waltham, Massachusetts, USA)	4368814
RIPA Buffer 10X	Millipore (Sigma Merck, Darmstadt, Germany)	1705061
Sodium Dodecyl Sulfate (SDS)	IBI Scientific (distributed by Thermo Fisher Scientific Waltham, Massachusetts, USA)	IB07062
Tris(hydroxymethyl)-aminomethane	GE Healthcare (Chicago, Illinois, USA)	17-1321-01
Tween 20	Promega (Madison, Wisconsin, USA)	H5152

2.2. Solutions

Unless otherwise specified, all buffers and reagents were prepared using milliQ water.

- Phosphate Buffered Saline

The buffer solution was commonly used for washing cells and precipitates. The phosphate buffered saline (PBS) solution was stored at 4 °C and used for washing cells and the removal of waste products, and suspension medium for cells in various protocols.

- Penicillin-Streptomycin

Solution used for cell cultures to avoid gram-positive and gram-negative bacteria contamination. The stock solution of penicillin-streptomycin (P/S) contains 10,000 units' penicillin and 10 mg/ml in a citrate buffer. Aliquots of 5 ml were prepared to be added to the cell culture medium at a 1% concentration. Storage at -20 °C.

- Fetal bovine serum

Fetal bovine serum (FBS) was used in cell cultures as media supplement. It was sterile-filtered, and delivers growth factors, vitamins, hormones, attachment and transport factors and other cell stimulating components. FBS solution was heated for 30 minutes at 60 °C to inactivate the complement system, then aliquots of 50 ml were prepared and stored at -20 °C. Each aliquot was defrosted and warmed to 37°C before being added to culture growth medium.

- Growth medium

Cell culture medium to support the growth of neuroblastoma SH-SY5Y cells was DMEM with low glucose. This was sterile-filtered, and supplemented with FBS (10%), P/S (1%) and L-glutamine (1%). Storage at 4 °C and heated to 37 °C prior to use.

- Differentiation medium

DMEM low glucose medium supplemented with 1% P/S, L-glutamine (1%) and 1% FBS was used. The low-serum medium promotes differentiation toward a neuron-like phenotype. It was stored at 4 °C and heated to 37 °C prior to use.

- Trypsin-EDTA

Trypsin is a 223-amino acid proteolytic enzyme. This work solution contains 0.5% Trypsin and 0.2% EDTA. It was used to detach SH-SY5Y adherent cells from the culture surface by the cleavage of peptides in the C-terminal side of lysine and arginine residues. Ethylenediaminetetraacetic acid (EDTA) was used as a chelating agent in order to neutralize calcium and magnesium ions, so the enzymatic activity is increased. The optimum temperature for its function is 37 °C. The solution was divided into aliquots and stored at -20 °C until use, then was stored at 4 °C and heated to 37 °C prior to use.

- SH-SY5Y Freezing media

SH-SY5Y freezing solution was composed by 90% FBS low endotoxins and 10% sterile dimethyl sulfoxide (DMSO). DMSO was used to allow a progressive freeze of the H₂O contained in the cells, thus avoiding formation of crystals that might break the membrane or other organelles.

- Retinoic acid

Retinoic Acid (RA) powder was dissolved in ethanol under N₂ to make a 3 mg/mL (10µM) stock solution, which was stored at -80 °C in aliquots.

- Phorbol Ester (TPA)

TPA was dissolved in ethanol to make a 0.01 M stock solution, which was stored at - 20 °C in aliquots.

- Protease inhibitor cocktail

Solution containing protease inhibitors for the inhibition of serine, cysteine, and metalloproteases. It was composed of 4-(2-Aminoethyl)benzenesulfonyl fluoride hydrochloride, Bestatin hydrochloride, Leupeptin, E-64, Aprotinin, Pepstatin A, and Phosphoramidon disodium salt. Stock solution was bought at 10X concentration and was stored at -20°C in aliquots.

- Phosphatase inhibitor cocktail

Solution composed of sodium orthovanadate to inhibit ATPases, tyrosine phosphatases and phosphate-transferring enzymes; sodium molybdate to inhibit acid and phosphoprotein

phosphatases; sodium tartrate to inhibit acid phosphatases; and imidazole to inhibit alkaline phosphatases. Stock solution was bought at 100X concentration and was stored at -20°C in aliquots.

- Radio-Immunoprecipitation Assay lysis buffer

Radio-Immunoprecipitation Assay (RIPA) lysis buffer allows protein extraction and solubilization from cell cultures. It is composed of 50 mM Tris-HCl, pH 8.0 buffer with 150 mM sodium chloride, 1.0% Igepal CA-630 (NP-40), 0.5% sodium deoxycholate, and 0.1% sodium dodecyl sulfate. The solution was stored at room temperature. Prior to use, RIPA lysis buffer 10X must be diluted to 1X and supplemented with protease and phosphatase inhibitor cocktail (1:100).

- Running buffer

Solution composed by 100 ml Tris-Glycine buffer (Tris base, Glycine), 10 ml SDS 10% (w/v) and dd H₂O up to 1000 ml.

- Transfer buffer

Solution used to transfer separated proteins from the 10 % gel to the polyvinylidene fluoride (PVDF) card. Composition: 100 ml Tris-Glycine buffer, 200 ml Methanol, dd H₂O up to 1000 ml.

- Probing blocking solution

Solution used to avoid non-specific binding of primary antibodies. Composition: 5 % (w/v) nonfat-dried milk from bovine in 0.1 % (v/v) Tween PBS.

- Probing wash buffer

Solution used to wash the PVDF card after blocking and antibody incubation. Composition: 0.1 % (v/v) Tween in PBS.

- Brain derived neurotrophic factor (BDNF)

BDNF lyophilized powder was dissolved in water to make a 100µg/mL stock solution, which was stored at -20 °C in aliquots

- MPP⁺

MPP⁺ powder was dissolved in growth medium to make a 10 mM stock solution, freshly prepared when needed.

- Rotenone

Rotenone was dissolved in DMSO to make a 300 μ M stock solution, which was stored at 8° C for a month.

- β NF

β NF powder was solubilized in DMSO in order to obtain a 4 mM stock solution, stored at 8° C for a maximum of three months.

- 10X PBS for FACS Flow

PBS used for the flow cytometer experiments was composed by 8 g NaCl, 0,2 g KCl, 1,44 g Na₂HPO₄, 0,24 g KH₂PO₄ in 1L, final pH 7.4. It was used diluted to 1X with water and filtered with 0.45 μ m filter before use.

- L-glutamine

L-glutamine is an essential amino acid that is a crucial component of culture media that serves as a major energy source for cells in culture. L-glutamine 200 mM stock solution was splitted up in 5 ml aliquots and stored at -20° C. Before being added to culture growth medium, was defrosted, and warmed at 37° C.

- Sample loading buffer 4X for WB

Buffer used to prepare samples for the SDS page. It contains TRIS at pH 6.8, Glycerol, 10 % SDS, 2 β -mercaptoethanol, 0,1 % bromo phenol blue. Loading buffer remove variables that cause lane-to-lane running anomalies.

- qRT-PCR probes

The probes were purchased from a company that supplied “reverse” and “forward” probes separately. They were therefore resuspended in RNA-free water to create stock solutions of 100 μ M and aliquoted in working solutions of 10 μ M. Both solutions were stored at -20° C.

- 2',7'-Dichlorofluorescein diacetate

DCFDA powder was stored at -20°C. A fresh solution 10 mmol/L in Ethanol was daily prepared, from which work solution 1 mmol/L diluted in PBS or distilled water was obtained.

- JC-1 200x Stock solution

JC-1 was resuspended in DMSO according to manufacturing indications, then was stored in aliquots at -20°C.

- Staining Mixture

Staining Mixture was prepared by mixing the Staining Solution (25 μ L of the 200xJC-1 Stock Solution in 4mL of milliQ H₂O) with an equal volume of the complete medium for cell growth.

- MTT

The MTT solution (0.5 mg/ml) was prepared in growth medium just before use and stored protected from light.

2.3. Instruments

- Bürker Chamber

Sigma Merck, Darmstadt, Germany.

- pH meter

pH meter (XS Instruments, Carpi, Italy) calibrated daily using standard pH buffers of pH 4.0, 7.0, and 10.0.

- Pipetting

A set of Gilson (Gilson, Middleton, USA) and Finpipette (Thermo FisherScientific Waltham, Massachusetts, USA) automatic pipettes was used for pipetting volumes within the range of 1 µl to 5 ml.

- Centrifuges

The following centrifuges were used:

Hermle Z 300 K centrifuge (Hermle Labortechnik GmbH, Wehingen, Germania) or ALC microcentrifuge 4114 (IT Instrument Teknik, Umea, Sweden).

- Reverse transcription and qRT-PCR

RNA samples were transcribed to cDNA in a 9800 Fast Thermal Cycler from Applied Biosystems (Thermo FisherScientific Waltham, Massachusetts, USA). PCR was carried out in a StepOne™ Real-Time PCR System (Thermo FisherScientific Waltham, Massachusetts, USA) and data was acquired with the StepOne 2.0 software (Thermo FisherScientific Waltham, Massachusetts, USA).

- Plate reader

UV-Vis plate reader was a Multiskan™ GO Microplate (Thermo FisherScientific Waltham, Massachusetts, USA) and results recorded with the software SkanIt™ 3.2 (Thermo Scientific Waltham, Massachusetts, USA). Fluorescence measurements were performed by using Fluoroskan Ascent fluorimeter, Thermo LabSystems, Helsinki, Finland.

- Western Blot

Western Blot (WB) was carried out with the BioRad Western Blot system (Hercules, California, USA). The PVDF cards were scanned for bands with Molecular Imager Gel Doc™ XR System (Thermo FisherScientific Waltham, Massachusetts, USA) and results were analyzed with Quantity One 1-D Analysis Software (BioRad, Hercules, California, USA).

- Flow cytometry

Samples were read with a FACSCalibur cytofluorimeter (BD Biosciences San Jose, CA, USA) equipped with two lasers (488 nm and 635 nm) and detectors for forward scatter, side scatter, and four fluorescence PMTs. Channels wavelengths are reported below.

Laser	Channel	Filter Info
Blue (488nm)	FL-1	515-545nm
	FL-2	564-601nm
	FL-3	670LP
Red (635nm)	FL-4	653-669nm

FACSCalibur was connected to a FACStation Data Management system featuring a Macintosh® computer and CELLQuest™ software version 3.3 (BD Biosciences San Jose, CA, USA) for data analysis.

- Microscopy

Cell growth was monitored with phase contrast microscopy LEICA DMI 4000 B (Leica Microsystems S.r.l., Wetzlar, Germany), using software Leica Application Suite X version 3.7.0.20979 (Leica Microsystems S.r.l., Wetzlar, Germany).

- NanoDrop 1000 Spectrophotometer

RNA amount of PCR samples was determined with the NanoDrop ND-1000 UV-Vis Spectrophotometer by (Thermo Fisher Scientific Waltham, Massachusetts, USA), using the software ND-1000 V3.3.0 (Thermo Fisher Scientific Waltham, Massachusetts, USA).

- Bioclass Thermo-shaker TS-100C

Bioclass S.r.l. Pistoia, Italy.

- Incubator for cells culturing

A SANYO CO2 Incubator (MCO-18 AIC Marshall Scientific, Hampton, USA) was used.

2.4. Cell culture

Neuroblastoma SH-SY5Y cells (Sigma Merck, Darmstadt, Germany) authenticated by gene typing (LGC Standards S.r.L., Milan, Italy) were cultured as described by Kovalevich and Langford¹⁶³ with some modifications. Undifferentiated SH-SY5Y cells were maintained in Dulbecco's Modified Eagle's Medium Low glucose, supplemented with 10% heat-inactivated FBS, 1% of L-glutamine and 1% Penicillin/Streptomycin (100 U/mL and 100 µg/mL), in the presence of 5% CO₂ in a humidified incubator at 37°C. Growth medium was refreshed every 2 days, and the cells were subcultured once 80-90% confluence was reached. All solutions for cell culture were heated to 37 °C before use.

2.4.2. Sub-culturing

An initial seed of 4×10^5 cells in a T-75 culture flask allow cells to be semi-confluent in approximately 7 days. Medium is aspirated and cells are washed very carefully with pre-warmed PBS to eliminate all the possible dead cells and debris. Then cells are detached from the flask after incubation with Trypsin/EDTA solution at 37 °C for 2 minutes. Trypsin is neutralized by adding the double volume of complete grow medium. The whole volume is collected and centrifuged at 1500 g for 5 minutes and pellet is resuspended in a known volume of complete medium. Concentration is then calculated as described below and approximately 3×10^5 cells are plated in a 75 cm² flask. To seed cells at the appropriate concentrations for experiments, cells were counted using the Trypan Blue exclusion procedure in a Bürker cell-counting chamber. Cells are allowed to adhere for 24 hours after sub-culturing or seeding before treatments were carried out. For the experiments, cells within passage 5-15 were used.

2.4.3. Cell counting

10 µl of resuspended cells is mixed with 90 µl of Trypan Blue, then 10 µl of this suspension is loaded into a Bürker Chamber. Cells are counted in at least 3 big squares and concentration is calculated according to the following formula:

¹⁶³ Kovalevich, J., & Langford, D. (2013). Considerations for the use of SH-SY5Y neuroblastoma cells in neurobiology. *Methods in molecular biology (Clifton, N.J.)*, 1078, 9–21.

$$C \text{ (cells}/\mu\text{l)} = \frac{N_T}{S_c \times S_s \times C_d} \times D_f$$

Where:

- NT: Total number of cells counted
- Sc: Number of large squares counted
- Ss: Surface of a large square (1 mm²)
- Cd: Chamber depth (0.1 mm)
- Df: Dilution factor (in this protocol, 10:100)

2.4.4. Cell freezing

Cells from centrifugation were resuspended in warm freezing media (90% FBS, 10% steril-filtered DMSO) to obtain approximately 10⁶ cells/ml. The suspension is transferred to a cryo-vial and placed at -80 °C overnight, then transferred to liquid nitrogen for long-term storage.

2.4.5. Cell seeding

SH-SY5Y neuroblastoma cells were seeded at the concentrations reported in the Figure 18. Following seeding, the cells were left overnight in the incubator to adhere to the bottom of the wells/flasks. The number reported for the differentiated cells represents the cell density of undifferentiated cells plated when starting the differentiation protocols to obtain a final cell density comparable to that of the undifferentiated experiments.

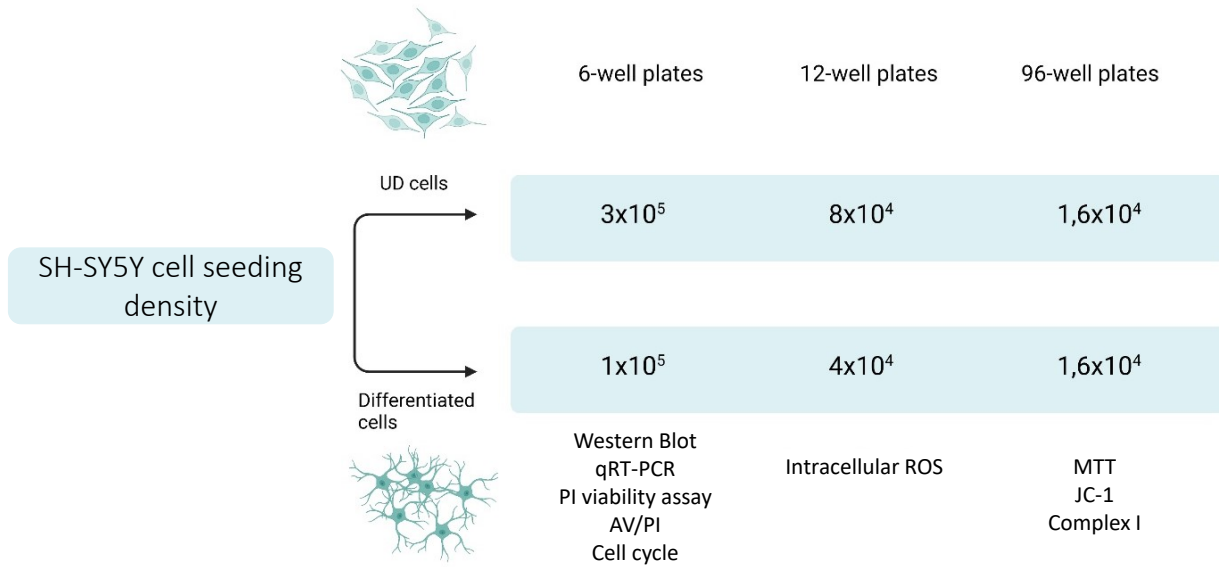


Figure 18. Seeding cell densities for undifferentiated (UD) and differentiated SH-SY5Y cells to run experiments in this study. The reported number for the differentiated cells represents the cell density of UD cells initially seeded when starting the differentiation protocols, to obtain a final cell density comparable to that of the undifferentiated experiments.

3. Task 1.

SH-SY5Y cell differentiation

3.1. Introduction

In neurobiology, the major types of cell culture models include primary neuronal cultures derived from rats and mice, and neuroblastoma cell lines such as rat B35 cells, Neuro-2A mouse cells, and rat PC12 cells. Although use of such cell lines has advanced the field significantly, there are several confounding factors associated with handling non-human cells and tissue. These include understanding species-specific differences in metabolic processes, phenotypes of disease manifestation, and pathogenesis when compared to humans. It is also important to note that there are significant differences between mouse and human gene expression and transcription factor signaling, highlighting the limitations of rodent models and the importance of understanding which pathways are conserved between rodents and humans.¹⁶⁴

Also given the difficulties in obtaining and maintaining a line of human primary neurons, the focus of the research has shifted to a model consisting in human neuronal cell lines. Many research groups have employed the use of human neuronal cell lines including the N-Tera-2 (NT2) human teratocarcinoma cell line and inducible pluripotent stem cells (iPSCs). These cell lines provide good models for *in vitro* human systems. However, differentiation of NT2 cells with retinoic acid (RA) results in the generation of a mixed population of neurons, astrocytes, and radial glial cells, necessitating an additional purification step to obtain pure populations of neurons.¹⁶⁵ Additionally, NT2 cells demonstrate a highly variable karyotype, with greater than 60 chromosomes in 72% of cells. iPSCs demonstrate variability in differentiation between different cell lines and changes in differentiation efficiency. It is therefore desirable to have a consistent and reproducible human neuronal cell model to complement these alternatives.

The present study was performed by using human SH-SY5Y cells. These have a stable karyotype consisting of 47 chromosomes and can be differentiated from a neuroblast-like state into mature human neurons through a variety of different mechanisms including the use of RA, phorbol esters, and specific neurotrophins such as brain-derived neurotrophic factor (BDNF).

¹⁶⁴ Shipley, M. M., Mangold, C. A., & Szpara, M. L. (2016). Differentiation of the SH-SY5Y Human Neuroblastoma Cell Line. *Journal of visualized experiments: JoVE*, (108), 53193.

¹⁶⁵ Shipley, M. M., Mangold, C. A., & Szpara, M. L. (2016). Differentiation of the SH-SY5Y Human Neuroblastoma Cell Line. *Journal of visualized experiments: JoVE*, (108), 53193.

For differentiation, several protocols have been developed¹⁶⁶ and some were proven to provide a straightforward and reproducible method to generate homogenous and viable human neuronal culture. In general, differentiation leads SH-SY5Y cells to a stable population, with a reduced rate of proliferation. In addition, various morphological changes are induced, mostly affecting the cell body (which can become more polarized) and neuritic processes (which grow both in number and in length).

As described previously, the treatment with RA of SH-SY5Y promotes the activation of TrkB receptors and the downstream signaling pathway, leading to an evident phenotypic change. RA-mediated differentiation of SH-SY5Y cells was associated with the induction of a cholinergic rather than DAergic phenotype. Therefore, to drive the differentiation toward a dopaminergic phenotype as a more realistic PD-model, the RA treatment is generally followed by other compounds such as phorbol esters, neurotrophic factors, Staurosporins and purines.

Specific aims of task 1.

Protocols that have been shown to effectively produce SH-SY5Y cell populations with dopaminergic like phenotype were selected and tested. They consisted in a first treatment with RA, followed by treatment with TPA or BDNF. Afterward, the evaluation of neuronal differentiation was performed by:

a) morphological analysis by contrast phase microscopy consisting in assessing changes in the length of neuritic processes and their number; b) expressions of different generic (NeuN, Synaptophysin, β -Tubulin III) and dopaminergic-specific (dopamine transporter, DAT) markers of mature neurons by western blot; c) basal expression of CYP isoforms CYP1A1, CYP2B6, CYP2D6, CYP2E1, CYP3A4 and MAO A and B enzymes.

The NeuN protein is located in the nuclei and in the perinuclear cytoplasm of neurons.¹⁶⁷ Its function is not yet fully understood, but from its localization within the nucleus and from its expression associated with neuronal differentiation, it appears to be a nervous system-specific nuclear

¹⁶⁶ Kovalevich, J., & Langford, D. (2013). Considerations for the use of SH-SY5Y neuroblastoma cells in neurobiology. *Methods in molecular biology (Clifton, N.J.)*, 1078, 9–21

¹⁶⁷ Gusel'nikova, V. V., & Korzhevskiy, D. E. (2015). NeuN As a Neuronal Nuclear Antigen and Neuron Differentiation Marker. *Acta naturae*, 7(2), 42–47.

regulatory molecule and is used as a reliable neuronal marker.¹⁶⁸ Synaptophysin is expressed in neurons and has been regarded as a specific presynaptic marker.¹⁶⁹ β -Tubulin III (*TUBB3*) is a marker protein involved in neuronal development of the cytoskeleton and is constitutively expressed in the central and peripheral nervous systems and in the testes, specifically in Sertoli cells.

DAT is a transmembrane protein selectively expressed in dopaminergic cells with a key role in dopamine (DA) reuptake. Indeed, DAT modulates quantal DA release at endplates also regulating DA storage in synaptic vesicles. Its expression on the presynaptic terminals reflects the striatal dopaminergic innervation, implying a direct relationship between its depletion and the loss of nigral cells.^{170,171}

The monoamine oxidases A and B subtypes are known to be linked to neurodegeneration phenomena.¹⁷² Experimental evidence suggest, in fact, that elevated astrocytes expression in MAO B and ensuing astrocytosis might promote dopaminergic neurodegeneration by increasing oxidative stress and /or directly bioactivating neurotoxins (i.e. MPTP and sasolinol).^{173, 174} This, prompted us to evaluate the modulation of their expression during the differentiation.

The expression of the above-mentioned markers was assessed also at intermediate stage, i.e. cells treated with RA only.

¹⁶⁸ Mullen RJ, Buck CR, Smith AM. NeuN, a neuronal specific nuclear protein in vertebrates. *Development*. 1992 Sep;116(1):201-11. PMID: 1483388.

¹⁶⁹ Bai, X., & Strong, R. (2014). Expression of synaptophysin protein in different dopaminergic cell lines. *Journal of biochemical and pharmacological research*, 2(4), 185–190.

¹⁷⁰ Sulzer, D., Cragg, S. J., & Rice, M. E. (2016). Striatal dopamine neurotransmission: regulation of release and uptake. *Basal ganglia*, 6(3), 123–148.

¹⁷¹ Palermo, G., Giannoni, S., Bellini, G., Siciliano, G., & Ceravolo, R. (2021). Dopamine Transporter Imaging, Current Status of a Potential Biomarker: A Comprehensive Review. *International journal of molecular sciences*, 22(20), 11234.

¹⁷² Tong, J., Rathitharan, G., Meyer, J. H., Furukawa, Y., Ang, L. C., Boileau, I., Guttman, M., Hornykiewicz, O., & Kish, S. J. (2017). Brain monoamine oxidase B and A in human parkinsonian dopamine deficiency disorders. *Brain : a journal of neurology*, 140(9), 2460–2474.

¹⁷³ Mallajosyula, J. K., Kaur, D., Chinta, S. J., Rajagopalan, S., Rane, A., Nicholls, D. G., Di Monte, D. A., Macarthur, H., & Andersen, J. K. (2008). MAO-B elevation in mouse brain astrocytes results in Parkinson's pathology. *PLoS one*, 3(2), e1616.

¹⁷⁴ Yao, L., Dai, X., Sun, Y., Wang, Y., Yang, Q., Chen, X., Liu, Y., Zhang, L., Xie, W., & Liu, J. (2018). Inhibition of transcription factor SP1 produces neuroprotective effects through decreasing MAO B activity in MPTP/MPP⁺ Parkinson's disease models. *Journal of neuroscience research*, 96(10), 1663–1676.

3.2. Methods

3.2.1. Cell Differentiation

Undifferentiated SH-SY5Y cells were seeded as reported in section 2.4.5. After 24 hours the medium was aspirated, cells were washed with PBS and differentiation medium were added. Two differentiation protocols were used (Figure 19):

- Protocol 1: Retinoic Acid and Phorbol-Ester: cells were treated with 10 μM RA in 1% FBS differentiation medium. After three days w/o medium change, cells were washed with PBS, added with 1% FBS differentiation medium containing 80 nM of TPA and maintained in these conditions for further three days.
- Protocol 2: Retinoic acid and Brain Derived Neurotrophic Factor: cells were treated with 10 μM RA in 1% FBS differentiation medium. After three days w/o medium change, cells were washed with PBS, added with 1% FBS differentiation medium containing 50 $\mu\text{g}/\text{mL}$ of BDNF and were thus maintained in these conditions for further three days.

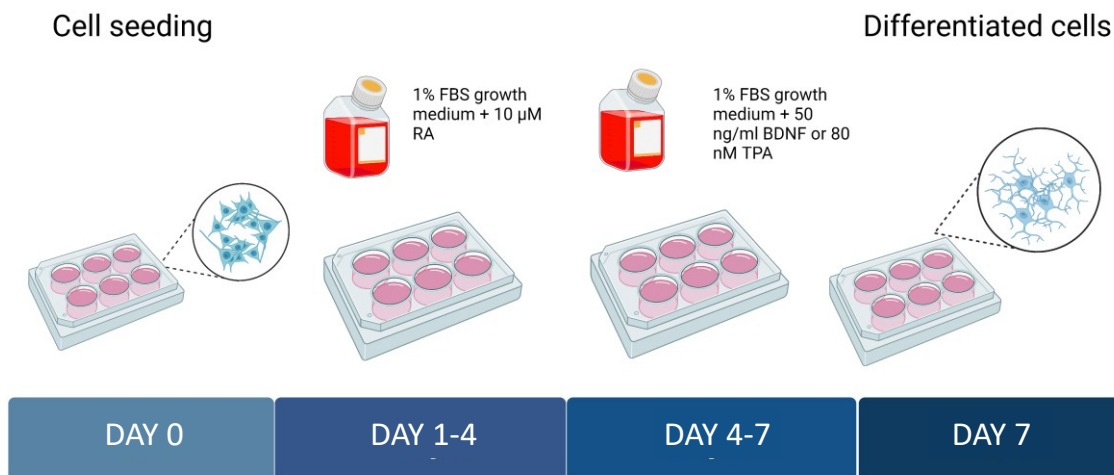


Figure 19. Differentiation protocols steps. On day 0, the UD neuroblastoma cells were plated in 6 multiwell plates. On day 1, the cells were treated with RA 10 μM in 1% FBS growth medium and left in this medium for 3 days. On day 4, the medium was switched to BDNF 50 ng/ml or TPA 80 nM 1% FBS medium. On day 7, cells were checked for differentiation markers.

All treatments were performed under dark conditions as the compounds used were photosensitive. Differentiation was daily monitored with phase contrast microscopy for neurite outgrowth and slowing of proliferation. On day 7, differentiated SH-SY5Y cells were checked for differentiation markers.

3.2.2. Morphological analysis

During and at the end of differentiation, the cells were observed under a phase-contrast microscope and photos were randomly taken. Morphological changes were quantified by an operator which was blind to the treatments by using ImageJ software (National Institute of Health, Bethesda, MD, USA, 1.37v). ImageJ offers the possibility to calculate various parameters based on the pixel values related to the regions of interest selected by the user. A total of 3-5 photos/well were taken (n> 3 wells for each experimental point) and n>3 representative cells were randomly selected for each photo. The neuritic processes were then counted and measured.

3.2.3. Western blot analysis

3.2.3.a. Protein Extraction

The protocol used was described by Peach et al.¹⁷⁵ with some modifications. The cells were washed twice with cold PBS and scraped by 1X RIPA lysis buffer containing protease and phosphatase inhibitor cocktail (1:100). The suspension was transferred to a new eppendorf, vortexed (30s) and incubated on ice (30 s) for approximately 5 minutes, then centrifuged at 13,000 g for 15 minutes at 4 °C. The supernatant was transferred in a new eppendorf and stored at -80 °C until use.

3.2.3.b. Protein concentration

Protein concentration was assessed according to the Bradford method¹⁷⁶ which is based on the formation of a complex between the dye Coomassie Brilliant Blue G-250 and the proteins of the sample via electrostatic interaction with protonated basic amino acids (lysine, arginine, and

¹⁷⁵ Peach, M., Marsh, N., Miskiewicz, E. I., & MacPhee, D. J. (2015). Solubilization of proteins: the importance of lysis buffer choice. *Methods in molecular biology (Clifton, N.J.)*, 1312, 49–60.

¹⁷⁶ Bradford M. M. (1976). A rapid and sensitive method for the quantitation of microgram quantities of protein utilizing the principle of protein-dye binding. *Analytical biochemistry*, 72, 248–254.

histidine)¹⁷⁷ and by hydrophobic interactions¹⁷⁸. The formation of this complex causes the conversion of the red form of Coomassie Brilliant Blue to the blue form, promoting a shift in the dye absorption maximum from 465 to 595, so the amount of protein is proportional to the amount of absorbance recorded. Protein samples were mixed with 250 µl of Bradford reagent (Sigma Merck, Germany) and absorbance was measured at 595 nm in a plate reader. The protein concentrations were then calculated by extrapolating absorbance data with a bovine serum albumin (BSA) standard curve with concentrations in the range 0-1.4 mg/ml.

3.2.3. c Electrophoresis

After protein extraction, electrophoresis was performed as described by Burnette.¹⁷⁹ 30 µg/sample were diluted in a final volume of 20 µl composed by 5 µl of loading buffer (4X) and milliQ H₂O. Samples were heated for 8 minutes at 95 °C in a Thermo-shaker. Samples and molecular weight markers were then loaded in a 10 % gel card for the electrophoresis stage. For protein separation, the gel was exposed to a current of 400 mA and an electric potential of 135 V during approximately 90 minutes.

3.2.3.d. Transfer

After electrophoresis, transfer was carried out as described by Komatsu¹⁸⁰ with some modifications according to manufacturer indications. The 10 % gel card was assembled in a sandwich with the PVDF card to transfer the separated proteins from the gel. The sandwich was then loaded in a tank containing transfer solution buffer and exposed to an electric potential of 100 V for 75-90 minutes.

¹⁷⁷ de Moreno, M. R., Smith, J. F., & Smith, R. V. (1986). Mechanism studies of coomassie blue and silver staining of proteins. *Journal of pharmaceutical sciences*, 75(9), 907–911.

¹⁷⁸ Fountoulakis, M., Juranville, J. F., & Manneberg, M. (1992). Comparison of the Coomassie brilliant blue, bicinchoninic acid and Lowry quantitation assays, using non-glycosylated and glycosylated proteins. *Journal of biochemical and biophysical methods*, 24(3-4), 265–274.

¹⁷⁹ Burnette W. N. (1981). "Western blotting": electrophoretic transfer of proteins from sodium dodecyl sulfate--polyacrylamide gels to unmodified nitrocellulose and radiographic detection with antibody and radioiodinated protein A. *Analytical biochemistry*, 112(2), 195–203.

¹⁸⁰ Komatsu S. (2015). Western Blotting Using PVDF Membranes and Its Downstream Applications. *Methods in molecular biology (Clifton, N.J.)*, 1312, 227–236.

3.2.3.e. Probing

The PVDF membrane was incubated in probing blocking solution for 1 hour, followed by three washes with probing wash buffer for 5 minutes each, then incubated overnight with primary antibodies and β -actin as housekeeping protein (see Table 2). The day after, the PVDF membrane was washed three times with probing wash buffer and incubated with secondary antibodies (see Table 2) for 1 hour. After incubation, the membrane was washed 2 times with probing wash buffer and once with buffer w/o Tween. Antibodies were kept in blocking solution during the whole procedure, in a final volume of 6 ml.

Target	Host	Concentration
NeuN	Rabbit	1:1000
Synaptophysin	Rabbit	1:1500
β tubulin III	Mouse	1:1000
MAO-A	Rabbit	1:100
MAO-B	Rabbit	1:100
DAT	Rabbit	1:500
β actin	Mouse	1:3000
<i>Secondary antibody Anti-Rabbit IgG– Peroxidase</i>	Goat	1:2000
<i>Secondary antibody Anti-Mouse IgG (H + L)-Hrp Conjugate</i>	Goat	1:3000

Table 2. Antibodies used for Western Blot experiments.

3.2.3.f. Scan and analysis

PVDF cards were scanned for bands and analyzed with the Molecular Imager Gel DocTM XR System. The intensity of each band was calculated with ImageJ software (Bethesda, Maryland, USA)¹⁸¹ and normalized with the β -actin.

¹⁸¹ <https://imagej.net/software/imagej/#publication>

3.2.4. Quantitative real-time PCR

3.2.4.a. RNA extraction

Gene expression was assessed by using quantitative real-time PCR (qRT-PCR). After treatments, the RNA was extracted with TRIzol reagent as described by Rio et al.¹⁸² with some modifications. Cells were scraped with 400 µl of TRIzol. After over night incubation stored at -80° C, cell lysate was centrifugated at 12,000 g at 4 °C for 10 minutes, then the supernatant was transferred to a new sterile eppendorf and mixed with 100 µl of chloroform then incubated on ice. After 30 minutes, the samples were centrifugated for 15 minutes at 12,000 g at 4 °C. The top layer produced in the tube and containing the RNA was transferred to a new sterile eppendorf and mixed with 250 µl of isopropanol. After 30 minutes of incubation on ice, the samples were centrifugated for 15 minutes at 8,000 g at 4 °C. The pellet was then resuspended in 250 µl of 75% EtOH and centrifugated for 5 minutes at 6,000 g at 4 °C. The pellet containing the RNA was left air drying and then resuspended in 15-25 µl of nuclease-free water. At this point, samples were read at Nanodrop and stored at -80 °C.

3.2.4.b. RNA concentration

The optic density (OD) at 260 and 280 nm of the samples was recorded to calculate the RNA concentration. Only the samples with an OD260/280 ratio (degree of purity) between 1.8 and 2.1 were selected.

Analysis was carried out with NanoDrop 1000 Spectrophotometer and the relative software ND 1000 V3.3.0.

3.2.4.c. cDNA Reverse transcription

Reverse transcription was performed as described by Bachman¹⁸³ with some modifications according to manufacturer indications. 1 µg of total RNA from each sample was diluted in 10 µl of RNase-free

¹⁸² Rio, D. C., Ares, M., Jr, Hannon, G. J., & Nilsen, T. W. (2010). Purification of RNA using TRIzol (TRI reagent). *Cold Spring Harbor protocols*, 2010(6), pdb. prot5439.

¹⁸³ Bachman J. (2013). Reverse-transcription PCR (RT-PCR). *Methods in enzymology*, 530, 67–74.

water. This RNA solution was mixed with 10 μl of master mix (see Table 3), transferred to a 200 μl eppendorf and placed in a 9800 Fast Thermal Cycler (Applied Biosystems).

Product	Volume (μL)
10X RT Buffer	2
25X dNTP mix 100 mM	0,8
10X RT Random Primers	2
Reverse Transcriptase	1
Nuclease Free H ₂ O	4,2
Total per reaction	10

Table 3. Master mix composition used for cDNA reverse transcription.

The volumes are calculated for a reverse transcription master mix of 10 μl , to be mixed with another 10 μl of RNA.

The reverse transcription was carried out according to the conditions showed in Table 4.

	Step 1	Step 2	Step 3	Step 4
Temperature ($^{\circ}\text{C}$)	25	37	85	4
Time (min)	10	120	5	∞

Table 4. Thermal cycler conditions used for reverse transcription reactions. Cycles of time and temperature were set for a reaction volume of 20 μl .

3.2.4.d. cDNA amplification by PCR

The resulting cDNA was used for a PCR amplification as described by Gibbs¹⁸⁴ and Williams et al. with some modifications according to manufacturer indications. 2 μl of cDNA samples were loaded in duplicate in the multi strip with 8 μl of mix solution (see Table 5). Samples were then placed in a StepOne™ Real-Time PCR System and analyzed. The thermal conditions started with an initial holding stage of 20 seconds at 95 $^{\circ}\text{C}$, followed by a two-step cycling stage, repeated for 45 cycles, 1 second denaturation at 95 $^{\circ}\text{C}$ and a subsequent annealing/extension step of 20 seconds at 60 $^{\circ}\text{C}$.

¹⁸⁴ Gibbs, L. S., & Shaffer, J. B. (1990). Nucleotide sequence of bovine copper/zinc superoxide dismutase cDNA generated by the polymerase chain reaction. *Nucleic acids research*, 18(23), 7171.

Component	Volume (μ l)
Reverse Primer	0,5
Forward Primer	0,5
Syber Green	5
H ₂ O Nuclease Free	2

Table 5. Master mix composition used for qRT-PCR. The volumes reported in this table are calculated for a master mix of 8 μ l, to be mixed with 2 μ l of cDNA.

The probes used in this work are listed below (Table 6).

Gene	Probe sequence (5'-3')
CYP1A1 "reverse"	TCTTGGATCTTTCTCTGTACC
CYP1A1 "forward"	CATTAACATCGTCTTGGACC
CYP2E1 "reverse"	TTCATTGAGGAAGTGTCTG
CYP2E1 "forward"	GACACCATTTTCAGAGGATAC
CYP2D6 "reverse"	TTTGGAACTACCACATTGC
CYP2D6 "forward"	CCTATGAGCTTTGTGCTG
CYP2B6 "reverse"	TTTCCATTGGCAAAGATCAC
CYP2B6 "forward"	AGGTTCCGAGAGAAATATGG
CYP3A4 "reverse"	ACATAATGAAGGGGAGAGTG
CYP3A4 "forward"	TAAAGCTCTGTCTGATCTGG
RPS 18 "reverse"	TATTTCTTCTTGGACACACC
RPS 18 "forward"	CAGAAGGATGTAAAGGATGG

Table 6. Probe sequence for each CYP isoform used for qRT-PCR assay. Probes were selected from the manufactured inventory of Sigma Merck.

3.2.4.e. Syber Green chemistry

SYBR® Green is one of the most used fluorescent dyes for performing real-time PCR analysis. It is an asymmetric cyanine dye that binds the minor groove of double-stranded DNA. During the denaturation procedure, the double-stranded DNA melts opening to single-stranded DNA. Then, PCR primers anneal to complementary regions of single-stranded DNA during the hybridization step. After each PCR cycle, the amount of the newly synthesized DNA strands, whose termini are defined by the 5' termini of the two primers, is measured. When bound to the double-stranded DNA, SYBR Green

increases its fluorescence by up to 1000-fold. The fluorescence intensity is directly related to the amount of DNA in the sample (Figure 20).¹⁸⁵

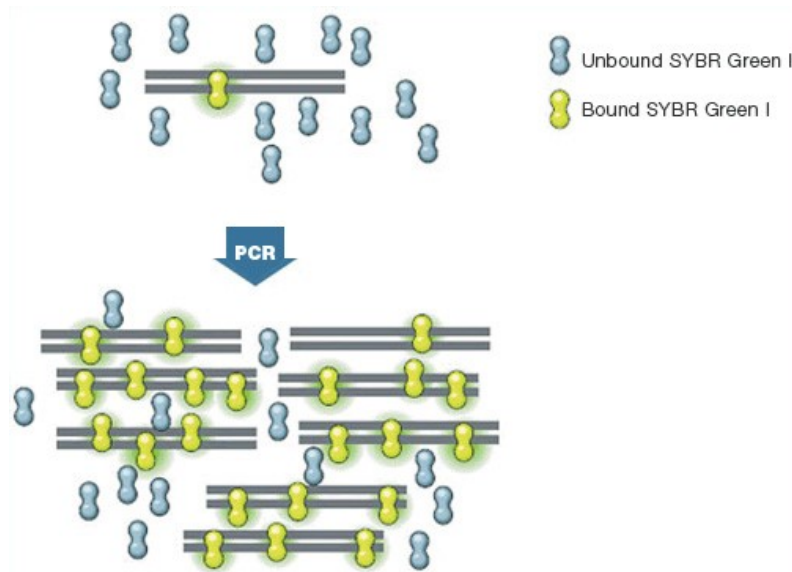


Figure 20. Principle of detection using SYBR[®] Green dye.

This technique aims at measuring the fold changes of samples compared to a “calibrator” (untreated sample) and to a “normalizer” (housekeeping gene expression). During the PCR, the signal of the reporter rises over the cycles, reaching a statistically significant increase over the baseline signal called “threshold”. For each reaction tube, the cycle at which the signal exceeds the threshold is called “threshold cycle” (C_t). The average threshold cycle (C_t) of the technical duplicates of each PCR reaction was used for quantification of the relative mRNA quantification for each isoform and was applied to the $2^{-\Delta\Delta C_t}$ method as described by Livak and Schmittgen¹⁸⁶ and Pfaffl¹⁸⁷. In brief, C_t s for the gene of interest in both the test samples and untreated samples are adjusted with the normalizer gene C_t from the same two samples. The resulting $\Delta\Delta C_t$ value is used to determine the fold difference according to the following formula:

¹⁸⁵ D. Rodríguez-Lázaro, M. Hernández, IDENTIFICATION METHODS | Real-Time PCR, Editor(s): Carl A. Batt, Mary Lou Tortorello, Encyclopedia of Food Microbiology (Second Edition), Academic Press, 2014, Pages 344-350, ISBN 9780123847331,

¹⁸⁶ Livak, K. J., & Schmittgen, T. D. (2001). Analysis of relative gene expression data using real-time quantitative PCR and the 2(-Delta Delta C(T)) Method. *Methods (San Diego, Calif.)*, 25(4), 402–408.

¹⁸⁷ Pfaffl M. W. (2001). A new mathematical model for relative quantification in real-time RT-PCR. *Nucleic acids research*, 29(9), e45.

$$\text{Fold difference: } 2^{-\Delta\Delta C_t}$$

$$\Delta C_{t \text{ sample}} - \Delta C_{t \text{ calibrator}} = \Delta\Delta C_t$$

$$C_{t \text{ GOI}}^S - C_{t \text{ norm}}^S = \Delta C_{t \text{ sample}}$$

$$C_{t \text{ GOI}}^C - C_{t \text{ norm}}^C = \Delta C_{t \text{ calibrator}}$$

In the present study, normalized results were shown as fold change values compared with the mean of control untreated samples.

3.2.4.f. Data Analysis

Results are reported as mean \pm SEM of at least 3 independent experiments and normalized to control values when appropriate. In the case of Western Blot and qRT-PCR, statistical analysis was performed by using One sample t test. For the other assays, one-way ANOVA followed by Bonferroni post test was used (GraphPad Prism version 6.01 for Windows, GraphPad Software, La Jolla California USA, www.graphpad.com). $P < 0.05$ was considered to be significant.

3.3. Results

3.3.1. Effect of differentiation with RA-TPA and RA-BDNF on SH-SY5Y: morphological analysis

3.3.1.a Morphological analysis

Undifferentiated SH-SY5Y cells (UD) demonstrate a large, flat, epithelial-like phenotype, tended to grow in clusters and had short, truncated processes extending from cells at the edges of the clusters (Figure 21, panel A). On the contrary, during the differentiation, SH-SY5Y cells underwent an important slowdown in the rate of proliferation and became a stable population. After three days of RA treatment, it was already possible to observe significant morphological changes: the cells no

longer grew in clusters but uniformly throughout the flask and the cell body presented a more pyramidal shape. In particular, cellular processes began to grow into long and extensive neurites connecting cells even very distant from each other, creating a dense network of interconnections (Figure 21, panel B). At day 7 of differentiation, following subsequent treatment with BDNF or TPA, the cells populations showed neuronal-similar morphology with more polarized cell bodies and numerous elongated processes (Figure 21, panel C and D).

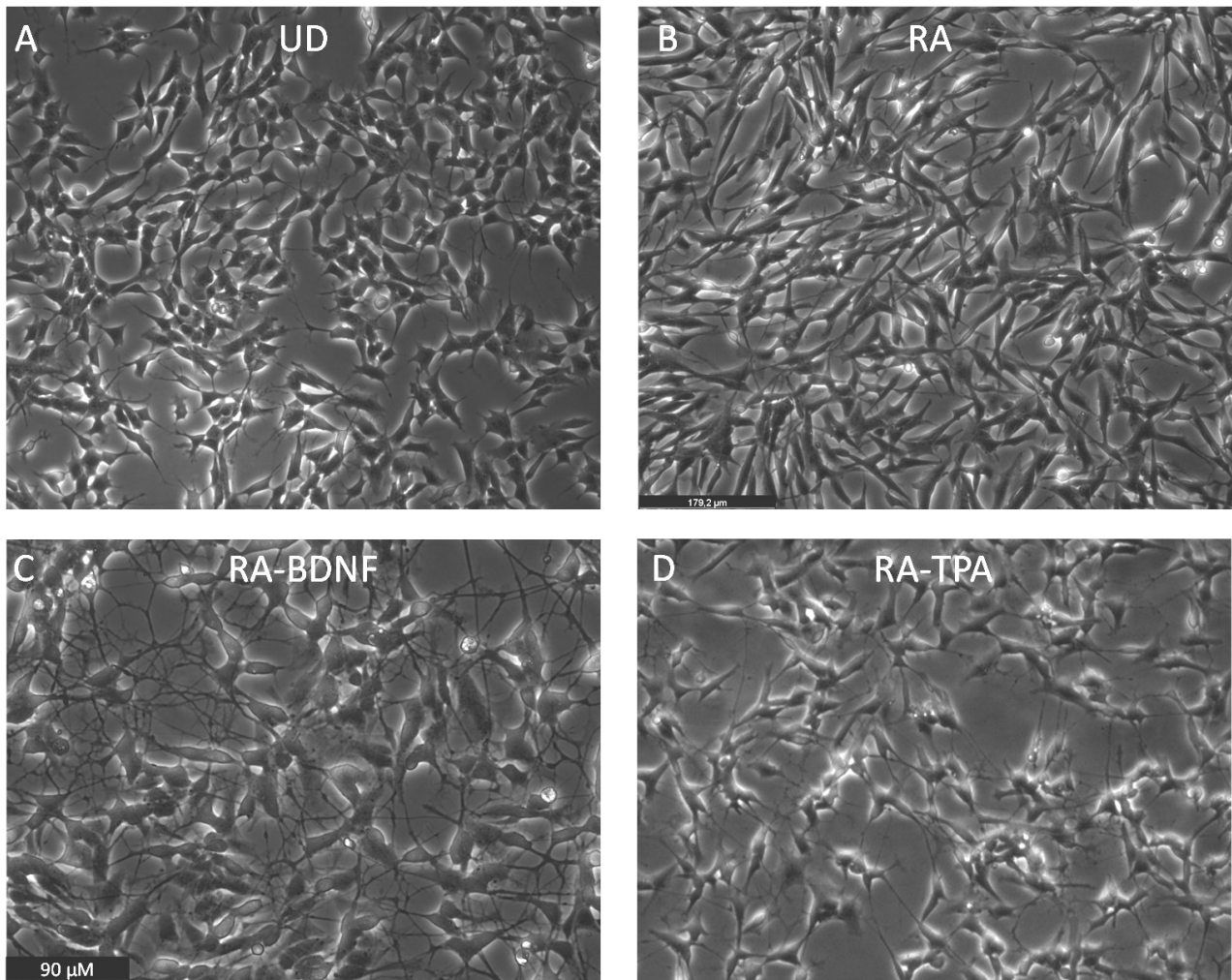


Figure 21. Morphological changes in SH-SY5Y cells promoted by differentiation. (A) The undifferentiated cells (UD) tend to grow in clusters and have a low polarized body with short neuritic processes. (B) In the 3 days RA-differentiated cells, a marked polarization of the cell body, an increase in the number and length of neuritic processes occurred. (C), The most striking difference was noted in the BDNF-differentiated protocol, causing cells with more rounded cell bodies, with dense and interconnected neuritic networks (D) The latter characteristics were reduced by the treatment with TPA, maintaining a more polarized cell body than in UD (scale bar 90 μ m).

As reported in Figure 22, both RA-TPA and RA-BDNF protocols caused a significant increase in the length of neuritic processes but not in their number. Specifically, neurite length increased 2.4-fold in the RA- BDNF cell population and 1.9-fold in RA-TPA cells.

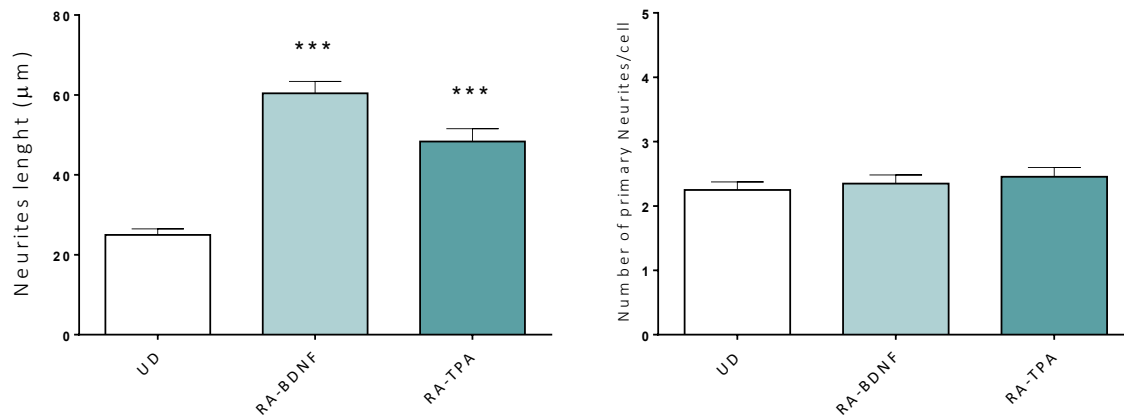


Figure 22. Effect of RA-TPA and RA-BDNF differentiation on the length (left panel) and number of neuritic processes (right panel). Undifferentiated SH-SY5Y cells (UD), grown in standard condition for the same period, were taken as matched controls. The average length of neurites was measured in at least 3 randomly selected images of differentiating SH-SY5Y cells by using ImageJ software. Data were reported as mean \pm SEM of at least 3 independent observations. Statistical analysis was carried out by one-way ANOVA followed by Bonferroni post test. *** $p < 0.001$ vs UD cells.

3.3.2. Expression of specific neuronal markers

To validate the differentiation protocols, the expression of three neuron-specific markers, namely β tubulin III, Synaptophysin and neuronal nuclear protein (NeuN) were analyzed, along with the specific marker for dopaminergic neurons, DAT (Figure 23).

RA, RA-TPA- and RA-BDNF-differentiated cells showed changes in the NeuN expression: this was in fact unchanged (RA) or increased (RA-BDNF) when compared to UD cells, while in RA-TPA population NeuN was elevated as well, though not significantly. Differentiation also rose Synaptophysin expression in RA-TPA- and RA-BDNF-differentiated cells (4.2- and 2.9- fold, respectively). TUBB3 was strikingly increased by 8- or 3.8-fold fold in RA- or RA-BDNF and RA-TPA differentiated cells, respectively. Interestingly, the dopaminergic marker DAT seemed to be halved in the RA-differentiated cells, while in the RA-BDNF- and RA-TPA-differentiated populations it was increased by 1,8 and 2.2-fold, respectively.

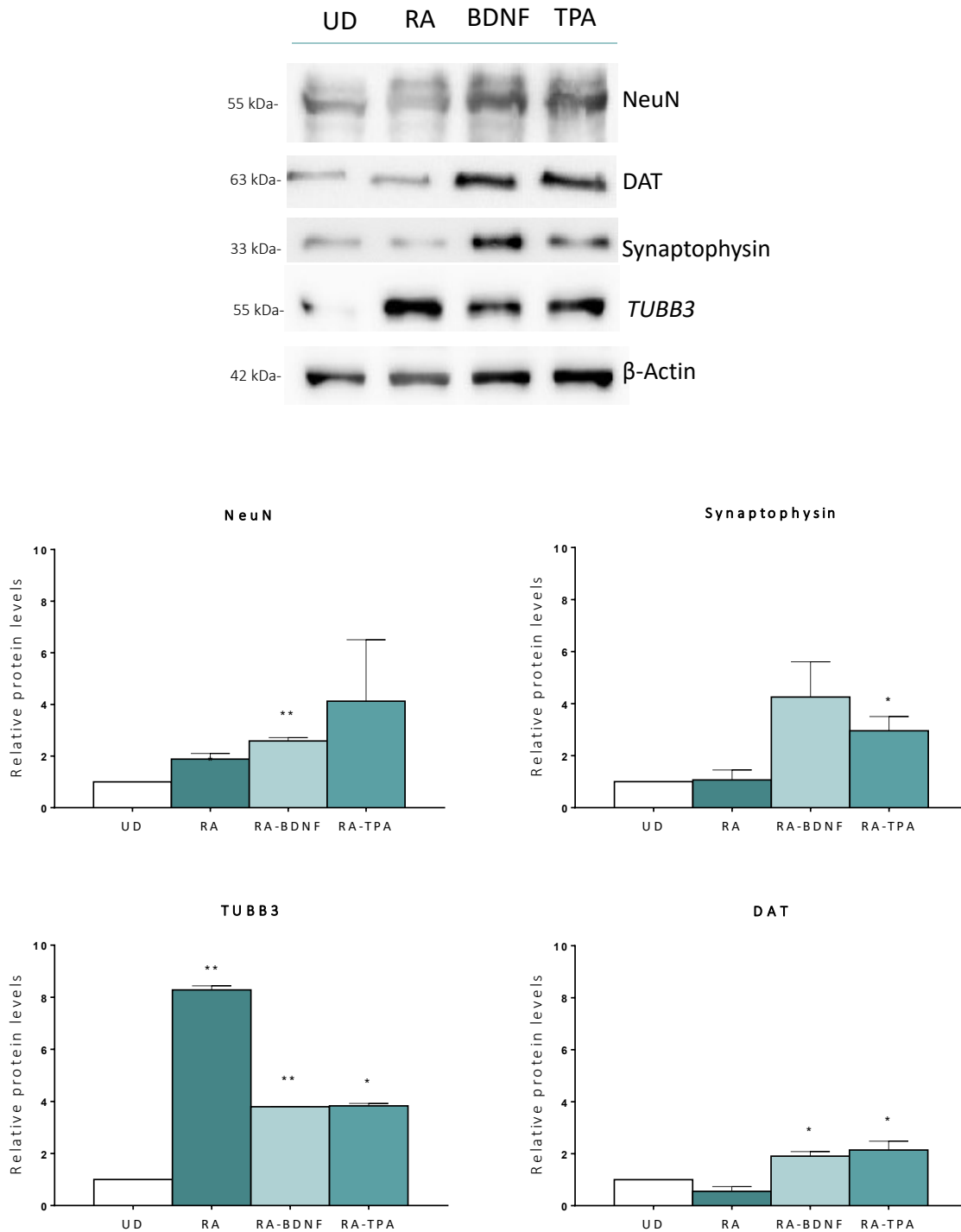


Figure 23. Neuronal protein marker levels in undifferentiated (UD) and differentiated SH-SY5Y cells.

WB analysis of undifferentiated (UD) or differentiated (RA, RA-BDNF, RA-TPA,) SH-SY5Y cell lisates. The top panel depicts a representative blot of proteins of interest in SH-SY5Y cells derived from 30 µg of total cellular lysate. Here and after, molecular mass standards (kDa) are reported on the left of each WB image. Bottom panels: quantitative analysis for the expression of proteins NeuN, Synaptophysin, *TUBB3* and DAT. Bars represent the mean ± SEM of at least three independent experiments. The values of the treated samples (differentiated cells) were compared to the respective control (undifferentiated cells, UD), which was taken as 1-fold level. All samples were normalised with β-actin as housekeeping protein. Statistical analysis was carried out by One sample t test. * $p < 0.05$ ** $p < 0.01$ vs. UD samples.

To further characterize the differentiated SH-SY5Y cell populations and to understand the differences in the expression of different enzymes involved in dopamine metabolism, the expression of MAO A and MAO B was also investigated.

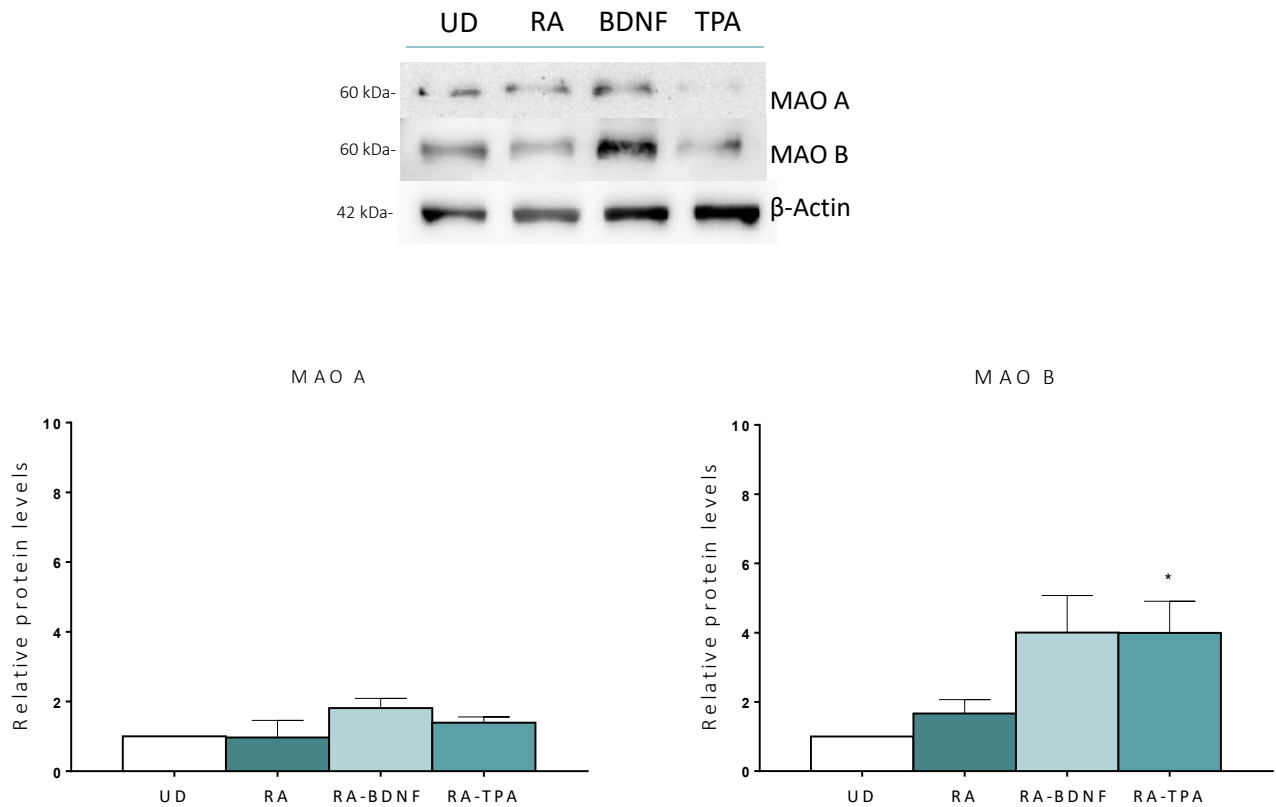


Figure 24. MAO A and MAO B protein levels of undifferentiated (UD) and differentiated SH-SY5Y cells.

WB analysis of undifferentiated (UD) or differentiated (RA, RA-BDNF, RA-TPA,) SH-SY5Y cell lysates. The top panel depicts a representative blot of proteins of interest in SH-SY5Y cells derived from 30 μ g of total cellular lysate. Bottom panels: quantitative analysis for the expression of MAO A and MAO B. Bars represent the mean \pm SEM of at least three independent experiments. The values of the treated samples (differentiated cells) were compared to the respective control (undifferentiated cells, UD), which was taken as 1-fold level. All samples were normalised with β -actin as housekeeping protein. Statistical analysis was carried out by one sample t test. * $p < 0.01$ vs. UD samples

As reported in Figure 24, the differentiation protocol did not promote any significant changes in MAO A expression. Conversely, an increased trend in MAO B protein was observed in fully differentiated cells with RA-BDNF and RA-TPA, respectively of 4- and 3.9-fold, a data preliminary confirmed by the analysis with qRT-PCR for MAO B. In this case, an increase in MAO A and MAO B mRNA expression was observed after the differentiation protocol (Figure 25).

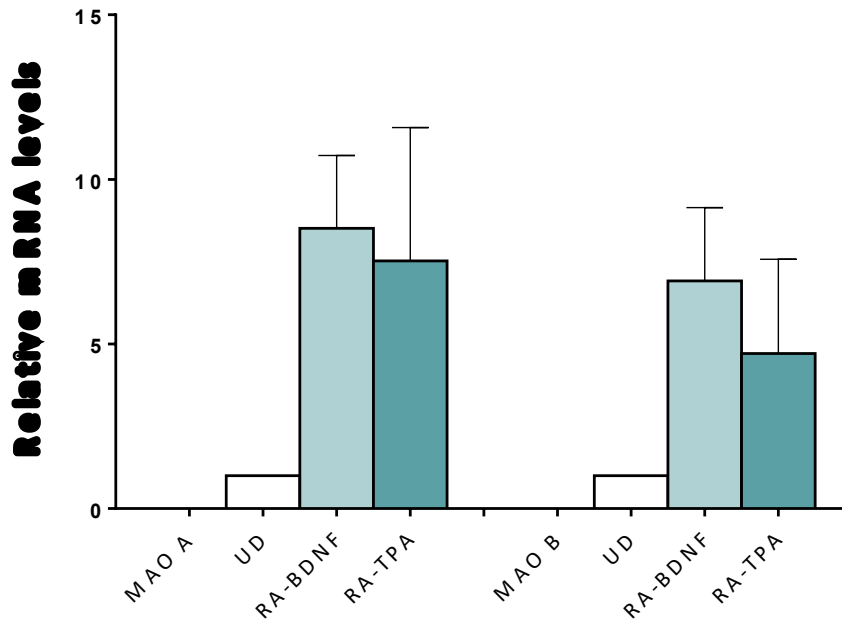


Figure 25. Relative basal mRNA levels of MAO A and MAO B in undifferentiated (UD) and differentiated SH-SY5Y cells. Data are the mean \pm SEM of at least three independent experiments. The values of the treated samples (differentiated cells) were compared to the respective controls (UD), which was taken as 1-fold level. All samples were normalised with RPS18 as housekeeping and statistical analysis was performed by One sample t test.

3.3.3. Effect of RA-BDNF and RA-TPA differentiation on basal CYP450 expression

To get an overview of the expression profile of the mRNA CYP450 in UD and differentiated SH-SY5Y cells, the mRNA basal levels of the isoforms CYP1A1, 3A4, 2D6, 2E1 and 2B6 were explored.

The results showed (Figure 26) that differentiation with RA-BDNF slightly affected the mRNA levels of **CYP1A1** (+2.2-fold), while RA-TPA protocol was most effective as a 5.9-fold increase was observed. The **CYP2D6** mRNA changes were just the opposite as these rose in the case of RA-BDNF (+5.6-fold) and remained unchanged in case of RA-TPA. Moreover, **CYP2E1** mRNA levels were affected by both protocols, increasing by 2.9-fold in RA-BDNF- and 9.8-fold in RA-TPA cells. Finally, the expression of **CYP3A4** is decreased by 0.8-fold in RA-BDNF cells, while RA-TPA protocol did not promote any marked change. The PCR amplification of CYP2B6 did not reveal the presence of this isoform in our *in vitro* model, neither in the undifferentiated SH-SY5Y cells nor in the two neuron-like cell populations obtained with the differentiation protocols.

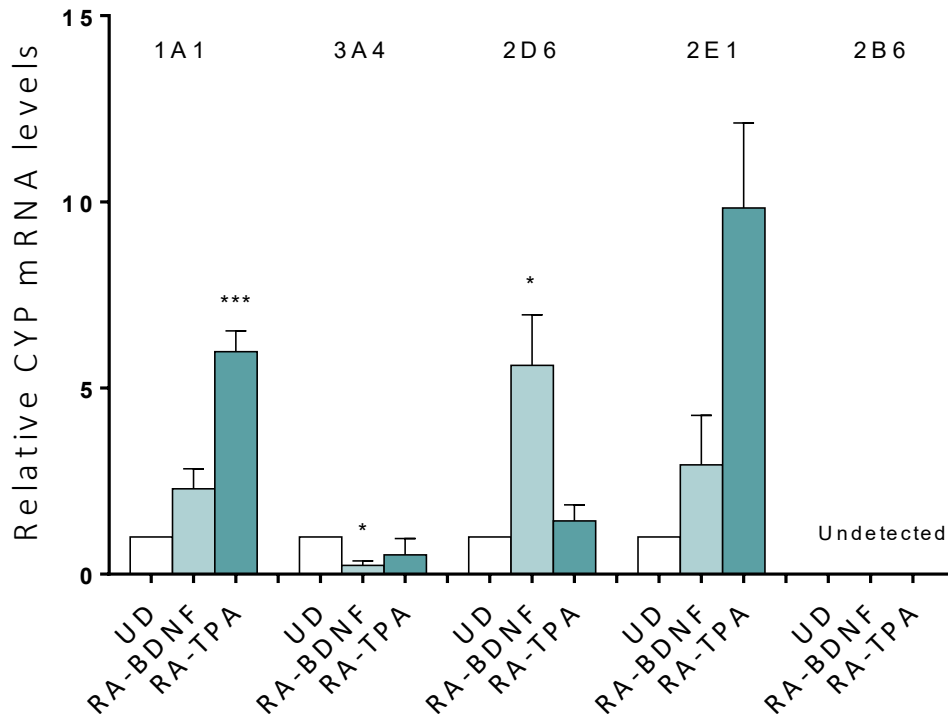


Figure 26. Relative basal mRNA levels of CYP 1A1, 2D6, 2E1 and 3A4 in undifferentiated (UD) and differentiated SH-SY5Y cells. Columns represent the mean \pm SEM of at least three independent experiments. The values of the treated samples (differentiated cells) were compared to the respective controls (undifferentiated cells, UD), which was taken as 1-fold level. All samples were normalised with RPS18 as housekeeping. Statistical analysis was carried out by One sample t test. *** $p < 0.001$, * $p < 0.05$ vs UD CTRL of the respective CYP isoform.

3.4. Discussion

The human cell line SH-SY5Y is often used as an *in vitro* cell model to study the pathogenesis of PD, as the cells have biochemical characteristics similar to human DAergic neurons such as the expression of D1 and D2 receptors, DA synthesis enzymes and DA transporter.^{188,189} Their usefulness for research also consists of the possibility of being differentiated into a more mature neuron-like phenotype cell population. In studies that need to use neuronal differentiated SH-SY5Y cells, however, it is vital to establish and validate a culture protocol that supports the growth of cells with this phenotype. This was the first task of the present study.

¹⁸⁸ Presgraves, S. P., Ahmed, T., Borwege, S., & Joyce, J. N. (2004). Terminally differentiated SH-SY5Y cells provide a model system for studying neuroprotective effects of dopamine agonists. *Neurotoxicity research*, 5(8), 579–598.

¹⁸⁹ McMillan, C. R., Sharma, R., Ottenhof, T., & Niles, L. P. (2007). Modulation of tyrosine hydroxylase expression by melatonin in human SH-SY5Y neuroblastoma cells. *Neuroscience letters*, 419(3), 202–206. 9

For the differentiation, several agents such as RA¹⁹⁰¹⁹¹, BDNF¹⁹², TPA¹⁹³¹⁹⁴, staurosporine¹⁹⁵¹⁹⁶ and conditioned medium of human neural stem cells (CM-hNSCs)¹⁹⁷ have been used to generate a homogenous population of neuronal-like cells. Most studies have either used single or combinations of two differentiating agents to generate and sustain differentiation of the SH-SY5Y cells.¹⁹⁸ Moreover, reducing the amount of FBS in culture medium was reported to facilitate the differentiation process as low FBS could inhibit cells from entering the synthesis (S) phase, causing them to remain for a longer period in the non-proliferative (G₀) phase of cell cycle.¹⁹⁹ Hence, some studies have used different FBS concentrations in the differentiation process; where the percentage of FBS could range from 10%²⁰⁰, 3%²⁰¹, 2.5%²⁰² to 1%²⁰³. On the contrary, serum starvation can cause environmental stress, which can lead to cellular stress response, autophagy, and apoptosis.²⁰⁴

¹⁹⁰ Qiao, J., Paul, P., Lee, S., Qiao, L., Josifi, E., Tiao, J. R., & Chung, D. H. (2012). PI3K/AKT and ERK regulate retinoic acid-induced neuroblastoma cellular differentiation. *Biochemical and biophysical research communications*, 424(3), 421–426.

¹⁹¹ Serdar B, Erkmen T, Ergür B et al (2020) Comparison of medium supplements in terms of the effects on the differentiation of SHSY5Y human neuroblastoma cell line. *Neurol Sci Neurophysiol* 37:82.

¹⁹² Goldie, B. J., Barnett, M. M., & Cairns, M. J. (2014). BDNF and the maturation of posttranscriptional regulatory networks in human SH-SY5Y neuroblast differentiation. *Frontiers in cellular neuroscience*, 8, 325.

¹⁹³ Feio-Azevedo, R., Costa, V. M., Ferreira, L. M., Branco, P. S., Pereira, F. C., Bastos, M. L., Carvalho, F., & Capela, J. P. (2017). Toxicity of the amphetamine metabolites 4-hydroxyamphetamine and 4-hydroxynorephedrine in human dopaminergic differentiated SH-SY5Y cells. *Toxicology letters*, 269, 65–76

¹⁹⁴ Presgraves, S. P., Ahmed, T., Borwege, S., & Joyce, J. N. (2004). Terminally differentiated SH-SY5Y cells provide a model system for studying neuroprotective effects of dopamine agonists. *Neurotoxicity research*, 5(8), 579–598.

¹⁹⁵ Filograna, R., Civiero, L., Ferrari, V., Codolo, G., Greggio, E., Bubacco, L., Beltramini, M., & Bisaglia, M. (2015). Analysis of the Catecholaminergic Phenotype in Human SH-SY5Y and BE (2)-M17 Neuroblastoma Cell Lines upon Differentiation. *PLoS one*, 10(8), e0136769.

¹⁹⁶ Ducray, A. D., Wiedmer, L., Herren, F., Widmer, H. R., & Mevissen, M. (2020). Quantitative Characterization of Phenotypical Markers After Differentiation of SH-SY5Y Cells. *CNS & neurological disorders drug targets*, 19(8), 618–629.

¹⁹⁷ Yang, H., Wang, J., Sun, J., Liu, X., Duan, W. M., & Qu, T. (2016). A new method to effectively and rapidly generate neurons from SH-SY5Y cells. *Neuroscience letters*, 610, 43–47.

¹⁹⁸ Presgraves, S. P., Ahmed, T., Borwege, S., & Joyce, J. N. (2004). Terminally differentiated SH-SY5Y cells provide a model system for studying neuroprotective effects of dopamine agonists. *Neurotoxicity research*, 5(8), 579–598.

¹⁹⁹ Fang, C. Y., Wu, C. C., Fang, C. L., Chen, W. Y., & Chen, C. L. (2017). Long-term growth comparison studies of FBS and FBS alternatives in six head and neck cell lines. *PLoS one*, 12(6), e0178960.

²⁰⁰ Khwanraj, K., Phruksaniyom, C., Madlah, S., & Dharmasaroja, P. (2015). Differential Expression of Tyrosine Hydroxylase Protein and Apoptosis-Related Genes in Differentiated and Undifferentiated SH-SY5Y Neuroblastoma Cells Treated with MPP(.). *Neurology research international*, 2015, 734703.

²⁰¹ Cheung, Y. T., Lau, W. K., Yu, M. S., Lai, C. S., Yeung, S. C., So, K. F., & Chang, R. C. (2009). Effects of all-trans-retinoic acid on human SH-SY5Y neuroblastoma as in vitro model in neurotoxicity research. *Neurotoxicology*, 30(1), 127–135.

²⁰² Shipley, M. M., Mangold, C. A., & Szpara, M. L. (2016). Differentiation of the SH-SY5Y Human Neuroblastoma Cell Line. *Journal of visualized experiments: JoVE*, (108), 53193.

²⁰³ Lopes, F. M., Schröder, R., da Frota, M. L., Jr, Zanotto-Filho, A., Müller, C. B., Pires, A. S., Meurer, R. T., Colpo, G. D., Gelain, D. P., Kapczynski, F., Moreira, J. C., Fernandes, M., & Klamt, F. (2010). Comparison between proliferative and neuron-like SH-SY5Y cells as an in vitro model for Parkinson disease studies. *Brain research*, 1337, 85–94.

²⁰⁴ Rashid, M. U., & Coombs, K. M. (2019). Serum-reduced media impacts on cell viability and protein expression in human lung epithelial cells. *Journal of cellular physiology*, 234(6), 7718–7724.

The RA-mediated differentiation of SH-SY5Y neuroblastoma cells promotes increased expression of choline acetyl transferase (ChAT), vesicular monoamine transporter (VMAT) and NA production, without affecting in the levels of tyrosine hydroxylase (TH) and dopamine transporter (DAT)²⁰⁵. With a few exceptions, the evidence reported by several studies suggests that these cells are shifted towards an adrenergic or cholinergic phenotype, and this is why this type of differentiation was not used herein.²⁰⁶ On the contrary, the differentiation protocol consisting in the treatment with RA followed by TPA leads SH-SY5Y cells to develop a DAergic phenotype with a high expression of D2 and D3 receptors, and increased expression of TH and DAT.²⁰⁷

We have thus focused on these differentiating agents but owing to the role played by the different treatments timing and by the various concentration of FBS to be used, some attempts aimed at finding the ideal conditions were first made. In particular, the protocols tested consisted in: Protocol 1 (3 days with 10 μ M RA+1 % FBS followed by 3 days with 80 nM with TPA+1% FBS) (RA-TPA), already described and widely used²⁰⁸²⁰⁹²¹⁰²¹¹; Protocol 2, based on the RA-BDNF combination. The RA treatment (10 μ M RA+1% FBS for 3 days) was thus followed by 50 ng/ml BDNF treatment that changed for timing and FBS concentration, taking as starting point data from literature²¹²²¹³ (see Figure 27).

²⁰⁵ Cheung, Y. T., Lau, W. K., Yu, M. S., Lai, C. S., Yeung, S. C., So, K. F., & Chang, R. C. (2009). Effects of all-trans-retinoic acid on human SH-SY5Y neuroblastoma as in vitro model in neurotoxicity research. *Neurotoxicology*, 30(1), 127–135. 1

²⁰⁶ Presgraves, S. P., Ahmed, T., Borwege, S., & Joyce, J. N. (2004). Terminally differentiated SH-SY5Y cells provide a model system for studying neuroprotective effects of dopamine agonists. *Neurotoxicity research*, 5(8), 579–598.

²⁰⁷ Ferrari, E., Cardinale, A., Picconi, B., & Gardoni, F. (2020). From cell lines to pluripotent stem cells for modelling Parkinson's Disease. *Journal of neuroscience methods*, 340, 108741.

²⁰⁸ Pählman, S., Ruusala, A. I., Abrahamsson, L., Mattsson, M. E., & Esscher, T. (1984). Retinoic acid-induced differentiation of cultured human neuroblastoma cells: a comparison with phorbol ester-induced differentiation. *Cell differentiation*, 14(2), 135–144.

²⁰⁹ Fernandes, C., Videira, A., Veloso, C. D., Benfeito, S., Soares, P., Martins, J. D., Gonçalves, B., Duarte, J., Santos, A., Oliveira, P. J., Borges, F., Teixeira, J., & Silva, F. (2021). Cytotoxicity and Mitochondrial Effects of Phenolic and Quinone-Based Mitochondria-Targeted and Untargeted Antioxidants on Human Neuronal and Hepatic Cell Lines: A Comparative Analysis. *Biomolecules*, 11(11), 1605.

²¹⁰ Magalingam, K. B., Radhakrishnan, A. K., Somanath, S. D., Md, S., & Haleagrahara, N. (2020). Influence of serum concentration in retinoic acid and phorbol ester induced differentiation of SH-SY5Y human neuroblastoma cell line. *Molecular biology reports*, 47(11), 8775–8788.

²¹¹ Presgraves, S. P., Ahmed, T., Borwege, S., & Joyce, J. N. (2004). Terminally differentiated SH-SY5Y cells provide a model system for studying neuroprotective effects of dopamine agonists. *Neurotoxicity research*, 5(8), 579–598.

²¹² Forster, J. I., Köglberger, S., Trefois, C., Boyd, O., Baumuratov, A. S., Buck, L., Balling, R., & Antony, P. M. (2016). Characterization of Differentiated SH-SY5Y as Neuronal Screening Model Reveals Increased Oxidative Vulnerability. *Journal of biomolecular screening*, 21(5), 496–509.

²¹³ Encinas, M., Iglesias, M., Liu, Y., Wang, H., Muhaisen, A., Ceña, V., Gallego, C., & Comella, J. X. (2000). Sequential treatment of SH-SY5Y cells with retinoic acid and brain-derived neurotrophic factor gives rise to fully differentiated, neurotrophic factor-dependent, human neuron-like cells. *Journal of neurochemistry*, 75(3), 991–1003

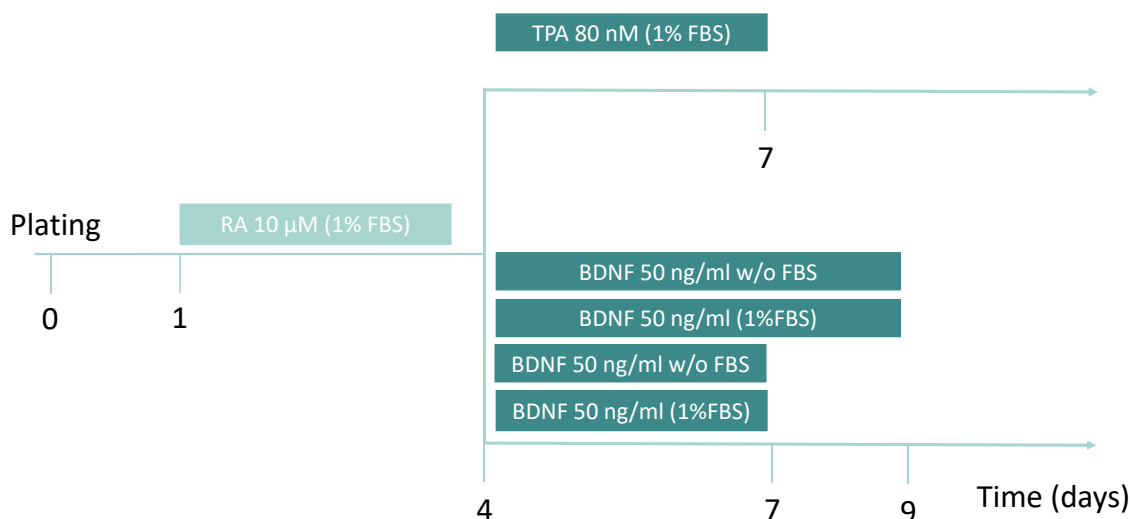


Figure 27. Protocols used to differentiate SH-SY5Y cells.

In Protocol 2, the SH-SY5Y cells responded differently according to the various FBS media supplements and differentiating time and among the tested conditions, that consisting in three days of BDNF 50 ng/ml with 1% FBS resulted to be the most efficient, giving the best results in terms of structural transformation to matured neuronal cells that possess significant striking neuronal cell characteristics such as branched or unbranched neurite outgrowth and elongated cell bodies, connection to the adjacent cells, reduced proliferation, and stability of the cell population. The protocol we have chosen is therefore based on that used by Forster²¹⁴, with some modifications (1% FBS vs 5%, DMEM low glucose vs neurobasal medium in the second step). Thus, the two protocols (RA-TPA and RA-BDNF) were further validated and the degree of neuronal differentiation was evaluated in respect to the alteration in morphological structure, as well as changes in gene and protein expression between the undifferentiated and differentiated SH-SY5Y cells, focusing on some characteristics of human dopaminergic neurones.

Undifferentiated SH-SY5Y cells are morphologically similar to neuroblasts with non-polarized cell bodies and few truncated neurites and grow with a high rate of proliferation forming clusters of cells, interconnected with each other with short neurites. Results showed that both differentiation protocols produced striking changes in these characteristics, making them morphologically more like primary neurons. The undifferentiated cells appeared clumped and with lower and shorter neurite-

²¹⁴ Forster, J. I., Köglberger, S., Trefois, C., Boyd, O., Baumuratov, A. S., Buck, L., Balling, R., & Antony, P. M. (2016). Characterization of Differentiated SH-SY5Y as Neuronal Screening Model Reveals Increased Oxidative Vulnerability. *Journal of biomolecular screening*, 21(5), 496–509.

like processes, poorly connected with to adjacent cells. Differentiation induced by both RA-TPA and RA-BDNF resulted in SH-SY5Y cells with considerably longer neurite processes, which also connect with adjacent cells. In these differentiation media, more SH-SY5Y cells were transformed into mature neurons with longer neurite projections compared to the undifferentiated cells, as outlined by the observed length and number of neurites.

RA-based differentiation of SH-SY5Y cells induces TrkB receptor expression²¹⁵, and their activation is induced by neurotrophins, like BDNF, triggering morphological changes towards neuronal phenotype.²¹⁶ Compared to cells treated with RA alone, in fact, fully differentiated cells (RA-BDNF) formed extended neurites, which were accompanied by low proliferation rate and, importantly, expression of mature neuronal markers. Similarly, the cells treated first with RA and subsequently with TPA behaved similarly in terms of cell growth and morphological changes induced by differentiation, as well as in the expression of mature neuronal markers, which were comparable to those found in the RA-BDNF population. An increase in NeuN expression was in fact observed in cells differentiated with both protocols used (RA- BDNF and RA-TPA), while RA treated cells were negative for NeuN, as also found elsewhere.²¹⁷

As already mentioned, full differentiation of SH-SY5Y cells results in changes in the expression of some genes encoding for neuronal markers, including synaptophysin.²¹⁸²¹⁹ The current results confirmed these data by showing how a significant increase in synaptophysin expression occurred in each cell population tested, particularly in RA-BDNF-differentiated SH-SY5Y.

RA differentiation followed by treatment with the phorbol ester TPA or BDNF significantly elevates the expression of DAT, in agreement with data from literature²²⁰. Moreover, a comparable DAT

²¹⁵ Edsjö, A., Lavenius, E., Nilsson, H., Hoehner, J. C., Simonsson, P., Culp, L. A., Martinsson, T., Larsson, C., & Pålman, S. (2003). Expression of trkB in human neuroblastoma in relation to MYCN expression and retinoic acid treatment. *Laboratory investigation; a journal of technical methods and pathology*, 83(6), 813–823.

²¹⁶ Kaplan, D. R., Matsumoto, K., Lucarelli, E., & Thiele, C. J. (1993). Induction of TrkB by retinoic acid mediates biologic responsiveness to BDNF and differentiation of human neuroblastoma cells. *Eukaryotic Signal Transduction Group. Neuron*, 11(2), 321–331.

²¹⁷ Agholme, L., Lindström, T., Kågedal, K., Marcusson, J., & Hallbeck, M. (2010). An in vitro model for neuroscience: differentiation of SH-SY5Y cells into cells with morphological and biochemical characteristics of mature neurons. *Journal of Alzheimer's disease: JAD*, 20(4), 1069–1082.

²¹⁸ Riegerová, P., Brejcha, J., Bezděková, D., Chum, T., Mašínová, E., Čermáková, N., Ovsepian, S. V., Cebecauer, M., & Štefl, M. (2021). Expression and Localization of AβPP in SH-SY5Y Cells Depends on Differentiation State. *Journal of Alzheimer's disease: JAD*, 82(2), 485–491.

²¹⁹ Ducray, A. D., Wiedmer, L., Herren, F., Widmer, H. R., & Mevissen, M. (2020). Quantitative Characterization of Phenotypical Markers After Differentiation of SH-SY5Y Cells. *CNS & neurological disorders drug targets*, 19(8), 618–629.

²²⁰ Presgraves, S. P., Ahmed, T., Borwege, S., & Joyce, J. N. (2004). Terminally differentiated SH-SY5Y cells provide a model system for studying neuroprotective effects of dopamine agonists. *Neurotoxicity research*, 5(8), 579–598.

expression in RA-TPA and RA-BDNF differentiated SH-SY5Y cells was also shown, suggesting that both these methods equally drive cells towards a DAergic neuronal phenotype.

CYP enzymes catalyze the biotransformation pathways of neuroactive endogenous substrates (neurosteroids, neurotransmitters) and are essential for the detoxification processes of the CNS. With the intention to make clear the basal CYPs profile in undifferentiated and differentiated SH-SY5Y cells, the expression of some isoforms (CYP1A1, 2B6, 2D6, 2E1, 3A4) were explored. Results showed that undifferentiated SH-SY5Y cells express mRNAs for all the above mentioned CYP isoform except for 2B6. Moreover, the differentiation protocol with RA-BDNF was more effective in increasing 2D6 and in some extent also 2E1, while 3A4 and 1A1 were decreased or unchanged respectively. The cell population differentiated with RA-TPA, on the other hand, showed a significant increase in the levels of expression of 1A1 and 2E1, while 3A4 and 2D6 seemed to be unaffected.

To our knowledge, our study is the first to systematically analyze the mRNA levels of these isoforms in both undifferentiated and differentiated SH-SY5Y cells, and results suggest that the differentiating protocols can differently drive the expression of specific CYP isoforms.

In conclusion, the protocols used in this study allowed to obtain differentiated stable SH-SY5Y cell populations, with morphological and biochemical characteristics typical of mature neurons. Overall, the parameters analyzed are in line with those present in the literature for comparable timing, concentrations and treatments used.

The change in MAO B levels found in differentiated cells are an interesting starting point for further study. As is well known, MAO B is one of the two subtypes (MAO A and MAO B) of the major monoamine metabolizing enzyme that oxidizes the neurotransmitter dopamine and breaks down other amines. MAO B is primarily localized primarily into astrocytes whereas MAO A is located largely to neurons in the brain.²²¹ PD and AD are characterized by an increase in MAO activity enzymes, although if this phenomenon is an ancillary process or a contribute to neurons loss is still under debate. In genetically engineered transgenic mice in which MAO-B levels could be specifically induced it was demonstrated that elevation in astrocytic MAO-B per se can induce several PD-related changes,

²²¹ Westlund, K. N., Denney, R. M., Rose, R. M., & Abell, C. W. (1988). Localization of distinct monoamine oxidase A and monoamine oxidase B cell populations in human brainstem. *Neuroscience*, 25(2), 439–456.

suggesting that MAO-B could be directly involved in multiple aspects of the disease neuropathology. The proposed molecular mechanism involves the increase in hydrogen peroxide production, along with its membrane permeability in DA-ergic neurones. This results in augmented dopamine oxidation to dopaminochrome which trigger increased mitochondrial superoxide formation, and finally neuronal degeneration, via interaction with mitochondrial complex I²²². In conclusion, the evidence that differentiation can modulate several proteins and enzymes involved in the metabolism of neurotoxins justify the use of this model in the study of the neurodegeneration promoted by exogenous- as well endogenous-compounds (i.e. salsolinole).

²²² Mallajosyula, J. K., Kaur, D., Chinta, S. J., Rajagopalan, S., Rane, A., Nicholls, D. G., Di Monte, D. A., Macarthur, H., & Andersen, J. K. (2008). MAO-B elevation in mouse brain astrocytes results in Parkinson's pathology. *PLoS one*, 3(2), e1616.

4. Task 2.

Induction of Cytochrome P450 isoforms in SH-SY5Y cells

4.1. Introduction

In the CNS, CYP isoforms have been identified as functional enzymes (although the overall expression is 0.5-2% compared to the liver) and are known to metabolize *in situ* a variety of compounds including centrally acting drugs, xenobiotics, neurotoxins and endogenous compounds such as fatty acids and steroids.²²³ CYP heterogeneous expression in different brain area allows them to reach levels even higher than those of hepatic microsomes and to contribute to local metabolism, influencing their clearance and response to pharmacological therapies or cell damage.

Many factors influence CYP expression and entail physiological- (age, sex, hormones, environment, and genetic polymorphisms) as well as pathological-conditions such as cancer, inflammation, and cholestasis.²²⁴

The marked brain regio-specific distribution²²⁵ of CYP isoforms also varies in response to various chemicals, often their substrates, and can be induced as well as liver isoforms. CYP induction in the brain can occur through various mechanisms: it is mainly transcriptional with a process involving de novo RNA and protein synthesis (receptor transcription factors including PXR, CAR, and AhR), but non-transcriptional mechanisms such as mRNA stabilization, enzymatic stabilization or inhibition of the protein degradation pathway have also been highlighted.²²⁶

The enzymes in the families 1-3 (CYP1A2, 2C9, 2C19, 2D6, 2E1 and 3A4) are the most active in the hepatic metabolism of xenobiotics, whereas the other families have important endogenous functions (see Table 7).

²²³ Miksys, S. L., & Tyndale, R. F. (2002). Drug-metabolizing cytochrome P450s in the brain. *Journal of psychiatry & neuroscience: JPN*, 27(6), 406–415.

²²⁴ Harvey, R. D., & Morgan, E. T. (2014). Cancer, inflammation, and therapy: effects on cytochrome p450-mediated drug metabolism and implications for novel immunotherapeutic agents. *Clinical pharmacology and therapeutics*, 96(4), 449–457.

²²⁵ Stamou, M., Wu, X., Kania-Korwel, I., Lehmler, H. J., & Lein, P. J. (2014). Cytochrome p450 mRNA expression in the rodent brain: species-, sex-, and region-dependent differences. *Drug metabolism and disposition: the biological fate of chemicals*, 42(2), 239–244.

²²⁶ Tompkins, L. M., & Wallace, A. D. (2007). Mechanisms of cytochrome P450 induction. *Journal of biochemical and molecular toxicology*, 21(4), 176–181.

Class of Substrates	CYP Enzymes
Sterols	1B1, 7A1, 7B1, 8B1, 11A1, 11B1, 11B2, 17A1, 19A1, 21A2, 27A1, 39A1, 46A1, 51A1
Xenobiotics	1A1, 1A2, 2A6, 2A13, 2B6, 2C8, 2C9, 2C18, 2C19, 2D6, 2E1, 2F1, 3A4, 3A5, 3A7
Fatty acids	2J2, 4A11, 4B1, 4F12
Eicosanoids	4F2, 4F3, 4F8, 5A1, 8A1
Vitamins	2R1, 24A1, 26A1, 26B1, 26C1, 27B1
Unknown	2A7, 2S1, 2U1, 2W1, 3A43, 4A22, 4F11, 4F22, 4V2, 4X1, 4Z1, 20A1, 27C1

Table 7. Classification of human P450s based on major substrate class ²²⁷

Considering this background and the evidence currently present in the literature, in this study we focused on some cytochrome isoforms involved in metabolism of xenobiotics (CYP3A4-2D6-2E1-1A1-2B6), studying the possibility to induce them upon the treatment with well-known inducers such as β NF and the EtOH²²⁸ in UD and differentiated SH-SY5Y cells. Changes in mRNA expression of the above-mentioned CYP isoforms were assessed by using qRT-PCR. Exposure time for maximal response of CYP induction potential treatments was extrapolated from studies in the literature on the kinetics of formation and degradation of CYP enzymes.²²⁹

4.2. Methods

4.2.1. Cell culture and cell differentiation

Undifferentiated SH-SY5Y cells were seeded as reported in section 2.4.5. Differentiation with RA+BDNF or RA+TPA was performed according to the protocols reported in section 3.2.1.

²²⁷ Manikandan, P., & Nagini, S. (2018). Cytochrome P450 Structure, Function and Clinical Significance: A Review. *Current drug targets*, 19(1), 38–54.

²²⁸ Fernandez-Abascal, J., Ripullone, M., Valeri, A., Leone, C., & Valoti, M. (2018). β -Naphthoflavone and Ethanol Induce Cytochrome P450 and Protect towards MPP⁺ Toxicity in Human Neuroblastoma SH-SY5Y Cells. *International journal of molecular sciences*, 19(11), 3369.

²²⁹ Zhang, J. G., Ho, T., Callendrello, A. L., Crespi, C. L., & Stresser, D. M. (2010). A multi-endpoint evaluation of cytochrome P450 1A2, 2B6 and 3A4 induction response in human hepatocyte cultures after treatment with β -naphthoflavone, phenobarbital and rifampicin. *Drug metabolism letters*, 4(4), 185–194.

4.2.2. CYP-induction

Cells separately were treated for 48 hours with the following well-known inducers β NF (4 μ M) and EtOH (100 mM). Afterward qRT-PCR was performed.

4.2.3. Quantitative real-time PCR

Quantitative real-time PCR was carried out as described in section 3.2.4.

4.3. Results

From a general point of view, both β NF and EtOH showed different effects both in of induction of single specific CYP isoforms and in terms of activity within the specif population of SH-SY5Y cells tested (UD, RA-TPA, RA-BDNF).

CYP1A1

The results showed that β NF increased CYP1A1 mRNA levels by 1.8- fold in UD cells, while it was less effective in RA-BDNF and in RA-TPA cells, in which differentiation already elevated this isoform levels (2.2- and 5.9- fold increase respectively). Changes in mRNA 1A1 levels were also observed when EtOH was used, as a 1.8-fold increase occurred in UD cells, while in RA-BDNF cells the expression was comparable to that of the controls (Figure 28 panel A).

CYP3A4

β NF was ineffective in changing CYP3A4 expression in all SH-SY5Y population under investigation. On the other hand, EtOH-mediated effects were similar, although an upward trend seemed to occur in UD, while in RA-BDNF a significant increase in mRNA levels by 2.3-fold occurred (Figure 28, panel B).

CYP2D6

CYP2D6 mRNA was found to be rised by both inducers used in UD cells, in which was observed an increase in its expression of 1.6- and 1.8-fold by β NF and EtOH, respectively (Figure 29, panel A). In

both differentiated cells populations both compounds seemed ineffective towards this CYP isoform, although an upward trend seemed to occur in the RA-TPA cells, while 2D6 mRNA was already upregulated by the differentiation in the RA-BDNF.

CYP2E1

β NF- and EtOH-mediated effects suggested a trend in the increase in 2E1 isoform in UD and RA-BDNF cells. These however were statistically significant in case β NF treatment in UD. (Figure 29 panel B). In the RA-TPA cell population, a basal increase in 2E1 mRNA expression was observed compared to UD cells (9.8-fold), and with both β NF and EtOH a downward trend seemed to occur.

CYP2B6

qRT-PCR did not reveal the presence of basal levels of the 2B6 isoform in our *in vitro* SH-SY5Y models, neither an induction was observed upon β NF and EtOH treatment (data not shown).

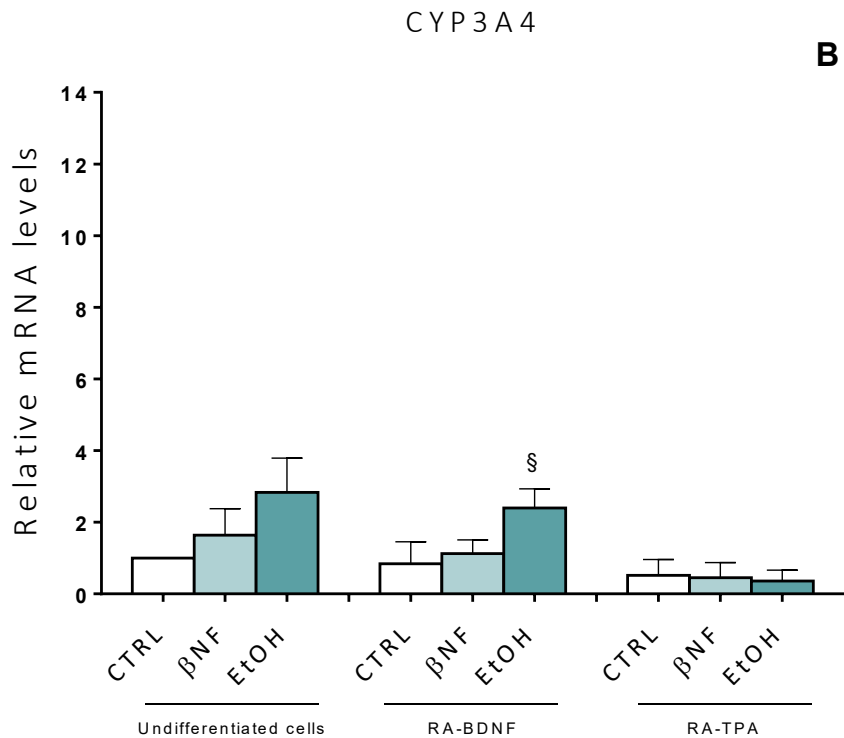
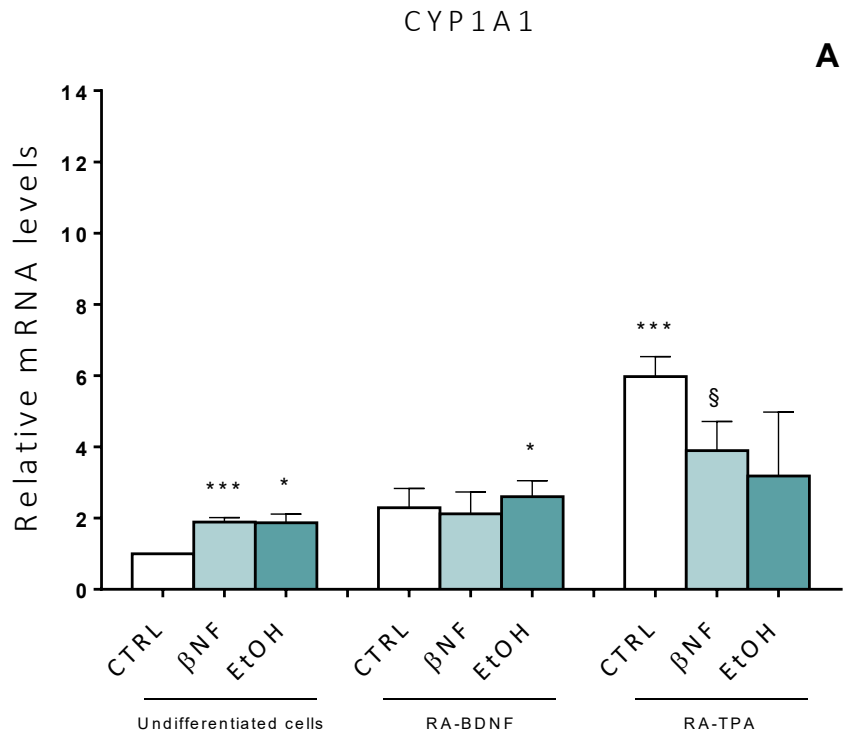


Figure 28. Relative mRNA levels of CYP1A1 (panel A) and CYP3A4 (panel B) in UD and differentiated SH-SY5Y cells following the treatment with βNF (4 μM, 48h) or EtOH (100 mM, 48h). Columns represent the mean ± SEM of at least three independent experiments. The values of the treated samples were compared to the control sample, which was taken as 1-fold level. All samples were normalised with RPS18 as housekeeping. Statistical analysis was carried out by One sample t test or by t test as appropriate *** $p < 0.001$, * $p < 0.05$ vs UD CTRL, § $p < 0.05$ vs respective CTRL (RA-BDNF or RA-TPA).

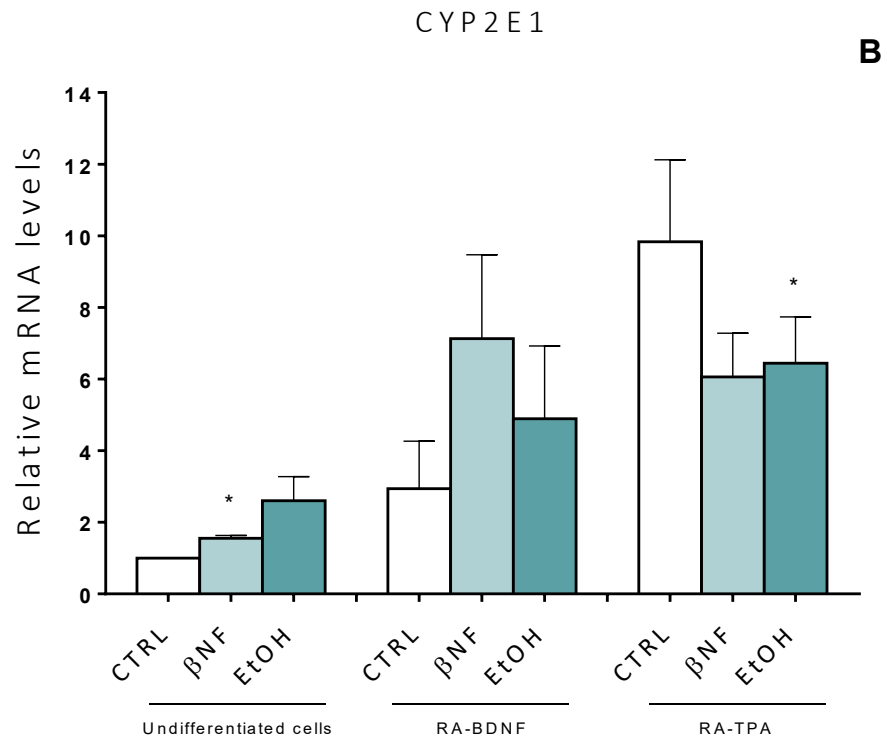
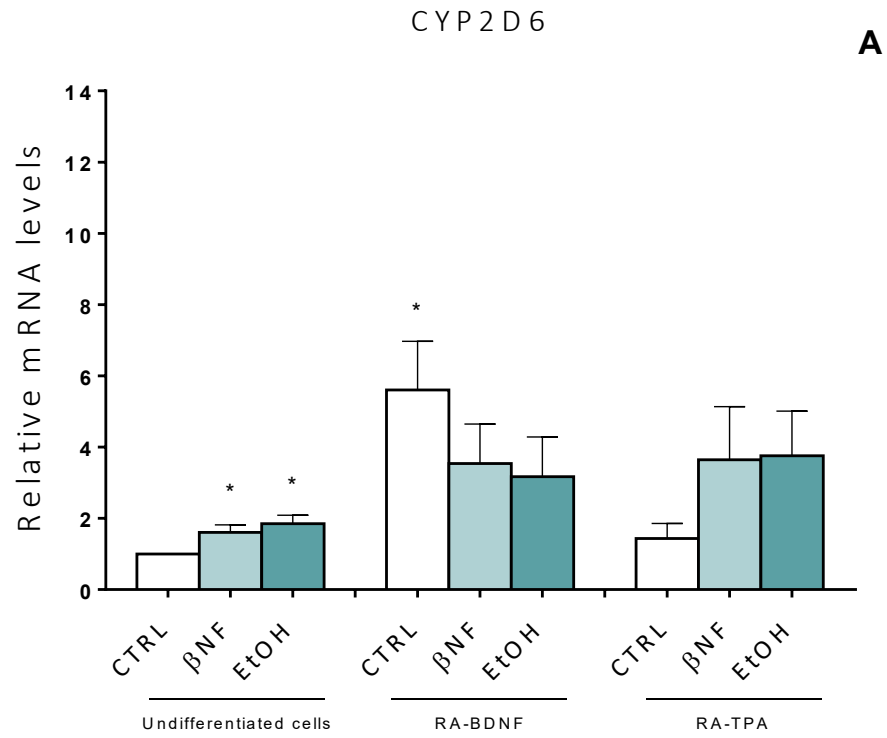


Figure 29. Relative mRNA levels of CYP2D6 (panel A) and CYP2E1 (panel B) in UD and differentiated SH-SY5Y cells following the treatment with β NF (4 μ M, 48h) or EtOH (100 mM, 48h). Columns represent the mean \pm SEM of at least three independent experiments. The values of the treated samples were compared to the control sample, which was taken as 1-fold level. All samples were normalised with RPS18 as housekeeping. Statistical analysis was carried out by One sample t test * $p < 0.05$ vs UD CTRL.

4.4. Discussion

The CYPs function and significance in brain is a research field of interest because most of the neuroactive drugs used in therapy today are not only substrates but also inducers of brain P450s. This can significantly impact the efficacy of drugs as well as the neurodegenerative processes promoted by xenobiotics. Cerebral CYP isoforms fulfill certain functions within specific cell types of the brain and their expression is differentially modulated by those in the liver.²³⁰ Several *in vitro* studies have reported unequal distribution, expression and inducibility of CYPs both in primary cultures of rat neuronal and glial cells and in immortal neuronal and glial cell lines.^{231,232} The potential induction of some isoforms in both undifferentiated and differentiated neuroblastoma SH-SY5Y cells was investigated with the final aim of elucidating the role of CYPs in the neuronal response to xenobiotics/neurotoxins.

PCR analysis revealed different behavior of the two inducers toward the CYPs isozymes. CYP1A1 was induced in UD cells while β NF and EtOH were ineffective in differentiated cells, in which the differentiation protocols already promoted an increase in mRNA expression of this isoform.

As previously observed in our laboratory,²³³ a different behavior was observed regarding the modulation of CYP2D6 and 2E1. In fact, both treatments increased the mRNA of CYP2D6 in UD. On the contrary, either β NF or EtOH seemed ineffective in differentiated cells. It is worth to note, however, that the differentiation procedure with RA-BDNF, but not that with RA-TPA, already upregulated CYP2D6.

Several studies indicate that in the liver 2D6 is not an inducible CYP isoform,²³⁴ while is differentially regulated in the brain. The pionieristic study of Tyndale group, in fact, demonstrated that the *in vivo* treatment with nicotine increased CYP2D6 in the brain of African green monkeys while remaining

²³⁰ Miksys, S., & Tyndale, R. F. (2006). Nicotine induces brain CYP enzymes: relevance to Parkinson's disease. *Journal of neural transmission. Supplementum*, (70), 177–180.

²³¹ Tripathi, V. K., Kumar, V., Singh, A. K., Kashyap, M. P., Jahan, S., Kumar, D., & Lohani, M. (2013). Differences in the expression and sensitivity of cultured rat brain neuronal and glial cells toward the monocrotophos. *Toxicology international*, 20(2), 177–185.

²³² Korashy, H. M., Abuhashish, H. M., & Maayah, Z. H. (2013). The role of aryl hydrocarbon receptor-regulated cytochrome P450 enzymes in glioma. *Current pharmaceutical design*, 19(40), 7155–7166.

²³³ Fernandez-Abascal, J., Ripullone, M., Valeri, A., Leone, C., & Valoti, M. (2018). β -Naphthoflavone and Ethanol Induce Cytochrome P450 and Protect towards MPP⁺ Toxicity in Human Neuroblastoma SH-SY5Y Cells. *International journal of molecular sciences*, 19(11), 3369.

²³⁴ Benedetti M. S. (2000). Enzyme induction and inhibition by new antiepileptic drugs: a review of human studies. *Fundamental & clinical pharmacology*, 14(4), 301–319.

unchanged in the liver.²³⁵ On the other hand, the EtOH-mediated CYP2D6 up-regulation observed in these results agrees with other reports describing an *in vitro* induction of this isoform by the same compound.²³⁶ The evidence of the induction of CYP2D6 in SH-SY5Y cells, in conflict with what occurs in hepatocytes, suggests that this isoform is differently controlled in the neuroblastoma cell line. Recently, Zhang, et al.²³⁷ suggested the involvement of PPARs in the regulation of CYP2D6 in both mouse brain and undifferentiated SH-SY5Y cells, but if this is the also the case of RA-BDNF differentiated population is a matter of future studies.

β NF was significantly effective in inducing the CYP2E1 isoform in all cell populations tested (UD SH-SY5Y, differentiated with RA-BDNF, differentiated with RA-TPA). This was found despite the fact that AhR receptor, of which β NF is a potent agonist, was not detected in both UD SH-SY5Y and RA-BDNF differentiated cells.²³⁸ CYP2E1 is transcriptionally activated by EtOH in the hippocampus and cerebellum²³⁹, while previous reports have shown that EtOH can induce CYP2E1 expression by activating multiple signaling pathways and transcription factors in cultured astrocytes²⁴⁰ and rat brain neuronal cells.²⁴¹ Conversely, the treatment with EtOH in our model did not increase of the CYP2E1 mRNA levels in undifferentiated SH-SY5Y and differentiated RA-BDNF cells. This contrasting results might be due to the fact that EtOH-mediated CYP2E1 induction seems to occur by translational, posttranslational (protein stabilization), and transcriptional mechanisms.²⁴² Thus, CYP2E1 induction involves posttranscriptional stabilization of CYP2E1, unlike other CYP isoform induction processes involving de novo RNA and protein synthesis. The induction of CYP2E1 seems to be regulated at the

²³⁵ Mann, A., Miksys, S., Lee, A., Mash, D. C., & Tyndale, R. F. (2008). Induction of the drug metabolizing enzyme CYP2D in monkey brain by chronic nicotine treatment. *Neuropharmacology*, 55(7), 1147–1155.

²³⁶ Hellum, B. H., & Nilsen, O. G. (2007). The in vitro inhibitory potential of trade herbal products on human CYP2D6-mediated metabolism and the influence of ethanol. *Basic & clinical pharmacology & toxicology*, 101(5), 350–358.

²³⁷ Zhang, F., Li, J., Na, S., Wu, J., Yang, Z., Xie, X., Wan, Y., Li, K., & Yue, J. (2018). The Involvement of PPARs in the Selective Regulation of Brain CYP2D by Growth Hormone. *Neuroscience*, 379, 115–125.

²³⁸ Imran, S., Ferretti, P., & Vrzal, R. (2015). Different regulation of aryl hydrocarbon receptor-regulated genes in response to dioxin in undifferentiated and neuronally differentiated human neuroblastoma SH-SY5Y cells. *Toxicology mechanisms and methods*, 25(9), 689–697.

²³⁹ Zhong, Y., Dong, G., Luo, H., Cao, J., Wang, C., Wu, J., Feng, Y. Q., & Yue, J. (2012). Induction of brain CYP2E1 by chronic ethanol treatment and related oxidative stress in hippocampus, cerebellum, and brainstem. *Toxicology*, 302(2-3), 275–284.

²⁴⁰ Vallés, S. L., Blanco, A. M., Pascual, M., & Guerri, C. (2004). Chronic ethanol treatment enhances inflammatory mediators and cell death in the brain and in astrocytes. *Brain pathology (Zurich, Switzerland)*, 14(4), 365–371.

²⁴¹ Kapoor, N., Pant, A. B., Dhawan, A., Dwivedi, U. N., Gupta, Y. K., Seth, P. K., & Parmar, D. (2006). Differences in sensitivity of cultured rat brain neuronal and glial cytochrome P450 2E1 to ethanol. *Life sciences*, 79(16), 1514–1522.

²⁴² Novak, R. F., & Woodcroft, K. J. (2000). The alcohol-inducible form of cytochrome P450 (CYP 2E1): role in toxicology and regulation of expression. *Archives of pharmacal research*, 23(4), 267–282.

posttranscriptional or posttranslational levels by the stabilization of mRNA²⁴³ or by protection against the rapid degradation of protein²⁴⁴ as seen in the liver. Further investigations are needed to clarify these controversial results.

The induction of CYP1A1 by β NF has already been reported in various *in vitro* models, including hepatocytes in which β NF caused increased mRNA, proteins, and enzymatic activity²⁴⁵, and partially in human neuroblastoma cells (mRNA only).²⁴⁶ In our experimental conditions, β NF increased CYP1A1 expression in UD cells, decreased in RA-TPA cells and remained stable in RA-BDNF population. On the other hand, EtOH treatment induced the 1A1 isoform in UD cells. In RA-BDNF and RA-TPA cells, in fact, its expression was comparable to those of the differentiated control. As described in literature, AhR is not expressed in undifferentiated or in the RA-BDNF differentiated-SH-SY5Y cells, although obtained by a different timing protocol respect to that used herein.^{247,248} Given this, the reason behind CYP1A1 induction in SH-SY5Y cells lacking AhR remains unclear. A plausible explanation for differentiated SH-SY5Y might involve epigenetic changes upon treatment with RA^{249,250}. Therefore,

²⁴³ Song, B. J., Matsunaga, T., Hardwick, J. P., Park, S. S., Veech, R. L., Yang, C. S., Gelboin, H. V., & Gonzalez, F. J. (1987). Stabilization of cytochrome P450j messenger ribonucleic acid in the diabetic rat. *Molecular endocrinology (Baltimore, Md.)*, 1(8), 542–547.

²⁴⁴ Roberts, B. J., Song, B. J., Soh, Y., Park, S. S., & Shoaf, S. E. (1995). Ethanol induces CYP2E1 by protein stabilization. Role of ubiquitin conjugation in the rapid degradation of CYP2E1. *The Journal of biological chemistry*, 270(50), 29632–29635.

²⁴⁵ Lněničková, K., Skálová, L., Stuchlíková, L., Sztotáková, B., & Matoušková, P. (2018). Induction of xenobiotic-metabolizing enzymes in hepatocytes by beta-naphthoflavone: Time-dependent changes in activities, protein and mRNA levels. *Acta pharmaceutica (Zagreb, Croatia)*, 68(1), 75–85.

²⁴⁶ Fernandez-Abascal, J., Ripullone, M., Valeri, A., Leone, C., & Valoti, M. (2018). β -Naphthoflavone and Ethanol Induce Cytochrome P450 and Protect towards MPP⁺ Toxicity in Human Neuroblastoma SH-SY5Y Cells. *International journal of molecular sciences*, 19(11), 3369.

²⁴⁷ Gassmann, K., Abel, J., Bothe, H., Haarmann-Stemmann, T., Merk, H. F., Quasthoff, K. N., Rockel, T. D., Schreiber, T., & Fritsche, E. (2010). Species-specific differential AhR expression protects human neural progenitor cells against developmental neurotoxicity of PAHs. *Environmental health perspectives*, 118(11), 1571–1577.

²⁴⁸ Imran, S., Ferretti, P., & Vrzal, R. (2015). Different regulation of aryl hydrocarbon receptor-regulated genes in response to dioxin in undifferentiated and neuronally differentiated human neuroblastoma SH-SY5Y cells. *Toxicology mechanisms and methods*, 25(9), 689–697.

²⁴⁹ Zuchegna, C., Aceto, F., Bertoni, A., Romano, A., Perillo, B., Laccetti, P., Gottesman, M. E., Avvedimento, E. V., & Porcellini, A. (2014). Mechanism of retinoic acid-induced transcription: histone code, DNA oxidation and formation of chromatin loops. *Nucleic acids research*, 42(17), 11040–11055.

²⁵⁰ Szychowski, K. A., Skóra, B., & Mańdziuk, M. (2021). Tris (2,3-Dibromopropyl) Isocyanurate (TDBP-TAZTO or TBC) Shows Different Toxicity Depending on the Degree of Differentiation of the Human Neuroblastoma (SH-SY5Y) Cell Line. *Neurotoxicity research*, 39(5), 1575–1588.

the possibility that CYP1A1 regulation may involve AhR receptor-independent mechanisms, such as miRNA²⁵¹ or PMTs, cannot be excluded.²⁵²

In all the cell populations tested, the expression of the 3A4 isoform was not affected after 48h treatment with β NF. On the other hand, EtOH significantly increased the expression levels of this isoform in SH-SY5Y cells differentiated with RA-BDNF. Furthermore, the basal expression of this isoform was significantly reduced during the differentiation process with RA-BDNF, while in RA-TPA cells was comparable to that found in UD. This difference may be due to changes in the global protein regulatory profile promoted by differentiation, such as miRNAs or activation/inactivation of signaling pathways.²⁵³²⁵⁴

Taken together, the present results suggest that CYP isozymes can be modulated by exposing cells to different compounds such as CYP inducers as well as differentiating agents. Further studies are, however, needed to understand the molecular mechanisms involved in the regulation of CYP isoforms in SH-SY5Y cells, since CYPs inducibility can extremely variate between undifferentiated and differentiated populations, as also reported for *in vivo* and *in vitro* liver and primary hepatocytes models.²⁵⁵

²⁵¹ Li, D., Tolleson, W. H., Yu, D., Chen, S., Guo, L., Xiao, W., Tong, W., & Ning, B. (2019). Regulation of cytochrome P450 expression by microRNAs and long noncoding RNAs: Epigenetic mechanisms in environmental toxicology and carcinogenesis. *Journal of environmental science and health. Part C, Environmental carcinogenesis & ecotoxicology reviews*, 37(3), 180–214.

²⁵² He, Z. X., Chen, X. W., Zhou, Z. W., & Zhou, S. F. (2015). Impact of physiological, pathological, and environmental factors on the expression and activity of human cytochrome P450 2D6 and implications in precision medicine. *Drug metabolism reviews*, 47(4), 470–519.

²⁵³ Pandey, A., Sarkar, S., Yadav, S. K., Yadav, S. S., Srikrishna, S., Siddiqui, M. H., Parmar, D., & Yadav, S. (2022). Studies on Regulation of Global Protein Profile and Cellular Bioenergetics of Differentiating SH-SY5Y Cells. *Molecular neurobiology*, 59(3), 1799–1818.

²⁵⁴ Xie, H. R., Hu, L. S., & Li, G. Y. (2010). SH-SY5Y human neuroblastoma cell line: in vitro cell model of dopaminergic neurons in Parkinson's disease. *Chinese medical journal*, 123(8), 1086–1092.

²⁵⁵ Berger, B., Donzelli, M., Maseneni, S., Boess, F., Roth, A., Krähenbühl, S., & Haschke, M. (2016). Comparison of Liver Cell Models Using the Basel Phenotyping Cocktail. *Frontiers in pharmacology*, 7, 443.

5. Task 3.

Role of CYP450 against dopaminergic neurotoxins- promoted damage

5.1. Introduction

The intracellular localization of CYPs is still under study, but it seems that this aspect, together with the different concentrations and relative distributions of the isoforms in the brain, together with the sensitivity to be inducible, may contribute to the variation of the therapeutic response and of the side effects to drugs and xenobiotics in general. It is established that, in general, hepatic CYPs are located in the ER. However, it has been shown that some isoforms can be present at the mitochondrial level in the brain.^{256,257} The localization of CYP in mitochondria can contribute to the bioactivation/detoxification processes of neurotoxins such as MPP⁺, paraquat, and Rotenone, that target the mitochondria and lead to the impairment of their functions. The results of our previous study reported that the 2D6 isoform is localized at mitochondria, and at a minor level, at ER in UD SH-SY5Y.²⁵⁸ This experimental evidence may represent another important perspective of the role of CYP2D6 in detoxification processes, since this isoform is proposed to be neuroprotective against xenobiotics targeting the mitochondria, such as the MPP⁺. In contrast, CYP2E1 appeared to partially localize in the ER, although other groups have indicated the possibility that CYP2E1 may target the mitochondria in other *in vitro* and *in vivo* models.^{259,260,261} Moreover, the localization images of CYP1A1 and 3A4 showed no preferential localization of these isoforms for either mitochondria or ER.

To study the role of CYPs in neuroprotection, specific isoforms were induced by using β NF and EtOH as reported in Task 2. This induction represents a powerful tool for studying the role of CYP in the metabolism of xenobiotics in cell cultures, thus bringing new insights into the molecular mechanisms

²⁵⁶ Marini, S., Nannelli, A., Sodini, D., Dragoni, S., Valoti, M., Longo, V., & Gervasi, P. G. (2007). Expression, microsomal and mitochondrial activities of cytochrome P450 enzymes in brain regions from control and phenobarbital-treated rabbits. *Life sciences*, *80*(10), 910–917.

²⁵⁷ Miksys, S. L., & Tyndale, R. F. (2002). Drug-metabolizing cytochrome P450s in the brain. *Journal of psychiatry & neuroscience: JPN*, *27*(6), 406–415.

²⁵⁸ Fernandez-Abascal, J., Ripullone, M., Valeri, A., Leone, C., & Valoti, M. (2018). β -Naphthoflavone and Ethanol Induce Cytochrome P450 and Protect towards MPP⁺ Toxicity in Human Neuroblastoma SH-SY5Y Cells. *International journal of molecular sciences*, *19*(11), 3369.

²⁵⁹ Bansal, S., Anandatheerthavarada, H. K., Prabu, G. K., Milne, G. L., Martin, M. V., Guengerich, F. P., & Avadhani, N. G. (2013). Human cytochrome P450 2E1 mutations that alter mitochondrial targeting efficiency and susceptibility to ethanol-induced toxicity in cellular models. *The Journal of biological chemistry*, *288*(18), 12627–12644.

²⁶⁰ Lavandera, J., Ruspini, S., Batlle, A., & Buzaleh, A. M. (2015). Cytochrome P450 expression in mouse brain: specific isoenzymes involved in Phase I metabolizing system of porphyrinogenic agents in both microsomes and mitochondria. *Biochemistry and cell biology = Biochimie et biologie cellulaire*, *93*(1), 102–107.

²⁶¹ Valencia-Olvera, A. C., Morán, J., Camacho-Carranza, R., Prospéro-García, O., & Espinosa-Aguirre, J. J. (2014). CYP2E1 induction leads to oxidative stress and cytotoxicity in glutathione-depleted cerebellar granule neurons. *Toxicology in vitro: an international journal published in association with BIBRA*, *28*(7), 1206–1214.

underlying the damage to dopaminergic neurons. In particular, UD and differentiated neuroblastoma SHSY5Y cells were treated with these two inducers before and during MPP⁺ and Rotenone exposure and cells viability, along with mitochondria performances were assessed.

5.2. Methods

5.2.1. Cell treatments

The cells were treated as reported in figures 30 and 31. After plating, the cells were treated for 24h with inducers, and for the next 24h with inducers and neurotoxins. Briefly, after plating, cells were treated with 4 μ M β NF or 100 mM EtOH for 24h (day 1). Afterward, the medium was removed and replaced by medium containing 1.5 mM MPP⁺ (neurotoxin treatment); 1.5 mM MPP⁺+4 μ M BNF (neurotoxin+inducer); 1.5 mM MPP⁺+100 mM EtOH (neurotoxin+inducer); 300 nM Rotenone (neurotoxin treatment); 300 nM Rotenone+4 μ M BNF (neurotoxin+inducer); 300 nM Rotenone+100 mM EtOH (neurotoxin+inducer). All treatment were performed for 24h (day 2), at the end of which data acquisition was performed.

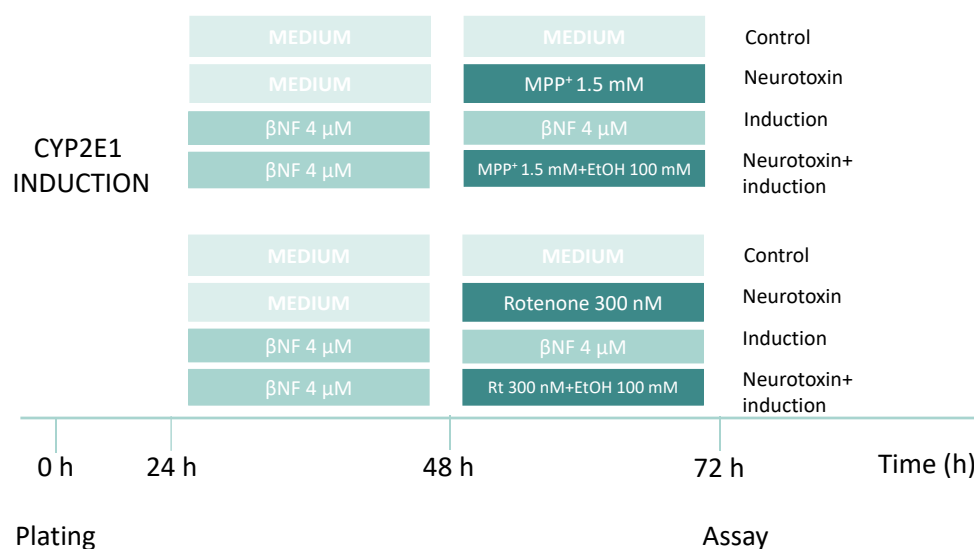


Figure 30. Experimental protocol for drug treatments. The day after plating the cells, they were treated for 24 hours with inducers of cytochrome P450. Afterward, the medium was replaced with fresh medium containing CYP inducers, neurotoxins, or a combination of both and left for additional 24h at the end of which assays were performed.

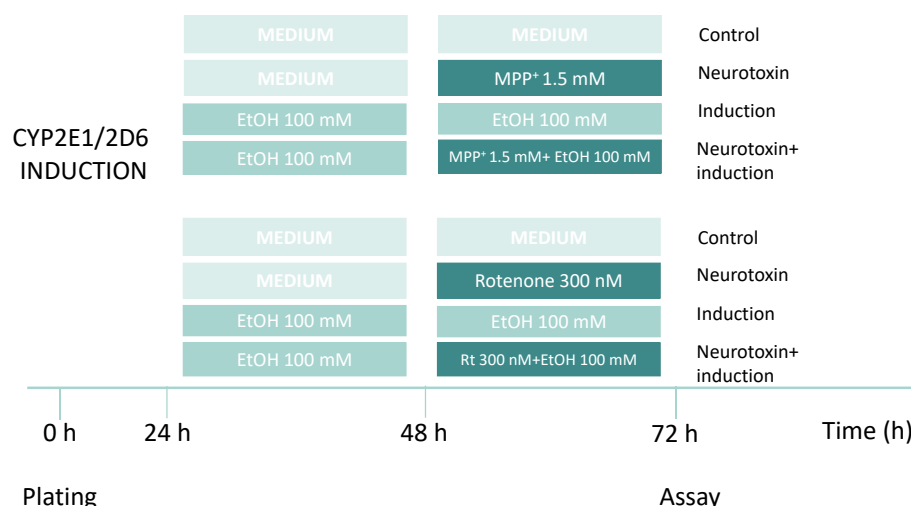


Figure 31. Experimental protocol for drug treatments. The day after plating the cells, they were treated for 24 hours with inducers of cytochrome P450. Afterward, the medium was replaced with fresh medium containing CYP inducers, neurotoxins, or a combination of both.

5.2.2. MTT viability assay

Cell viability was assessed using MTT (3- (4,5-dimethylthiazol-2-yl) -2,5-diphenyltetrazolium bromide) according to Fernandez-Abascal (2018)²⁶². It is a standard colorimetric assay for measuring the activity of enzymes that reduce MTT to formazan, giving the substance a blue / purplish color. This occurs mainly in the mitochondria where the succinate dehydrogenase enzyme, active only in living cells, reduces the tetrazolium ring of MTT (yellow colored powder) with the formation, consequently, of another compound, formazan (a blue salt). Formazan is insoluble in the intracellular environment and is unable to cross the wall, so it accumulates in cells where electron transport systems, such as mitochondrial dehydrogenases, are still metabolically active.

For the assay, the cells were plated in multiwell 96 at a density of 16,000 cells/well. After treatments, 200 µl of MTT solution (0.5 mg/ml in culture medium) was added to each well and they were incubated for 90 minutes at 37° C. After this period the supernatant is aspirated and 200 µl of DMSO are added, thus allowing the extraction and solubilization of the formazan salts. Absorbance is measured by spectrophotometric reading of the sample, at a wavelength of 540 nm in absorbance with a plate reader.

²⁶² Fernandez-Abascal, J., Ripullone, M., Valeri, A., Leone, C., & Valoti, M. (2018). β-Naphtoflavone and Ethanol Induce Cytochrome P450 and Protect towards MPP⁺ Toxicity in Human Neuroblastoma SH-SY5Y Cells. *International journal of molecular sciences*, 19(11), 3369.

5.2.3. Propidium Iodide viability assay

Flow cytometry is a quick and reliable method to quantify viable cells. One method to test cell viability is using dye exclusion. Live cells have membranes that are still intact and exclude a variety of dyes that easily penetrate the damaged, permeable membranes of non-viable cells. Propidium iodide (PI) is a membrane impermeant dye that is generally excluded from viable cells. It binds to double stranded DNA by intercalating between base pairs. PI is excited at 488 nm and, with a relatively large Stokes shift, emits at a maximum wavelength of 617 nm.

For the assay, cells were detached with trypsin-EDTA, centrifugated at 13.000 g for 1 minute and washed once in cold PBS. After that, staining with PI was performed by adding to each sample 1µl of PI (100 µg/ml), and left to incubate 30 seconds at room temperature before the cytofluorimetric analysis. PI fluorescence was assessed by using the FL-2 channel (filter 585/42 nm, detection range 564-606 nm).

5.2.4. Annexin V/PI assay

Exposed phosphatidylserine was detected by flow cytometry using the Alexa fluor 488™-Annexin V/PI double staining kit according to manufacturer indications with some modifications.²⁶³ The co-staining with annexin V and PI allows the quantitative distinction between viable (healthy) cells (AV negative, PI negative), early (AV positive, PI negative) or late AV positive, PI positive) apoptotic or necrotic (AV negative, PI positive) cells.

For the assay, cells were detached with trypsin-EDTA, centrifugated at 13.000 g for 1 minute and washed once in cold PBS. After that, cells were resuspended in the supplier Annexin-binding buffer 1X (2x10⁵ cells in 100 µl) and stained with 5 µl of Annexin V Alexa fluor 488 stock solution diluted in AV-binding buffer 1:20 (15 minutes at room temperature). At the end of the incubation, the samples were placed on ice and 400 µl of cold annexin binding buffer were added to stop the annexin V

²⁶³ Chiaino, E., Micucci, M., Cosconati, S., Novellino, E., Budriesi, R., Chiarini, A., & Frosini, M. (2020). Olive Leaves and Hibiscus Flowers Extracts-Based Preparation Protect Brain from Oxidative Stress-Induced Injury. *Antioxidants (Basel, Switzerland)*, 9(9), 806.

reaction. Staining with PI was performed by adding to each sample 1µl of PI (100 µg / ml) and left to incubate 30 seconds at room temperature before the cytofluorimetric analysis.

5.2.4.a. Cytofluorimetric data acquisition and analysis

Samples were read with a FACSCalibur™ cytofluorimeter with CELLQuest software version 3.3. The excitation of both fluorochromes was made with an argon-ion laser at 488 nm, and annexin V and PI emission was recorded with FL1 (filter 530/30 nm, detection range 515-545 nm) and FL2 (filter 585/42 nm, detection range 564-606 nm). The fluorescent parameters were set at logarithmic gain, and 10,000 total events per sample were acquired. Cells were scored according to the following criteria: PI negative, AV negative: viable cells. AV positive, PI negative, early apoptotic cells. AV positive, PI positive, late apoptotic cells. AV negative, PI positive, necrotic cells.

5.2.5. Analysis of Cell cycle

The following protocol already established in our laboratory was used²⁶⁴. Cells were rinsed twice with PBS, detached with Trypsin-EDTA, centrifugated at 5000 rpm for 5 minutes and resuspended in 1 mL of PBS. The samples were vortexed briefly, centrifugated at 5000 rpm for 5 minutes and resuspended in 300 µl of cold PBS. To fix the cells, each sample was added with 700 µl of cold EtOH, upon slowly stirring on the vortex. The samples obtained were then left at -20°C o/n. The day after, these were centrifugated at 13.000 rpm for 1 minute and the pellets washed with 1 ml of PBS. After centrifugation (13.000 rpm, 1 min. ambient temperature), the pellet was resuspended in 300 µl of PB, loaded with 3 µl of RNase (10 mg/ml) and incubated for 30 minutes at ambient temperature. The samples were centrifugated at 13.000 rpm for 1 minute, resuspended in 1 ml of cold PBS and incubated for 30 minutes with 10 µl of PI (2 mg/ml, protected from light). Afterward, the samples were gently and carefully resuspended by an insulin syringe and filtered with a 30 µm diameter filter before flow cytometry analysis.

²⁶⁴ Chiaino E, Micucci M, Durante M, Budriesi R, Gotti R, Marzetti C, Chiarini A, Frosini M (2020). Apoptotic-Induced Effects of Acacia Catechu Willd. Extract in Human Colon Cancer Cells. *International Journal of Molecular Sciences* 19;21(6):2102.

5.2.5.a. Cytofluorimetric data acquisition and analysis

Samples were read with a FACSCalibur™ cytofluorimeter with CELLQuest software version 3.3. The excitation of PI was made with an argon-ion laser at 488 nm, and PI emission was recorded with FL2 (filter 585/42 nm, detection range 564-606 nm). As there is at most a two-fold difference in fluorescence intensity between a cell in G0/G1 and a cell in G2/M, DNA staining was assessed on a linear scale. Forward scatter (FS) and side scatter (SS) were used to identify single cells, and pulse processing to exclude cell doublets from the analysis (pulse area vs. pulse width). For analysis, gate on the single cell population using pulse width vs. pulse area was drawn and then this gate was applied to the scatter plot to gate out obvious debris. Combined gates were then applied to the PI histogram plot. 10,000 total events per sample were acquired.

5.2.6. Intracellular ROS

The intracellular ROS levels were detected using the oxidation-sensitive fluorescent probe DCFDA as previously described.²⁶⁵ After the treatments, the cells were rinsed twice with PBS, detached with Trypsin-EDTA and washed with 1 mL of PBS, centrifuged at 13,000 g for 1 min and re-suspended in 0.7 mL of PBS. 500 µl were loaded with with 2',7'-Dichlorofluorescein diacetate (DCFDA 10 µM, 500 µL /tube, 15 min at 37°C), and the remaining 200 µl used for protein determinations. 300 µl of DCFDA-loaded samples were transferred in a 96-well plate and the intracellular fluorescence read at 504 nm excitation, 529 nm emission. The fluorescence was then normalized to the amount of proteins of each sample and expressed as percentage values respect to controls.

5.2.7. Mitochondrial Membrane Potential measure

Mitochondria generate a potential across their membranes due to the activities of enzymes of the electron transport chain. During apoptosis, collapse of the mitochondrial membrane potential (MMP)

²⁶⁵ Chiaino, E., Micucci, M., Cosconati, S., Novellino, E., Budriesi, R., Chiarini, A., & Frosini, M. (2020). Olive Leaves and Hibiscus Flowers Extracts-Based Preparation Protect Brain from Oxidative Stress-Induced Injury. *Antioxidants (Basel, Switzerland)*, 9(9), 806.

coincides with the opening of the mitochondrial permeability transition pores, leading to the release of cytochrome *c* into the cytosol, which in turn triggers other downstream events in the apoptotic cascade. JC-1 is a cationic, lipophilic dye that forms reversible red-fluorescent JC-1 aggregates in the mitochondria of cells with a polarized mitochondrial membrane. In apoptotic cells, MMP collapse results in the failure to retain JC-1 in the mitochondria and a return of the dye to its monomeric, green, fluorescent form.

The Mitochondrial membrane potential was measured according to manufacturing indications with some modifications. At the end of the experimental session, cells were rinsed with PBS and Staining Mixture was added. After 20' of incubation at 37° C, Staining Mixture was aspirated, cells were rinsed twice with growth medium and the fluorescence was measured (490 nm excitation wavelength and 530 nm emission wavelength for JC-1 monomers, 525 nm excitation wavelength and 590 nm emission wavelength for JC-1 aggregates). Then, the RATIO between JC-1 monomers and aggregates was calculated. Valinomycin (0.2 ng/μL for 20 min) that permeabilizes the mitochondrial membrane for K⁺ ions, and thus, dissipates the mitochondrial electrochemical potential, was used as positive control to prevent JC-1 aggregation.

5.2.8. Mitochondrial complex I activity

Cells were plated at a concentration of $1,6 \times 10^4$ cells/well in a 96-well plate. The day after, they were treated for 48 hours with either β-NF (4 μM) or EtOH (100 mM). After incubation with inducers, they were ready for mitochondrial complex I activity experiments according to manufacturer indications and as reported by Brown and Brand²⁶⁶ with some modifications.

In brief, medium was changed for assay buffer containing KCN (100 mM) for mitochondrial complex IV inhibition, fatty acid free BSA (1:20), and bovine heart mitochondria (1:50). Then, test compound (MPP⁺, 1,5 mM final concentration), positive control (rotenone, 1 μM final concentration), or vehicle, diluted in assay buffer, was added to each well. Finally, buffer containing NADH-reagent (1:23) and ubiquinone reagent (1:34) was added to each well. Immediately after, data was acquired in a plate reader (Multiskan GO, SkanIT software version 3.2) at 340 nm absorbance every 30 seconds during 15 minutes at room temperatures. The rate of NADH oxidation is measured by a decrease in

²⁶⁶ Brown, G. C., & Brand, M. D. (1988). Proton/electron stoichiometry of mitochondrial complex I estimated from the equilibrium thermodynamic force ratio. *The Biochemical journal*, 252(2), 473–479.

absorbance at 340 nm and is proportional to the activity of complex I. Absorbance of each well was plotted versus time and slope was calculated. The complex I activity (%) was determined by the following formula:

$$\text{Complex I Activity (\%)} = \left[\frac{\text{Slope of sample}}{\text{Slope of control}} \right] \times 100$$

5.3. Statistical analysis

Data were collected as as triplicate from at least three independent experiments. The results were expressed as means±SEMs. Data were expressed as percentage of untreated cells. Statistical significance was assessed by using ANOVA followed by Bonferroni post test (GraphPad Prism version 6, GraphPad Software Inc., San Diego, CA, USA).

5.4. Results

5.4.1. Effects of β NF and EtOH on MPP⁺- and Rotenone-mediated injury in UD and differentiated SH-SY5Y

To study whether the induction of CYP by β NF and EtOH could protect towards MPP⁺- and Rotenone-induced toxicity, the two neurotoxins were used in presence or absence of the two inducers.

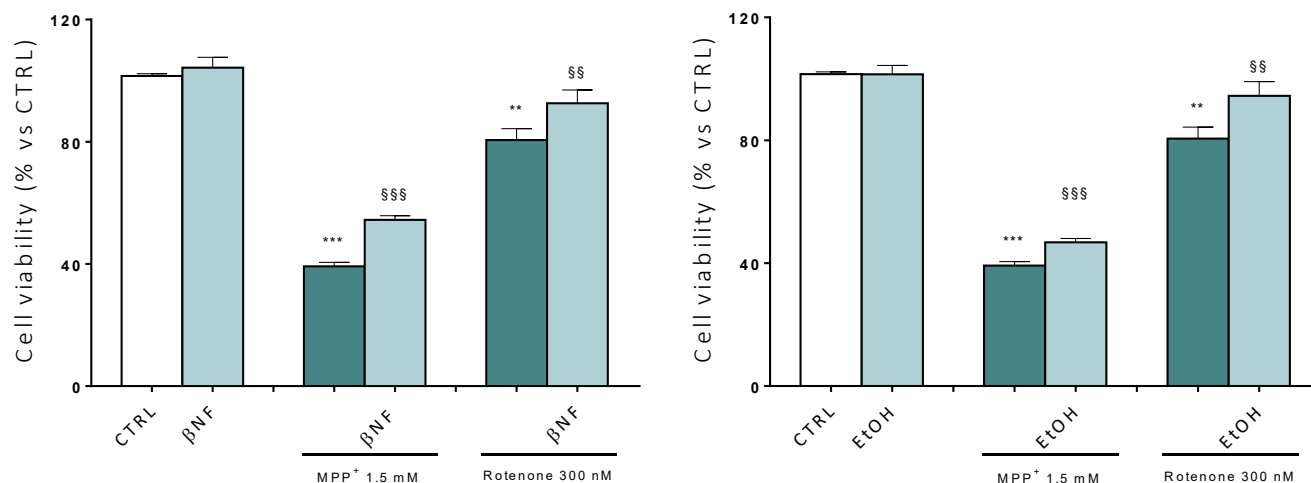


Figure 32. Effect of β NF and EtOH on MPP⁺- and Rotenone-mediated neurotoxicity in UD SH-SY5Y cells. Data are reported as mean \pm SEM of at $n \geq 3$ independent experiments. Statistical analysis was carried out by ANOVA followed by Bonferroni post test. *** $p < 0.001$, ** $p < 0.01$ vs CTRL. §§§ $p < 0.001$, §§ $p < 0.01$ vs cells treated with the same neurotoxin (MPP⁺ or Rotenone).

As shown in Figure 32, the two neurotoxins caused a reduction in metabolic activity of 60% (MPP⁺) and 20% (Rotenone), respectively. When cells were treated with both β NF and EtOH before and during exposure to the same MPP⁺, the neurotoxic damage was reverted (+ 15% β NF, + 7% EtOH). In the case of damage mediated by Rotenone, the two inductors restored the cell viability to values close to untreated cells (+12% β NF, + 14% EtOH).

The target in the MTT assay, succinate dehydrogenase, however, is a mitochondrial enzyme, that is the sub-cellular target of both neurotoxins, thus we wanted to confirm the data obtained with a further viability assay having a different mechanism, the assay with the DNA intercalator Propidium iodide.

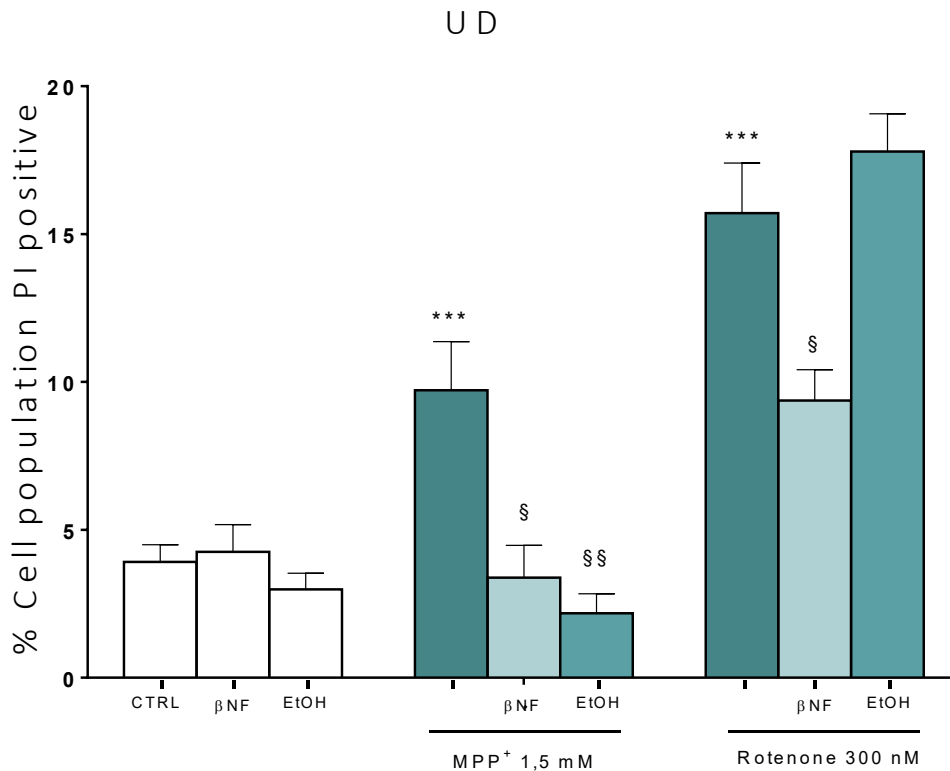


Figure 33. Effect of βNF and EtOH on MPP⁺- and Rotenone-mediated neurotoxicity in UD SH-SY5Y cells. Data are reported as mean ± SEM of at $n \geq 3$ independent experiments. Statistical analysis was carried out by one-way ANOVA and Bonferroni post test. *** $p < 0.001$ vs CTRL. § $p < 0.05$, §§ $p < 0.01$ vs cells treated with the same neurotoxin.

As reported in Figure 33, the two neurotoxins increased the positive PI population by 5.8% (MPP⁺) and 11.8% (Rotenone). When cells were treated with both βNF and EtOH prior and during exposure to MPP⁺ itself, cell viability was restored to values close to untreated cells.

On the other hand, in the case of Rotenone-mediated injury, only βNF produced a significant protection.

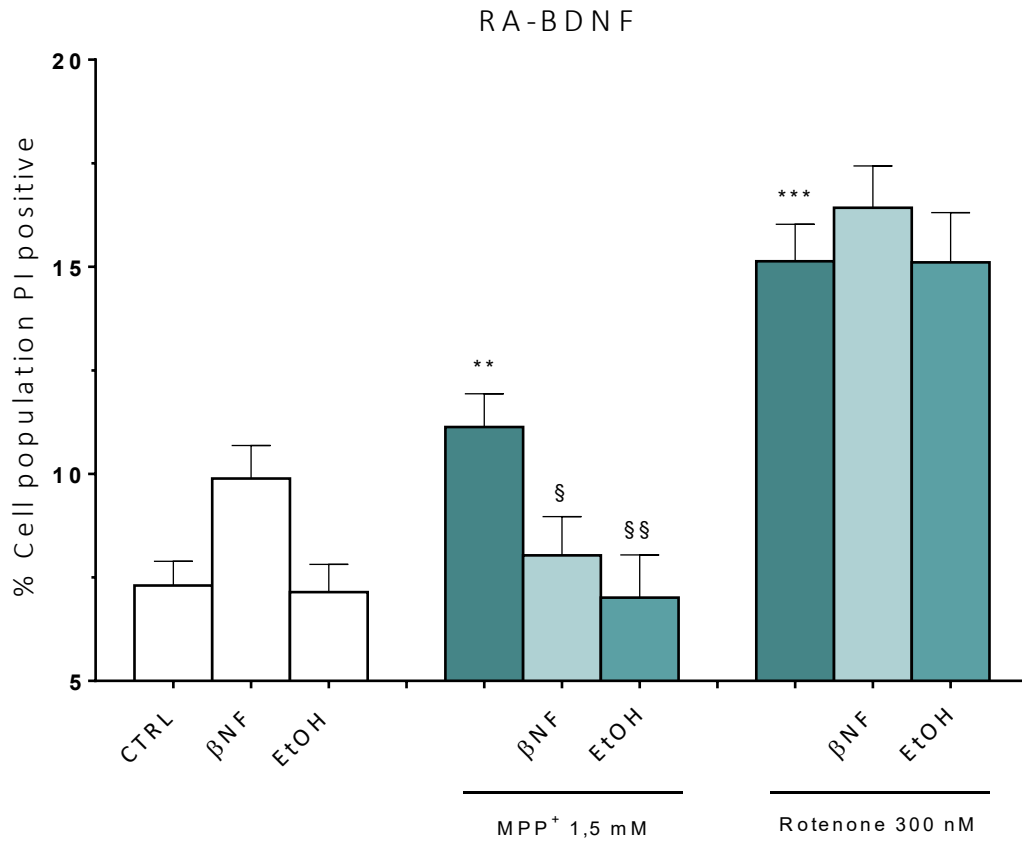


Figure 34. Effect of βNF and EtOH on MPP⁺- and Rotenone-mediated neurotoxicity in RA-BDNF differentiated SH-SY5Y cells. Data are reported as mean ± SEM of at $n \geq 3$ independent experiments. Statistic analysis was carried out with ANOVA and Bonferroni post test. *** $p < 0.001$, ** $p < 0.01$ vs CTRL. § $p < 0.05$, §§ $p < 0.01$ vs cells treated with the same neurotoxin.

In the RA-BDNF differentiated SH-SY5Y cells, an increase in PI positive population occurred after the challenge MPP⁺- and Rotenone. MPP⁺ toxicity was significantly reduced by βNF and EtOH treatment while neither βNF nor EtOH were effective toward the damage caused by Rotenone (Figure 34).

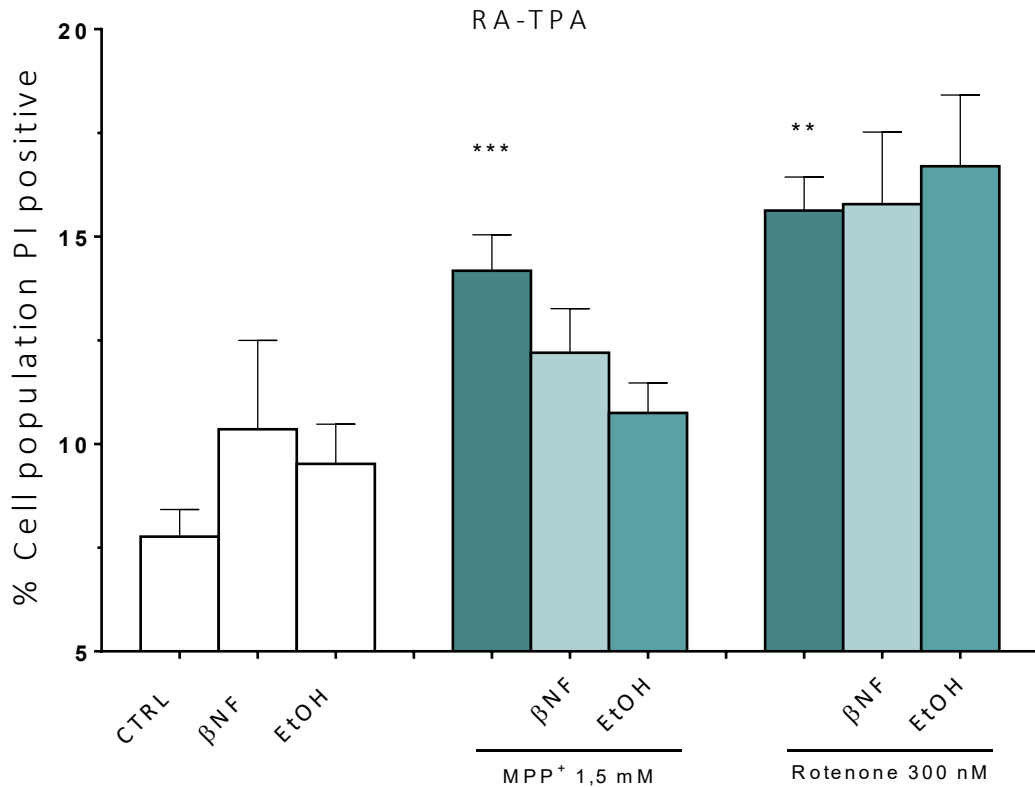


Figure 35. Effect of βNF and EtOH on MPP⁺- and Rotenone-mediated neurotoxicity in RA-TPA differentiated SH-SY5Y cells. Data are reported as mean ± SEM of at $n \geq 3$ independent experiments. Statistic analysis was carried out with ANOVA and Bonferroni post test. *** $p < 0.001$, ** $p < 0.01$ vs CTRL.

In the RA-TPA cell population, the injury due to neurotoxins increased in the PI positive cell population by approximately 6.4% (MPP⁺) or 7.8% (Rotenone). As already observed for cells differentiated with RA-BDNF, even in those treated with RA-TPA, βNF and EtOH did not reverse the cytotoxic effect of Rotenone. Instead, both inducers rescued MPP⁺-mediated effects, with a reduction of the positive PI population of 1.9% with βNF and 3.4% with EtOH (Figure 35).

The protective effect of CYP induction by βNF or EtOH was further investigated by analyzing the formation of apoptotic/necrotic cells.

In undifferentiated SH-SY5Y cells MPP⁺ promote a significant increase in the early apoptotic (+17%), the late apoptotic (+14%) and the necrotic populations (+6%) which was however reverted by βNF. On the other hand, Rotenone-mediated cytotoxic effects consisted in a significant increase in early apoptotic and necrotic populations (+7% and +12%, respectively), and in this case a neuroprotection was observed with the βNF treatment (Figure 36).

UD

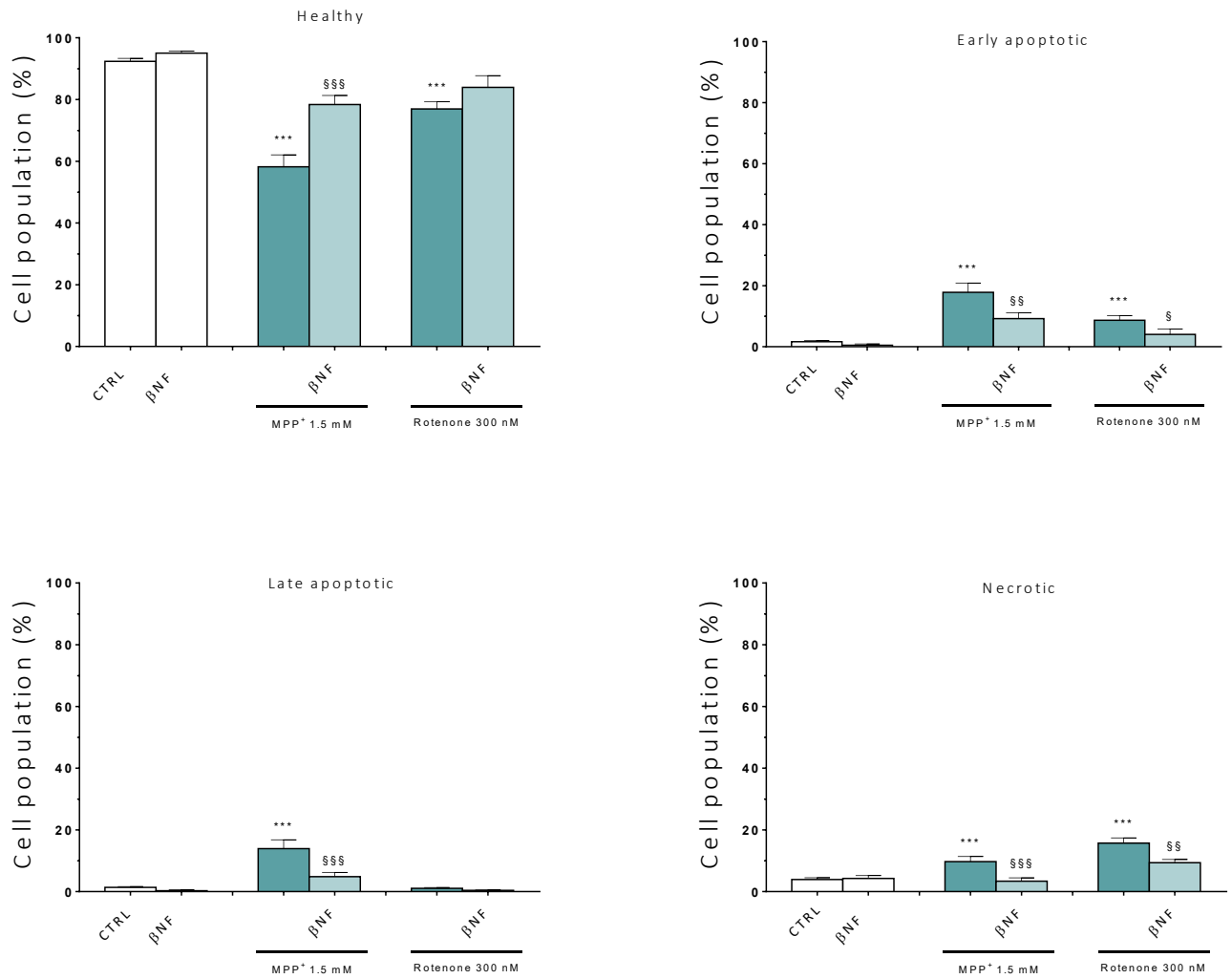


Figure 36. Effect of β NF on MPP⁺- and Rotenone-mediated apoptosis in UD SH-SY5Y cells via Annexin V/PI double staining. Data are reported as mean \pm SEM of at $n \geq 3$ independent experiments. Statistical analysis was carried out with ANOVA and Bonferroni post test. *** $p < 0.001$ vs CTRL, §§§ $p < 0.001$, §§ $p < 0.01$, § $p < 0.05$ vs. neurotoxins treatments (MPP⁺ or Rotenone).

UD

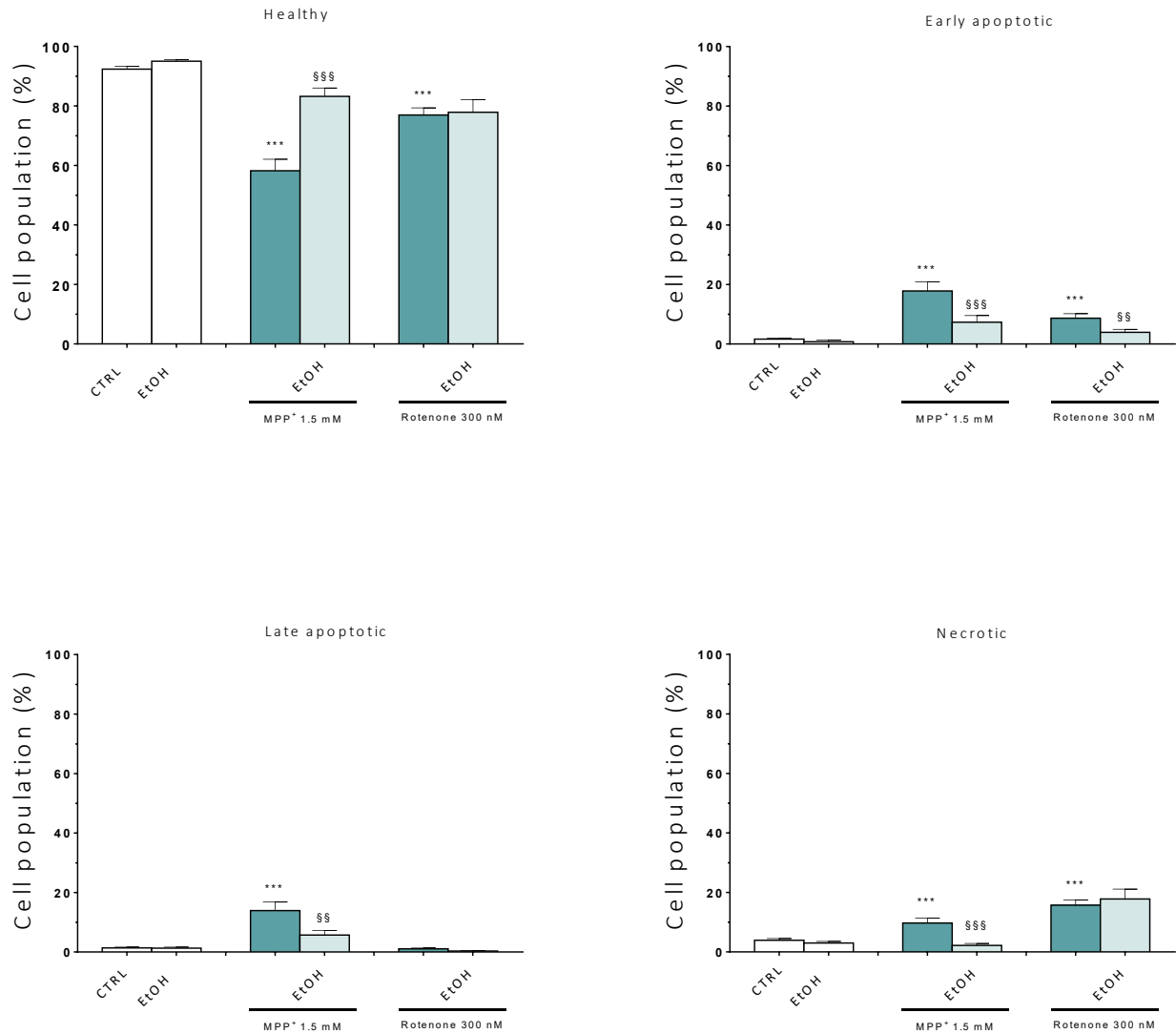


Figure 37. Effect of EtOH on MPP⁺- and Rotenone-mediated apoptosis in UD SH-SY5Y cells via cell viability assay with Annexin V/PI double staining. Data are reported as mean \pm SEM of at $n \geq 3$ independent experiments. Statistical analysis was carried out with ANOVA and Bonferroni post test. *** $p < 0.001$ vs CTRL, \$\$\$ $p < 0.001$, \$\$ $p < 0.01$ vs. neurotoxins treatments (MPP⁺ or Rotenone).

Similarly to β NF, EtOH reverted the damage promoted by MPP⁺ on early apoptotic (from 17.8% to 7.3%), late apoptotic (from 13.9% to 5.6%) and necrotic (from 9.7% to 2.1%) cell populations. Furthermore, treatment with EtOH was also effective in reverting the cytotoxicity caused by Rotenone on the early apoptotic cell population, while it was ineffective in restoring necrotic cell population (Figure 37).

In the RA-BDNF differentiated cells, MPP⁺, but not Rotenone, caused a significant increase in the early apoptotic cell population (+19.5%), which was reduced by β NF. On the other hand, the necrotic cells population were not affected by MPP⁺ but rose strikingly upon Rotenone challenge (+19%), an effect not reverted by β NF (Figure 38).

EtOH showed neuroprotection, too. This compound, in fact, prevented the MPP⁺-induced increase in early apoptotic cells, allowing them to regain basal values. Conversely, EtOH was ineffective towards rotenone effects. (Figure 39)

The **RA-TPA** differentiated cell population reported poor changes after treatment with the two neurotoxins used. These mainly concerned the necrotic population, which rose slightly (+7% with MPP⁺ and +5% with Rotenone) and seemed to be insensitive to both β NF (Figure 40) and EtOH (figure 41), the latter being also able to further rise necrotic cells.

RA-BDNF

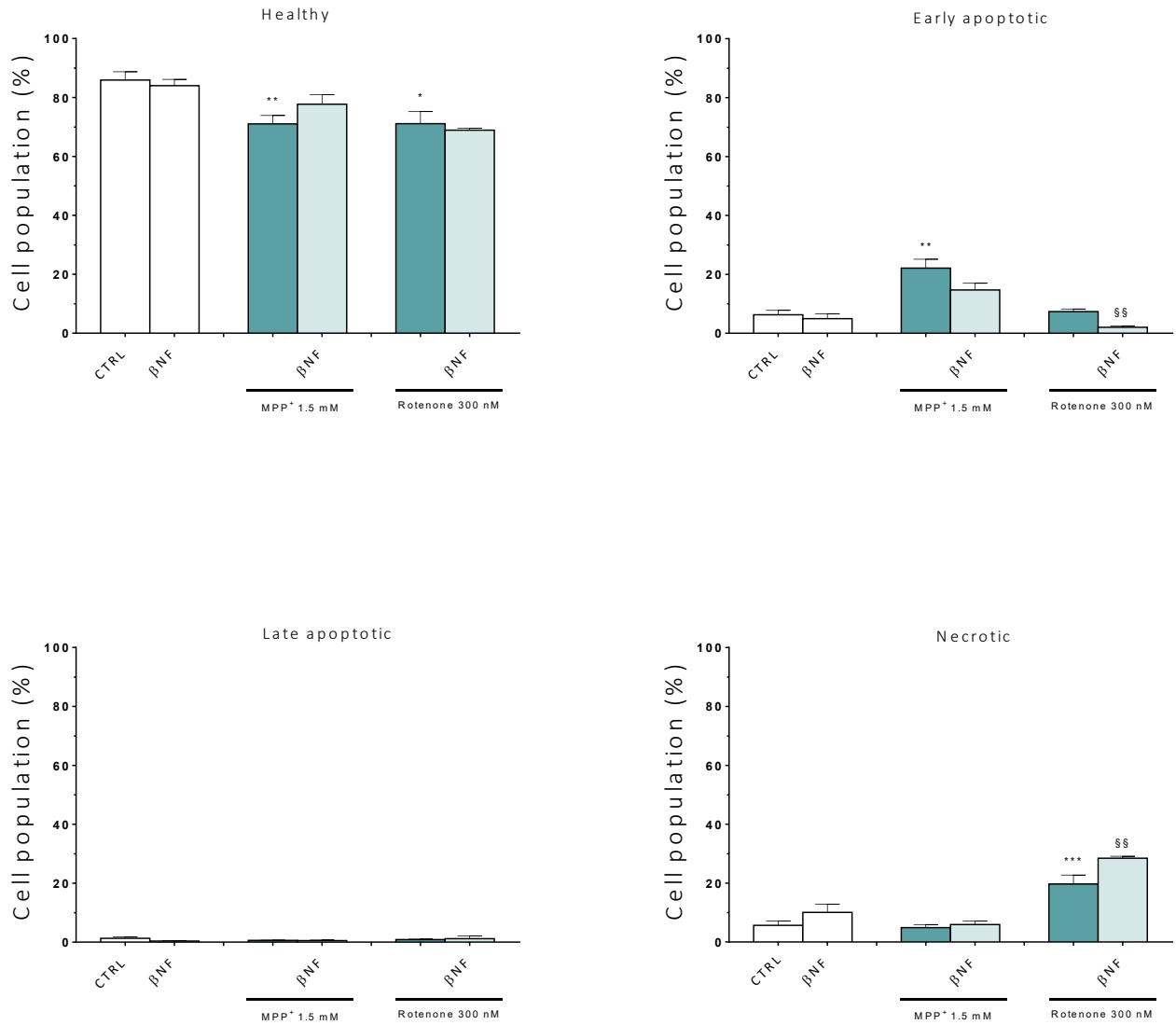


Figure 38. Effect of β NF on MPP⁺- and Rotenone-mediated apoptosis in differentiated (RA-BDNF) SH-SY5Y cells: Annexin V/PI double staining. Data are reported as mean \pm SEM of at $n \geq 3$ independent experiments. Statistical analysis was carried out by ANOVA and Bonferroni post test. *** $p < 0.001$, ** $p < 0.01$, * $p < 0.05$ vs CTRL, §§ $p < 0,01$ vs. neurotoxins treatments (MPP⁺ or Rotenone).

RA-BDNF

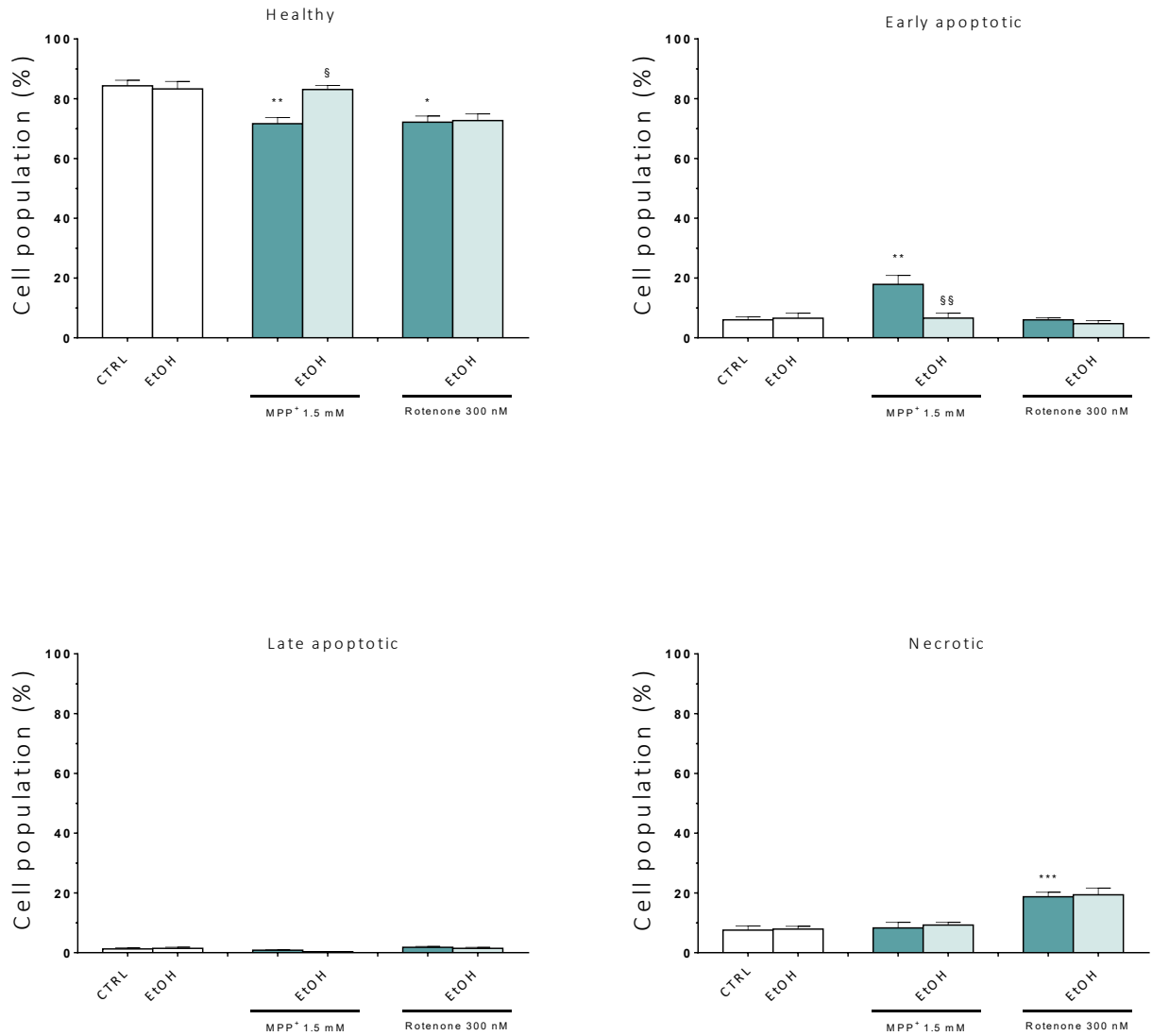


Figure 39. Effect of EtOH on MPP⁺- and Rotenone-mediated apoptosis in differentiated (RA-BDNF) SH-SY5Y cells: Annexin V/PI double staining. Data are reported as mean \pm SEM of at $n \geq 3$ independent experiments. Statistical analysis was carried out by ANOVA and Bonferroni post test. *** $p < 0.001$, ** $p < 0.01$, * $p < 0.05$ vs CTRL, §§ $p < 0.01$, § $p < 0.05$ vs. neurotoxins treatments (MPP⁺ or Rotenone).

RA-TPA

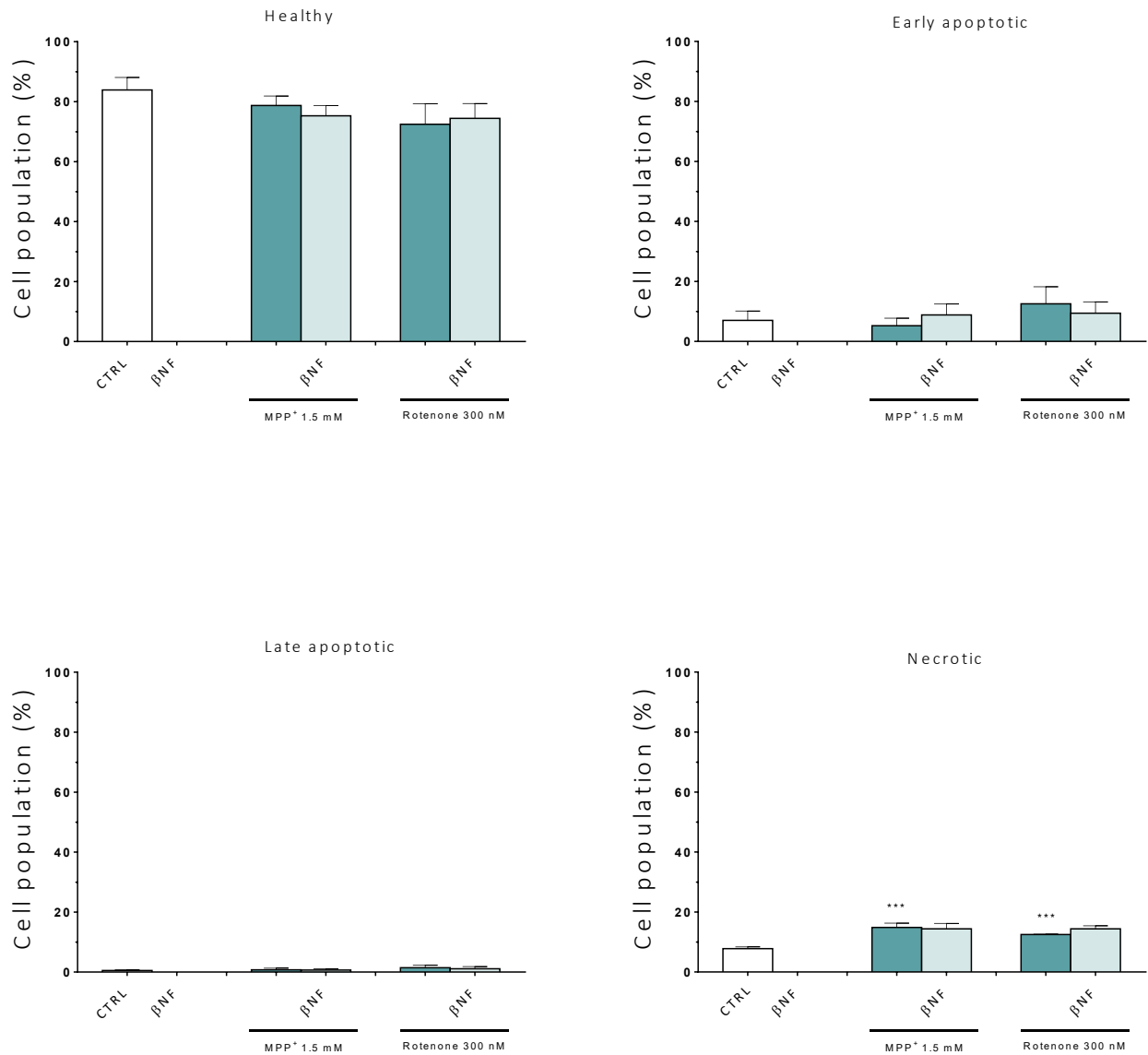


Figure 40. Effect of βNF on MPP⁺- and Rotenone-mediated apoptosis in differentiated (RA-TPA) SH-SY5Y cells: Annexin V/PI double staining. Data are reported as mean ± SEM of at $n \geq 3$ independent experiments. Statistical analysis was carried out by ANOVA and Bonferroni post test. *** $p < 0.001$ vs CTRL.

RA-TPA

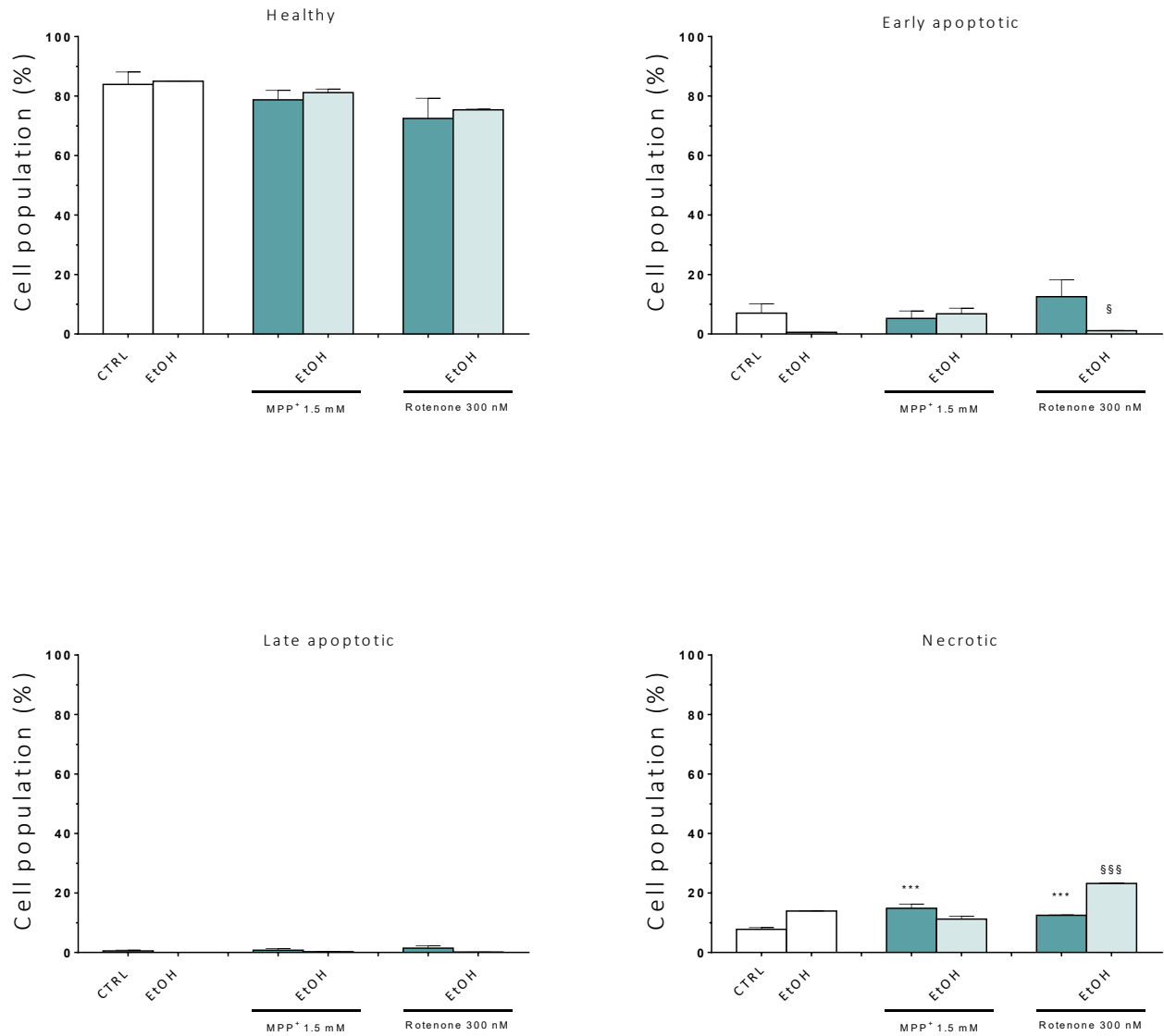


Figure 39. Effect of EtOH on MPP⁺- and Rotenone-mediated apoptosis in differentiated (RA-TPA) SH-SY5Y cells: Annexin V/PI double staining. Data are reported as mean \pm SEM of at $n \geq 3$ independent experiments. Statistical analysis was carried out by ANOVA and Bonferroni post test. *** $p < 0.001$ vs CTRL, §§§ $p < 0.001$, § $p < 0.05$ vs. neurotoxins treatments (MPP⁺ or Rotenone).

5.4.2. Effects of β NF and EtOH on cell cycle changes promoted by MPP⁺ and Rotenone in UD SH-SY5Y

As reported in Figure 42, both MPP⁺ and Rotenone increased subG0/G1 population by 7.5% and 7%, respectively. Interestingly, when cells were treated with β NF, the percentage of cells in this phase was lower (MPP⁺) or comparable (Rotenone) to that caused by the neurotoxins. Interestingly, at variance with MPP⁺, Rotenone caused an arrest in G2/M phase of SH-SY5Y cells, which was however not restored by β NF.

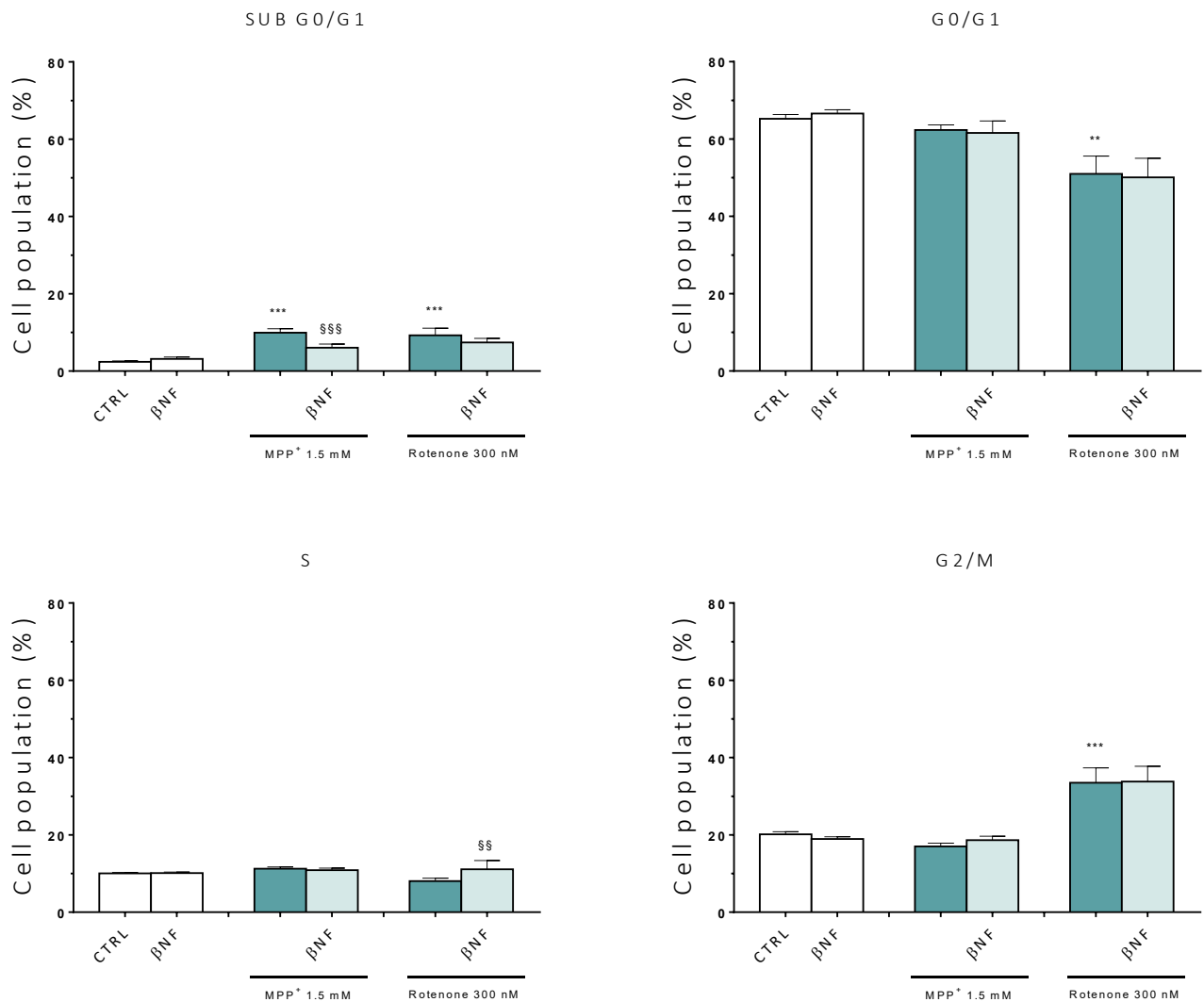


Figure 42. Effect of β NF on MPP⁺- and Rotenone-mediated changes in cell cycle phases in UD SH-SY5Y cells. Data are reported as mean \pm SEM of at $n \geq 3$ independent experiments. Statistical analysis was carried out by ANOVA and Bonferroni post test. *** $p < 0.001$, ** $p < 0.01$ vs CTRL, §§§ $p < 0.001$, §§ $p < 0.01$ vs. neurotoxins treatments (MPP⁺ or Rotenone).

On the other hand, when cells were treated with the EtOH, the decrease in subG0 / G1 cells occurred only in the case of the samples treated with MPP⁺, while no variation was observed in the case of the samples with damage caused by Rotenone (Figure 43).

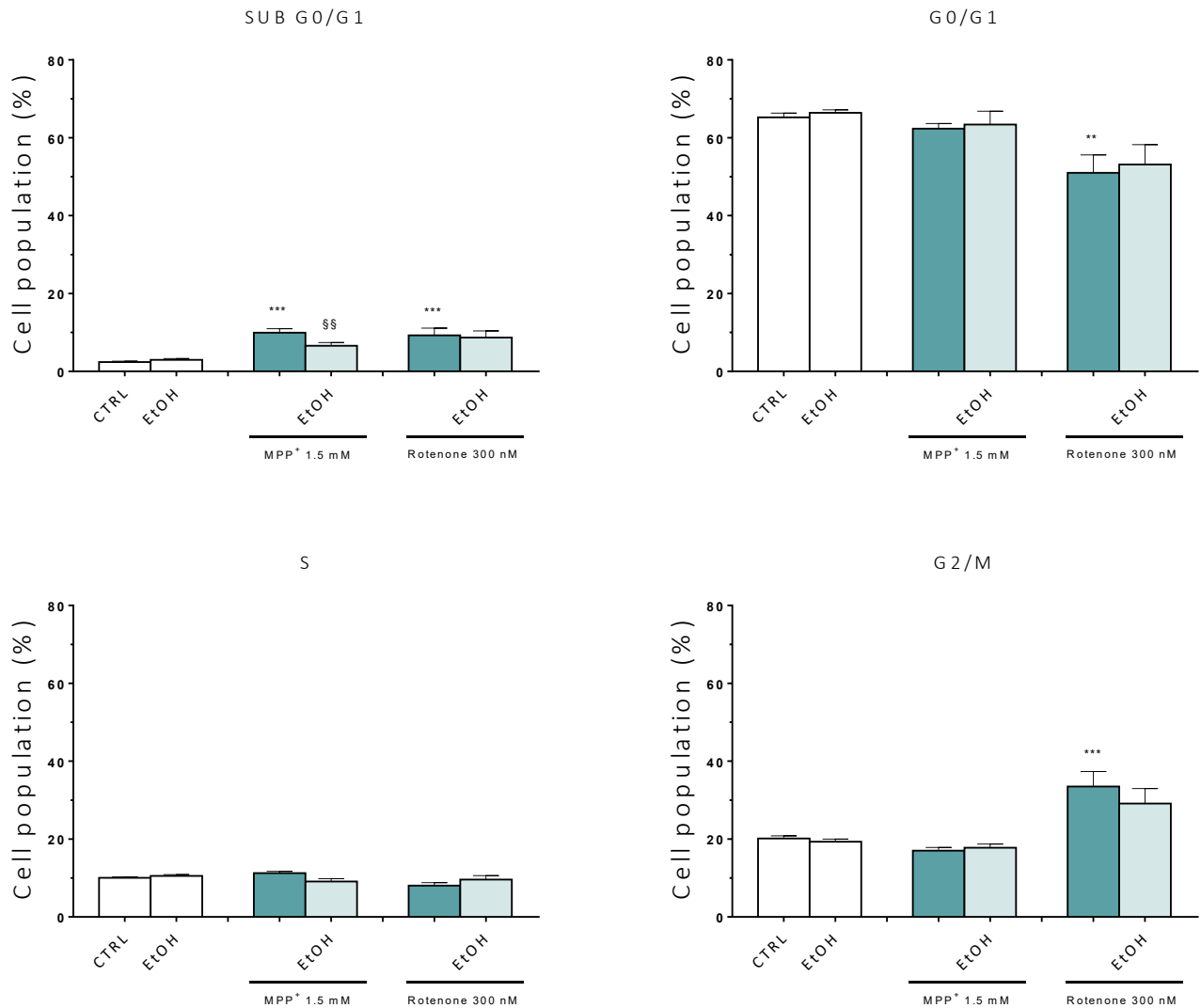


Figure 43. Effect of EtOH on MPP⁺- and Rotenone-mediated changes in cell cycle phases in UD SH-SY5Y cells. Data are reported as mean \pm SEM of at $n \geq 3$ independent experiments. Statistical analysis was carried out by ANOVA test, followed by Bonferroni post test. *** $p < 0,001$, ** $p < 0,01$ vs CTRL, §§§ $p < 0,001$, §§ $p < 0,01$ vs neurotoxins treatments (MPP⁺ or Rotenone).

5.4.3. Effects of β NF and EtOH on intracellular ROS formation promoted by MPP⁺ and Rotenone in UD and differentiated SH-SY5Y

As reactive oxygen species (ROS) and mitochondria play an important role in apoptosis, ROS formation and the possible protective effect of CYP induction by β NF and EtOH were investigated by using DCFA assay. In undifferentiated SH-SY5Y cells, MPP⁺ and Rotenone increased DCFA fluorescence by 120% and 34%, respectively (Figure 44). Interestingly, when cells were treated with β NF and EtOH, the ROS production was significantly lower as a decrease in fluorescence of -139% (β NF+MPP⁺), -21% (β NF+Rotenone), -106% (MPP⁺ + EtOH) and -22 % (Rotenone + EtOH) respect to neurotoxin-treated samples occurred.

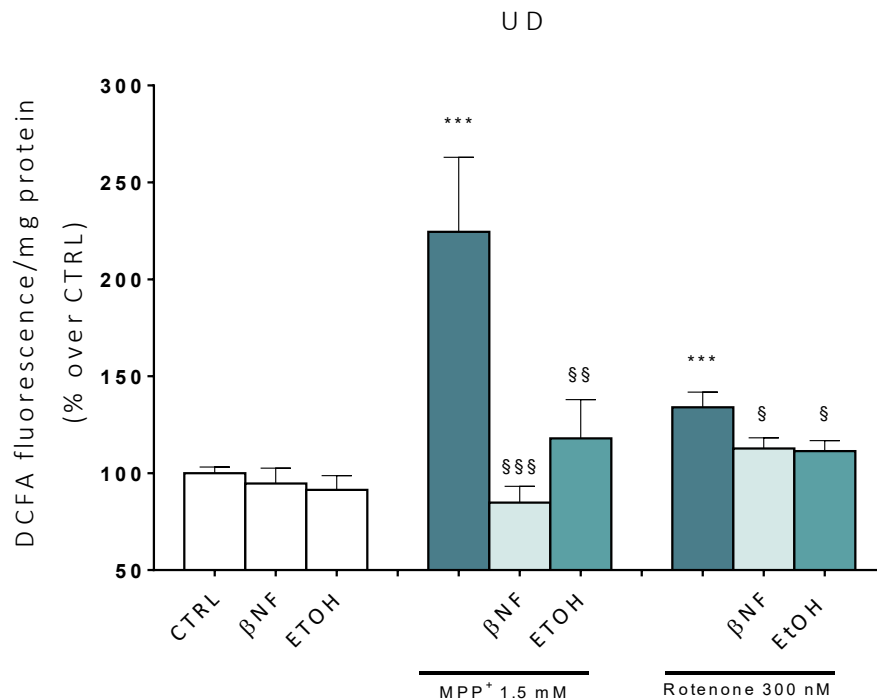


Figure 44. Effect of β NF and EtOH on MPP⁺- and Rotenone-mediated intracellular ROS formation in UD SH-SY5Y cells. Data are reported as mean \pm SEM of at $n \geq 3$ independent experiments. Statistical analysis was carried out by ANOVA followed by Bonferroni post test. *** $p < 0.001$ vs CTRL, §§§ $p < 0.001$, § $p < 0.05$ vs. neurotoxins treatments (MPP⁺ or Rotenone).

In the RA-BDNF-differentiated cell population, MPP⁺ and Rotenone promoted an increase in DCFA fluorescence of 69% and 45%, respectively (Figure 45). β NF significantly reduced fluorescence in MPP⁺-treated samples, but was less effective in the case of Rotenone. On the other hand, EtOH behaves just the opposite, as it hampered ROS formation caused by Rotenone- but not by MPP⁺-treatment.

In RA-TPA-differentiated cell population, ROS production mediated by the neurotoxins used was comparable (+ 47%). Interestingly, in the case of MPP⁺, a reduction in the ROS content was observed in the samples treated with both inducers, while these were ineffective in the case of Rotenone, although a descending trend was observed.

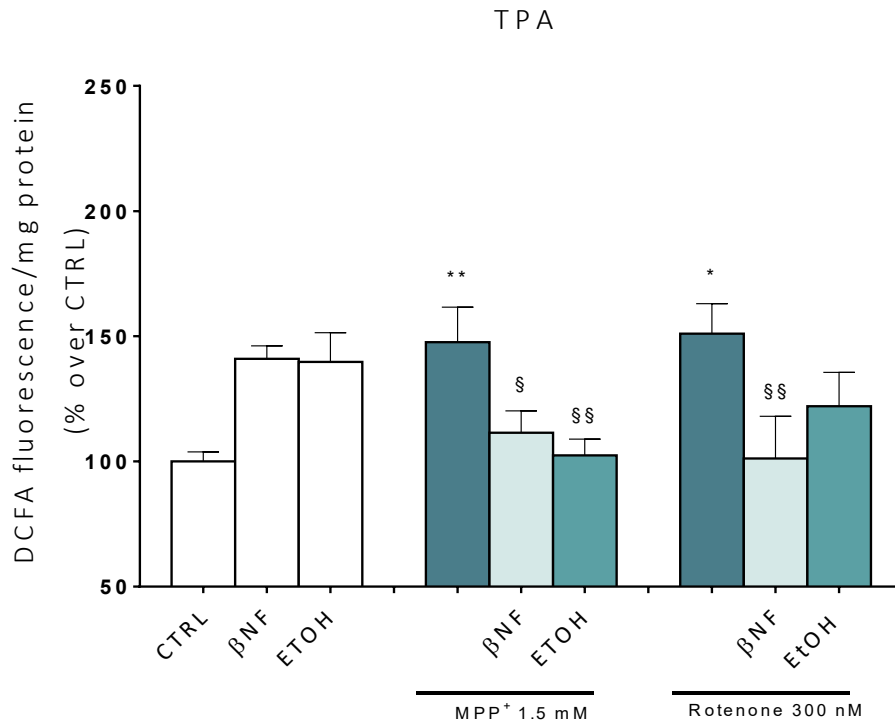
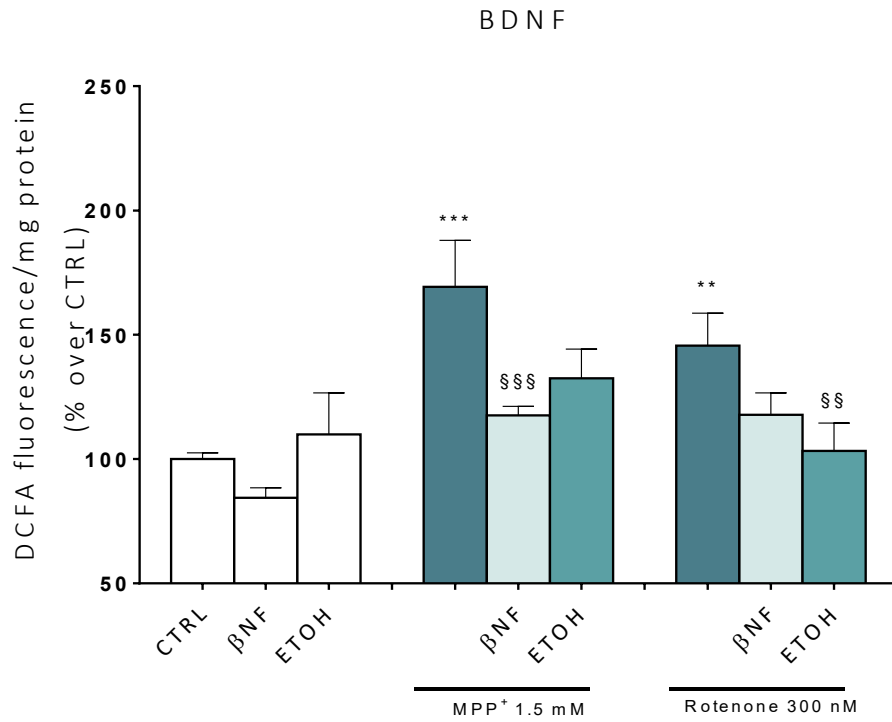


Figure 45. Effect of β NF and EtOH on MPP⁺- and Rotenone-mediated intracellular ROS formation in differentiated RA-BDNF and RA-TPA SH-SY5Y cells. Data are reported as mean \pm SEM of at $n \geq 3$ independent experiments. Statistical analysis was carried out by ANOVA followed by Bonferroni post test. ** $p < 0.01$, * $p < 0.05$ vs CTRL, §§ $p < 0.01$, § $p < 0.05$ vs. neurotoxins treatments (MPP⁺ or Rotenone).

5.4.4. Effects of β NF and EtOH on $\Delta\psi_m$ loss promoted by MPP⁺ in UD SH-SY5Y cells

We then assessed whether the treatments with inducers would also be able to restore the $\Delta\psi_m$. The red/green fluorescent intensity ratio observed when cells were treated with MPP⁺ was 23% lower than control samples, indicating a higher accumulation of 5,5',6,6'-tetrachloro-1,1',3,3'-tetraethylbenzimidazolocarboyanine iodide (JC-1) monomers (Figure 46).

Both β NF and EtOH treatments were able to partially reverse this decrease and showed a significant recover (+12% and +13%, respectively) in the red/green ratio. An important decrease in JC-1 aggregates in valinomycin control samples confirmed that the observed changes were due to dissipation of the electrochemical potential. These data suggest that the possible protection exerted by the treatments affects mechanisms that are upstream to any impairment of mitochondrial functioning promoted by MPP⁺ toxicity.

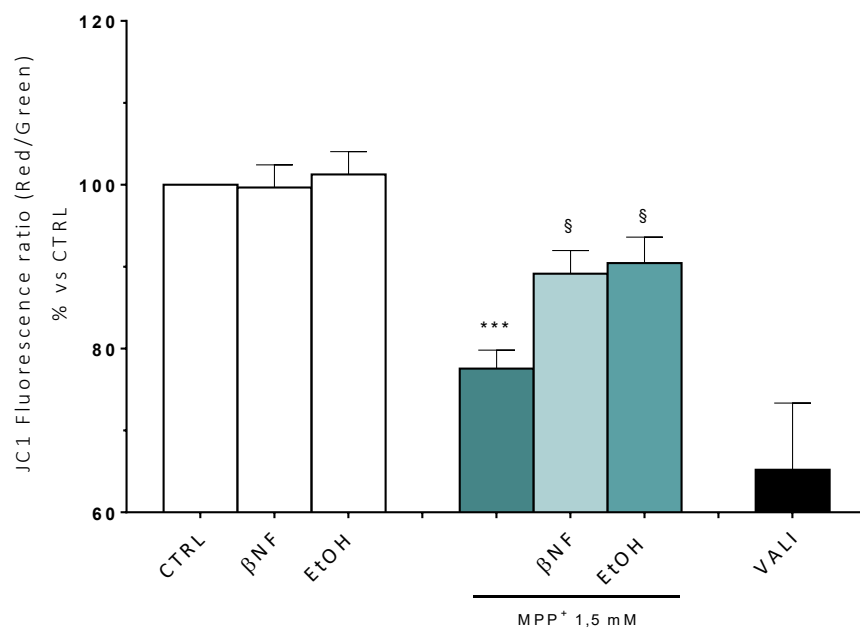


Figure 46. Effect of β NF and EtOH on MPP⁺-mediated $\Delta\psi_m$ in UD SH-SY5Y cells. Data are reported as mean \pm SEM of at $n \geq 3$ independent experiments. Valinomycin (VALI, 0.2 ng/ μ L for 20 min) that permeabilizes the mitochondrial membrane for K⁺ ions, and thus, dissipates the mitochondrial electrochemical potential, was used as positive control to prevent JC-1 aggregation. Statistical analysis was carried out by ANOVA followed by Bonferroni post test. *** $p < 0.001$ vs CTRL, § $p < 0.05$ vs. neurotoxin treatment.

5.4.5. Effects of β NF and EtOH Complex I disruption promoted by MPP⁺ in UD SH-SY5Y cells

To assess whether CYP inducers protect the correct functioning of mitochondria from MPP⁺, a complex I activity assay was carried out. Cells were pre-incubated for 48 hours with β NF or EtOH at reported concentrations, then treated with MPP⁺ at the moment of data acquisition. We observed a decrease in the complex I activity of 56% compared to control (Figure 47). The inhibition of complex I activity obtained by rotenone confirmed that complex I was involved in the NADH reduction measured in this assay. Both pre-treatments with β NF and EtOH significantly reduced the toxic effect of MPP⁺, showing only 33% and 11% decreases of complex I activity, respectively.

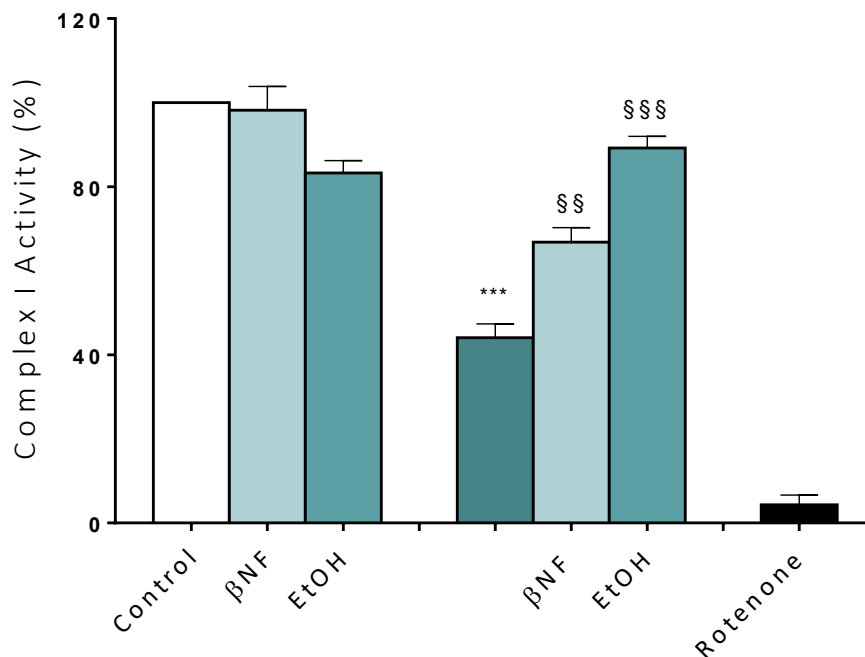


Figure 47. Analysis of mitochondrial Complex I activity after MPP⁺-mediated damage in UD SH-SY5Y cells. Columns represent the mean \pm SEM of three independent experiments. Results were normalised by considering the activity in control samples as a 100%. Statistical analysis was carried out by ANOVA followed by Bonferroni post test. *** $p < 0.001$ vs CTRL, §§§ $p < 0.001$, §§ $p < 0.01$ vs. MPP⁺ treatment.

5.5. Discussion

In neurodegenerative diseases, and more specifically in PD, the etiology appears to be a complex interplay of genetic and environmental factors.²⁶⁷ The oxidative stress²⁶⁸ and mitochondrial dysfunction²⁶⁹ promoted by the exposure to xenobiotics or their metabolism is one of the main causes that contributes to apoptosis.²⁷⁰ A pivotal role in these events is played by CYP-mediated metabolism, which is involved in the clearance of both endogenous and exogenous compounds and, at the same time, in the production of oxidative stress due to its metabolic activity.^{271,272} Various *in vitro* models have been developed for the study of PD, including those currently in use neurotoxins-based. These compounds exert their cytotoxic effect through the degeneration of nigrostriatal dopaminergic neurons, such as 6-hydroxydopamine (6-OHDA), 1-methyl-4-phenyl1,2,3, 6-tetrahydropyridine (MPTP), paraquat and rotenone.²⁷³ Unfortunately, none of these neurotoxic patterns perfectly reproduce all the characteristics of PD. Despite this, these pharmacological models have still contributed enormously to our understanding of disease processes.

In this context, MPP⁺ have been used as one of the most potent tools for *in vitro* models to study this neurodegeneration due to its selective damage of dopaminergic neurons in the substantia nigra.²⁷⁴ MPP⁺ exert its toxic effect by inhibiting Complex I of the electron transport chain, with increase of ROS production, as here demonstrated, and altered fusion-fission dynamics. However, other toxic compounds like Rt or PQ has been showed as a useful tool for the study of oxidative stress and

²⁶⁷ Schapira A. H. (2006). Etiology of Parkinson's disease. *Neurology*, 66(10 Suppl 4), S10–S23.

²⁶⁸ Jenner P. (2003). Oxidative stress in Parkinson's disease. *Annals of neurology*, 53 Suppl 3, S26–S38.

²⁶⁹ Winklhofer, K. F., & Haass, C. (2010). Mitochondrial dysfunction in Parkinson's disease. *Biochimica et biophysica acta*, 1802(1), 29–44.

²⁷⁰ Ramsay, R. R., Majekova, M., Medina, M., & Valoti, M. (2016). Key Targets for Multi-Target Ligands Designed to Combat Neurodegeneration. *Frontiers in neuroscience*, 10, 375.

²⁷¹ McMillan, D. M., & Tyndale, R. F. (2018). CYP-mediated drug metabolism in the brain impacts drug response. *Pharmacology & therapeutics*, 184, 189–200.

²⁷² Zhao, M., Ma, J., Li, M., Zhang, Y., Jiang, B., Zhao, X., Huai, C., Shen, L., Zhang, N., He, L., & Qin, S. (2021). Cytochrome P450 Enzymes and Drug Metabolism in Humans. *International journal of molecular sciences*, 22(23), 12808.

²⁷³ Zeng, X. S., Geng, W. S., & Jia, J. J. (2018). Neurotoxin-Induced Animal Models of Parkinson Disease: Pathogenic Mechanism and Assessment. *ASN neuro*, 10, 1759091418777438.

²⁷⁴ Schober A. (2004). Classic toxin-induced animal models of Parkinson's disease: 6-OHDA and MPTP. *Cell and tissue research*, 318(1), 215–224.

neurodegeneration due to their ability to cause mitochondrial dysfunction and dopaminergic cell loss in the SNpc.²⁷⁵²⁷⁶

To clarify the implication of some CYP isoforms in the metabolism of xenobiotics in all phenotypes of neuroblastoma SH-SY5Y cells, we performed an experimental approach with some well-known inducers that have been used to increase the CYP expression and to study its effect against xenobiotic-mediated cytotoxicity. Among the very few publications that can be found regarding MPP⁺ or Rotenone and their CYP-mediated metabolism, most of them report a greater affinity of the CYP system towards MPP⁺.²⁷⁷²⁷⁸

Mann and Tyndale demonstrated that the enzymatic activity of CYPs is involved in the response to the cytotoxic damage promoted by MPP⁺. In fact, selective inhibition of CYP2D6 by quinidine in SH-SY5Y cells resulted in increase of toxicity promoted by MPP⁺ treatment. This, although indirectly, underline a neuroprotective effect of CYP.²⁷⁹ Moreover, it was demonstrated that the inhibition of mitochondrial fraction of CYP2D6 in primary culture neurons protected the cells from MPP⁺-mediated injury.²⁸⁰ On the contrary, in astrocytes, the inhibition of CYP2E1 reduced the toxic damage promoted by MPP⁺.²⁸¹

In the present study, the induction of CYP isozymes led to a partial recovery in SH-SY5Y cell viability treated with both MPP⁺ and Rotenone (PI staining assay). The protective effect of EtOH and β NF was further investigated and confirmed by analyzing the formation of apoptotic/necrotic cells and by the cell cycle analysis. Moreover, it is worth noting that EtOH had a different effect compared to β NF. The former, in fact, recovered the cell viability in all SH-SY5Y phenotypes when treated with MPP⁺, while it was ineffective towards Rotenone.

²⁷⁵ Saravanan, K. S., Sindhu, K. M., & Mohanakumar, K. P. (2005). Acute intranigral infusion of rotenone in rats causes progressive biochemical lesions in the striatum similar to Parkinson's disease. *Brain research*, 1049(2), 147–155.

²⁷⁶ Mouhape, C., Costa, G., Ferreira, M., Abin-Carriquiry, J. A., Dajas, F., & Prunell, G. (2019). Nicotine-Induced Neuroprotection in Rotenone In Vivo and In Vitro Models of Parkinson's Disease: Evidence for the Involvement of the Labile Iron Pool Level as the Underlying Mechanism. *Neurotoxicity research*, 35(1), 71–82.

²⁷⁷ Caboni, P., Sherer, T. B., Zhang, N., Taylor, G., Na, H. M., Greenamyre, J. T., & Casida, J. E. (2004). Rotenone, deguelin, their metabolites, and the rat model of Parkinson's disease. *Chemical research in toxicology*, 17(11), 1540–1548.

²⁷⁸ Mann, A., & Tyndale, R. F. (2010). Cytochrome P450 2D6 enzyme neuroprotects against 1-methyl-4-phenylpyridinium toxicity in SH-SY5Y neuronal cells. *The European journal of neuroscience*, 31(7), 1185–1193.

²⁷⁹ Mann, A., & Tyndale, R. F. (2010). Cytochrome P450 2D6 enzyme neuroprotects against 1-methyl-4-phenylpyridinium toxicity in SH-SY5Y neuronal cells. *The European journal of neuroscience*, 31(7), 1185–1193.

²⁸⁰ Bajpai, P., Sangar, M. C., Singh, S., Tang, W., Bansal, S., Chowdhury, G., Cheng, Q., Fang, J. K., Martin, M. V., Guengerich, F. P., & Avadhani, N. G. (2013). Metabolism of 1-methyl-4-phenyl-1,2,3,6-tetrahydropyridine by mitochondrion-targeted cytochrome P450 2D6: implications in Parkinson disease. *The Journal of biological chemistry*, 288(6), 4436–4451.

²⁸¹ Hao, C., Liu, W., Luan, X., Li, Y., Gui, H., Peng, Y., Shen, J., Hu, G., & Yang, J. (2010). Aquaporin-4 knockout enhances astrocyte toxicity induced by 1-methyl-4-phenylpyridinium ion and lipopolysaccharide via increasing the expression of cytochrome P4502E1. *Toxicology letters*, 198(2), 225–231.

High oxidative stress and disruption of mitochondrial membrane potential lead to a change in morphology and alteration in mitochondrial fusion-fission dynamics.²⁸² These events disrupt the overall mitochondrial homeostasis, promoting apoptosis, the release of pro-apoptotic factors, and contributing to neurodegeneration in PD and other diseases. We investigated the oxidative stress and the consequential disruption of mitochondrial functionality after the exposure to MPP⁺ and Rotenone. EtOH and β NF were able to avoid the MPP⁺- and Rotenone-mediated increase in intracellular ROS formation. Furthermore, the analysis of the integrity of mitochondria highlighted that both inducers reverted the $\Delta\psi_m$ loss and reduced the Complex I impairment due to the MPP⁺-mediated damage in UD cells.

Overall, these results suggest that CYP induction predisposes the undifferentiated SH-SY5Y to be more efficient in avoiding the toxicity produced by MPP⁺ and partially by Rotenone.

The differentiated cells response presents substantial differences compared to undifferentiated cells. Interestingly, the first finding is that the cytotoxic injury promoted by the neurotoxins used was less severe in both full differentiated populations. In fact, except for a few cases, upon the MPP⁺ and Rotenone challenge the populations stained by Annexin V or Propidium Iodide increased to a lesser extent compared to their own control. Accordingly, in the case of MPP⁺, ROS production in both differentiated populations was also lower than that occurring in UD. It can be hypothesized that the molecular mechanism behind this different behavior may lie in the complex set of biochemical, molecular, ultrastructural, morphological, and electrophysiological changes that SH-SY5Y cells undergo during the differentiation process. In particular, cells modifications are accompanied by metabolic and energetic alterations, in which mitochondria play a pivotal role.²⁸³ Retinoic acid affects

²⁸² Subramaniam, S. R., & Chesselet, M. F. (2013). Mitochondrial dysfunction and oxidative stress in Parkinson's disease. *Progress in neurobiology*, 106-107, 17–32.

²⁸³ Zhang, H., Menzies, K. J., & Auwerx, J. (2018). The role of mitochondria in stem cell fate and aging. *Development (Cambridge, England)*, 145(8), dev143420.

mitochondria and energy metabolism via TrkB activation,^{284,285,286} and this can be further enhanced by the BDNF.^{287,288,289}

Contrary to undifferentiated cells, which present an energetical profile mainly based on glycolysis to obtain their energy requirements for ATP generation as any other common proliferating cells^{290,291}, differentiated cells are extremely dependent on mitochondria and oxidative phosphorylation (OXPHOS) to survive.²⁹² Several studies investigated the effect of differentiation on mitochondrial function and cellular bioenergetics. Specifically, the RA treatment enhances the metabolic activity of neuroblastoma cells, increases the spare respiratory capacity of mitochondria and the oxygen consumption rate (OCR) without changing mitochondrial number,²⁹³ promotes a greater stimulation of mitochondrial respiration, an increased bioenergetic reserve capacity and an increased mitochondrial membrane potential, which confers resistance to oxidative stress-induced cell death and alterations in mitochondrial function.²⁹⁴ Moreover, this effect is confirmed in full differentiated SH-SY5Y cells with RA-BDNF, which present higher OCR and lower extracellular acidification rate

²⁸⁴ Xun, Z., Lee, D. Y., Lim, J., Canaria, C. A., Barnebey, A., Yanonne, S. M., & McMurray, C. T. (2012). Retinoic acid-induced differentiation increases the rate of oxygen consumption and enhances the spare respiratory capacity of mitochondria in SH-SY5Y cells. *Mechanisms of ageing and development*, 133(4), 176–185.

²⁸⁵ Truckenmiller, M. E., Vawter, M. P., Cheadle, C., Coggiano, M., Donovan, D. M., Freed, W. J., & Becker, K. G. (2001). Gene expression profile in early stage of retinoic acid-induced differentiation of human SH-SY5Y neuroblastoma cells. *Restorative neurology and neuroscience*, 18(2-3), 67–80.

²⁸⁶ Schneider, L., Giordano, S., Zelickson, B. R., S Johnson, M., A Benavides, G., Ouyang, X., Fineberg, N., Darley-USmar, V. M., & Zhang, J. (2011). Differentiation of SH-SY5Y cells to a neuronal phenotype changes cellular bioenergetics and the response to oxidative stress. *Free radical biology & medicine*, 51(11), 2007–2017.

²⁸⁷ Forster, J. I., Köglberger, S., Trefois, C., Boyd, O., Baumuratov, A. S., Buck, L., Balling, R., & Antony, P. M. (2016). Characterization of Differentiated SH-SY5Y as Neuronal Screening Model Reveals Increased Oxidative Vulnerability. *Journal of biomolecular screening*, 21(5), 496–509.

²⁸⁸ Arcangeli, A., Rosati, B., Crociani, O., Cherubini, A., Fontana, L., Passani, B., Wanke, E., & Olivetto, M. (1999). Modulation of HERG current and herg gene expression during retinoic acid treatment of human neuroblastoma cells: potentiating effects of BDNF. *Journal of neurobiology*, 40(2), 214–225.

²⁸⁹ Encinas, M., Iglesias, M., Liu, Y., Wang, H., Muhaisen, A., Ceña, V., Gallego, C., & Comella, J. X. (2000). Sequential treatment of SH-SY5Y cells with retinoic acid and brain-derived neurotrophic factor gives rise to fully differentiated, neurotrophic factor-dependent, human neuron-like cells. *Journal of neurochemistry*, 75(3), 991–1003.

²⁹⁰ Vander Heiden, M. G., Cantley, L. C., & Thompson, C. B. (2009). Understanding the Warburg effect: the metabolic requirements of cell proliferation. *Science (New York, N.Y.)*, 324(5930), 1029–1033.

²⁹¹ Lees, J. G., Gardner, D. K., & Harvey, A. J. (2017). Pluripotent Stem Cell Metabolism and Mitochondria: Beyond ATP. *Stem cells international*, 2017, 2874283.

²⁹² Riestler M, Xu Q, Moreira A, Zheng J, Michor F, Downey R (2018) The Warburg effect: persistence of stem-cell metabolism in cancers as a failure of differentiation. *Ann Oncol* 29(1):264–270

²⁹³ Xun, Z., Lee, D. Y., Lim, J., Canaria, C. A., Barnebey, A., Yanonne, S. M., & McMurray, C. T. (2012). Retinoic acid-induced differentiation increases the rate of oxygen consumption and enhances the spare respiratory capacity of mitochondria in SH-SY5Y cells. *Mechanisms of ageing and development*, 133(4), 176–185.

²⁹⁴ Schneider, L., Giordano, S., Zelickson, B. R., S Johnson, M., A Benavides, G., Ouyang, X., Fineberg, N., Darley-USmar, V. M., & Zhang, J. (2011). Differentiation of SH-SY5Y cells to a neuronal phenotype changes cellular bioenergetics and the response to oxidative stress. *Free radical biology & medicine*, 51(11), 2007–2017.

(ECAR) and a higher OCR/ECAR ratio compared to UD.²⁹⁵ The Authors suggest that this is a consequence of the proliferative rate of undifferentiated SH-SY5Y cells, which have a high endogenous demand for ATP and exhibit greater dependence on glycolysis. Furthermore, since the respiratory capacity of a cell is necessary for it to respond effectively to the increased demand for ATP and to stress, such as reactive oxygen species or oxidized lipids,²⁹⁶ differentiated SH-SY5Y cells consequently possess a greater capacity to withstand stress compared to undifferentiated SH-SY5Y.²⁹⁷ The discrepancy of the results with with RA-TPA differentiated SH-SY5Y suggests that TPA does not probably nullify the activation of the pathways necessary for the bioenergetic change induced by the treatment with RA.

However, pieces of evidence of less sensitivity towards the neurotoxins on differentiated SH-SY5Y should be attributed to the highest CYP isozymes expression promoted by differentiation processes. Therefore, the subsequent exposure of cells with inducers does not promote an extent increase in CYP content and keeps the cells protected versus MPP⁺.

The lower protective effects of CYP-induction towards Rotenone-induced toxicity support the evidence that CYP-dependent metabolism did not play a key role in these mechanisms.

Caboni et al.²⁹⁸ demonstrated that for rotenone metabolism CYP3A4 is more active than the other P450 enzymes, 2E1 is ineffective, while 2D6 is barely involved. This observation can be at the basis of the lower protection exerted by CYPs towards rotenone in our experimental model. The differentiation process, in fact, promoted a decrease in CYP3A4 activity compared to the undifferentiated cells, and upregulated 2E1 and 2D6, not involved in rotenone metabolism as previously outlined.

Taken together, these results support the possible role of CYP isoforms in the neuroprotection against xenobiotic insult, especially as regards the metabolic activity of CYP2D6 and CYP2E1. However, it would be interesting to investigate the induction dynamics of the CYPs analyzed here and understand

²⁹⁵ Pandey, A., Sarkar, S., Yadav, S. K., Yadav, S. S., Srikrishna, S., Siddiqui, M. H., Parmar, D., & Yadav, S. (2022). Studies on Regulation of Global Protein Profile and Cellular Bioenergetics of Differentiating SH-SY5Y Cells. *Molecular neurobiology*, 59(3), 1799–1818.

²⁹⁶ Dranka, B. P., Hill, B. G., & Darley-Usmar, V. M. (2010). Mitochondrial reserve capacity in endothelial cells: The impact of nitric oxide and reactive oxygen species. *Free radical biology & medicine*, 48(7), 905–914.

²⁹⁷ Schneider L, Giordano S, Zelickson BR, Johnson MS, Benavides GA, Ouyang X, Fineberg N, Darley-Usmar VM, Zhang J (2011) Differentiation of SH-SY5Y cells to a neuronal phenotype changes cellular bioenergetics and the response to oxidative stress. *Free Radical Biol Med* 51(11):2007–2017

²⁹⁸ Caboni, P., Sherer, T. B., Zhang, N., Taylor, G., Na, H. M., Greenamyre, J. T., & Casida, J. E. (2004). Rotenone, deguelin, their metabolites, and the rat model of Parkinson's disease. *Chemical research in toxicology*, 17(11), 1540–1548.

the pathways promoted by β NF, EtOH that lead to the induction of CYP. Moreover, the impact that this isoform has in the metabolism of other drugs, together with the results reported here, bring new insights for future therapeutic approaches.

6. Conclusions

6.1 Conclusions

In the results shown in the first part of this thesis (chapter 3), we found that SH-SY5Y cells can be differentiated towards cellular phenotypes like mature primary neurons, in which the expression of characteristics of dopaminergic neurons was increased. The cell populations obtained can then be used as a reproducible and reliable *in vitro* model for pathophysiological studies of Parkinson's disease, being thus a useful tool of research.

The results from CYP induction confirmed that β NF and EtOH can modulate the expression of different CYP isoforms both in the undifferentiated SH-SY5Y cells and in the two populations obtained following the RA-BDNF and RA-TPA differentiation protocols. Overall, undifferentiated SH-SY5Y cells showed a greater propensity for induction of the CYP system by the two inducers used. Indeed, β NF produced a significant increase in isoforms 2D6 2E1 and 1A1. On the other hand, EtOH promoted an increase in CYP2D6, CYP1A1.

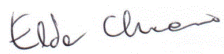
Given these data, the same compounds were used to evaluate the role of CYP isoforms induction upon the toxicity of MPP⁺ and Rotenone. In this context, it may be noted how the greater recovery in response to neurotoxin-mediated damage following CYP-induction in undifferentiated cells overlaps with the greater response to induction observed in Task 2. In fact, the differentiated cells, characterized by a higher expression of CYPs, showed a lower capability to reverse the insult. In the present findings about viability and apoptosis, the neuroprotective effects promoted by β NF against MPP⁺ were evident in both undifferentiated and RA-BDNF-differentiated cells, while a reversal effect was observed in all cell populations as regards the production of ROS. Treatment with EtOH significantly promoted an effective cellular response to MPP⁺-mediated damage only in undifferentiated cells. In cells differentiated with RA-BDNF, in fact, a recovery was observed only in the case of MPP⁺ but not with Rotenone, while a decrease in ROS production was reported in RA-BDNF and partially in RA-TPA.

On the other hand, treatment with the inducers reverted the cytotoxic damage in the UD exposed to Rotenone to a lower extent than the cells exposed to MPP⁺. β NF and EtOH were effective in reverting the cell viability and in decreasing ROS production in UD, while no significant protective effects were

reported in differentiated populations. These differences suggest CYPs isoforms investigated in this study and induced by β NF and EtOH are probably not involved in Rotenone toxicity.

Further studies regarding the CYP induction will be needed to better understand the underlying mechanisms. As an example, the mRNA levels should be accompanied by the assessment of the expression of the protein itself via Western Blot. Furthermore, it will be interesting to evaluate whether the neuroprotection that seems prompted by the induction of CYPs by β NF and EtOH involving the defense towards the mitochondria also occurs against the damage promoted by Rotenone and above all if the differentiated cells exhibit different behaviors

Hereby, the results showed in this thesis address the inducibility of some CYP isoforms and more specifically, the potential neuroprotective role of the CYP2D6 against the toxicity promoted by MPP⁺ in undifferentiated and differentiated neuroblastoma SH-SY5Y cells. Given this, the presented work aims at contributing to the knowledge about the metabolic activity of the CYPs in the CNS, thus giving new insight for the future development of therapeutic approaches in neurodegenerative diseases.

DocuSigned by:

1DDB601DD520453...